SEALING OF SMALL MOVEMENT BRIDGE EXPANSION JOINTS – PHASE 2: FIELD DEMONSTRATION AND MONITORING

Dr. Ramesh B. Malla, Principal Investigator
Dr. Montgomery Shaw, co-Principal Investigator
Mr. Brian Swanson, Graduate Research Assistant, and
Mr. Thomas Gionet, Graduate Research Assistant

Prepared for
The New England Transportation Consortium
July 31, 2011
NETCR-86 **Project No. 02-6 (Phase 2)**

ACKNOWLEDGEMENTS

The authors gratefully acknowledge the financial support received from the Federal Highway Administration/United States Department of Transportation through the New England Transportation Consortium (NETC). First and foremost, sincere thanks are due to the NETC Technical Committee members for this project. The following are the members of the Technical Committee that developed the scope of work for the project and provided technical oversight throughout the course of the research:

Robert Fura, Rhode Island DOT, Chairperson
Lew Benner, Maine DOT
Timothy Boodey, New Hampshire DOT
David Hall, FHWA
Andrew J. Mroczkowski, Connecticut DOT
Mohammed Nabulsi, Massachusetts DOT
Peter Weykamp, New York DOT

Their advice, comments, and assistance throughout the project duration, especially in the field installation of the sealants sealant were vital to the accomplishments and success of this research project. We would also like to thank the Departments of Transportation of Connecticut, New Hampshire, Rhode Island, and New York for providing the bridge sites, traffic control, and help in the field application/installation of the sealants. Special thanks go to Mr. Boodey, Mr. Fura, Mr. David Hiscox (CT DOT), and Mr. Weykamp for coordinating to bring all the logistics together for (and being personally present at) the field installation of the sealants in their states' bridges. The authors would like to express their thanks to Watson Bowman Acme Corporation for their continued interest in the project and for providing their existing bridge sealant materials. Thanks are also due to Bibek Shrestha, a graduate student, for his help in a part of this project. Finally, the authors want to thank the Department of Civil & Environmental Engineering and Connecticut Transportation Institute, University of Connecticut, Storrs, CT for providing lab research facilities and logistics support for the project.

Technical Report Documentation Page

1. Report No.	2. Government Accession No.	3. Recipient's Catalog No.
NETCR 02-6 Phase 2	N/A	N/A

4. Title and Subtitle	5. Report Date / 6. Performing Organization Code
Sealing of Small Movement Bridge Expansion Joints-Phase 2: Field Demonstration and Monitoring	5. Report Date: July 31, 2011 6. Performing Organization Code: N/A
7. Author(s)	8. Performing Organization Report No.
Ramesh B. Malla, Ph.D., Associate Professor (PI); Montgomery Shaw, Ph.D., Professor (co-PI); Brian Swanson, Graduate Research Assistant; and Thomas Gionet, Graduate Research Assistant	NETCR-86
9. Performing Organization Name and Address	10 Work Unit No. (TRAIS) / 11. Contract or Grant No.
Department of Civil and Environmental Engineering 261 Glenbrook Road, Unit 2037 Storrs, CT 06269-2037	10 Work Unit No. (TRAIS): N/A 11. Contract or Grant No.: N/A
12. Sponsoring Agency Name and Address	13. Type of Report and Period Covered / 14. Sponsoring Agency Code
New England Transportation Consortium C/o Advanced Technology & Manufacturing Center University of Massachusetts Dartmouth 151 Martine Street Fall River, MA 02723	13. Type of Report and Period Covered: FINAL REPORT 14. Sponsoring Agency Code: NETC 02-6 Phase 2. A study conducted in cooperation with the U.S. DOT

15 Supplementary Notes

N/A

16. Abstract

A silicone foam sealant was developed to provide an easy-to-use and economical joint sealant for small-movement bridge expansion joints. In studies reported in Phase 1, various laboratory tests were conducted to evaluate the performance of the sealant using concrete as the bonding substrate. In the present study (Phase 2), laboratory tests on the sealant were conducted using other substrates found in practice, including steel, asphalt, and polymer concrete. Tension, repair, oven-aged bonding, salt water immersion, freeze-thaw, and cure rate (modulus vs. time) tests were performed to determine the engineering/mechanical properties of the foam sealant. These tests were also performed on a commercially available silicone sealant for comparison. A method to produce the foam sealant in larger quantity for field application was successfully accomplished. A procedure was developed to apply the foam sealant into bridge expansion joints. This development consisted of determining the proper applicator tools, a step-by-step application process, and the rehearsal of the sealing of a prototype 7-ft long x 2-in wide joint in the laboratory prior to field installation. After successful laboratory experimentation, the newly developed foam sealant along with the commercially available sealant were installed in the expansion joints of four bridges, one each in Connecticut, New Hampshire, Rhode Island, and New York. Over the course of approximately 20 months, post-installation monitoring of the sealants was conducted at the bridge joints to evaluate of the physical condition of the applied sealants. Through the laboratory tests, field installation, and monitoring, it has been observed that the silicone foam sealant has the ability to bond to various substrate materials, can accommodate deformation typical of small-movement expansion joints in bridges, is easy to install, and has displayed durability over the course of approximately 20 months in the field environment. The silicone foam sealant has been seen to provide as good as or in several cases superior engineering/mechanical properties in laboratory testing and better resiliency and performance in the four bridge expansion joints during the field testing.

17. Key Words	18. Distribution Statement
Bridges, expansion joints, silicone foam sealant, elastomer, monitoring.	No restrictions. This document is available to the public through the National Technical Information Service, Springfield, Virginia 22161.

19. Security Classif. (of this report)	20. Security Classif. (of this page)	21. No. of Pages	22. Price
Unclassified	Unclassified	137	N/A

Form DOT F 1700.7 (8-72) Reproduction of completed page authorized

SI* (MODERN METRIC) CONVERSION FACTORS

APPROXIMATE CONVERSIONS TO SI UNITS

Symbol	When You Know	Multiply By	To Find	Symbol
		LENGTH		
in	inches	25.4	millimetres	mm
ft	feet	0.305	metres	m
yd	yards	0.914	metres	m
mi	miles	1.61	kilometres	km
		AREA		
in^2	square inches	645.2	millimetres squared	mm^2
ft^2	square feet	0.093	metres squared	m^2
yd^2	square yards	0.836	metres squared	m^2
ac	acres	0.405	hectares	ha
mi^2	square miles	2.59	kilometres squared	km^2
		VOLUME		
fl oz	fluid ounces	29.57	millilitres	mL
gal	gallons	3.785	Litres	L
ft^3	cubic feet	0.028	metres cubed	m^3
yd^3	cubic yards	0.765	metres cubed	m^3

NOTE: Volumes greater than 1000 L shall be shown in m^3

Symbol	When You Know	Multiply By	To Find	Symbol
		MASS		
oz	ounces	28.35	grams	g
lb	pounds	0.454	kilograms	kg
T	short tons (2000 lb)	0.907	megagrams	Mg
		TEMPERATURE (exact)		
^0F	Fahrenheit temperature	5(F-32)/9	Celcius temperature	^0C

* SI is the symbol for the International System of Measurement

APPROXIMATE CONVERSIONS TO SI UNITS

Symbol	When You Know	Multiply By	To Find	Symbol
		LENGTH		
mm	millimetres	0.039	inches	in
m	metres	3.28	feet	ft
m	metres	1.09	yards	yd
km	kilometres	0.621	miles	mi
		AREA		
mm^2	millimetres squared	0.0016	square inches	in^2
m^2	metres squared	10.764	square feet	ft^2
ha	hectares	2.47	acres	ac
km^2	kilometres squared	0.386	square miles	mi^2
		VOLUME		
mL	millilitres	0.034	fluid ounces	fl oz
L	litres	0.264	gallons	gal
m^3	metres cubed	35.315	cubic feet	ft^3
m^3	metres cubed	1.308	cubic yards	yd^3
		MASS		
g	grams	0.035	ounces	oz
kg	kilograms	2.205	pounds	lb
Mg	megagrams	1.102	short tons (2000 lb)	T
		TEMPERATURE (exact)		
^oC	Celcius temperature	1.8C+32	Fahrenheit temperature	^oF

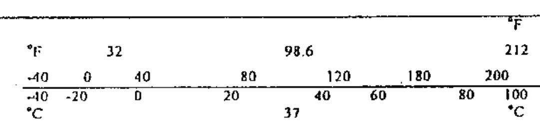

SEALING OF SMALL MOVEMENT BRIDGE EXPANSION JOINTS – PHASE 2: FIELD DEMONSTRATION AND MONITORING

by
Ramesh B. Malla, Ph.D., Associate Professor (Principal Investigator)
Montgomery Shaw, Ph.D., Professor (co-Principal Investigator)
Brian Swanson, Graduate Research Assistant
and
Thomas Gionet, Graduate Research Assistant

Department of Civil and Environmental Engineering
University of Connecticut
261 Glenbrook Road, Storrs, CT 06269-2037

Prepared for
The New England Transportation Consortium

NETCR-86 Project No. NETC 02-6 (Phase 2)

EXECUTIVE SUMMARY

A silicone foam sealant was developed to provide an easy-to-use and economical joint sealant for small-movement bridge expansion joints. The silicone foam sealant investigated in this research was made from five ingredients: a commercially available two-part silicone sealant (termed herein as “solid sealant”), water, crosslinker, and a platinum catalyst following the method and procedure developed in Phase 1 of this project (see Malla et al. 2006, 2007, and 2010). In the study reported previously (Phase 1), various laboratory tests were conducted to evaluate the performance of the sealant using concrete as the bonding substrate. In the present study (Phase 2), laboratory tests on the sealant were conducted using other substrates found in practice, including steel, asphalt, and polymer concrete. The laboratory tests, including tension, repair, oven-aged bonding, salt water immersion, freeze-thaw, and a modulus over time tests, were conducted to evaluate the mechanical properties of the sealant. For comparison purpose, these laboratory tests were also performed on the commercially available two-part silicone sealant (solid sealant) that was the base element for the foam sealant. The following covers the conclusions drawn from the laboratory experiments:

- The foam sealant exhibits an ability to accommodate movement of small-movement expansion joints as these types of joints are designed to expand as much as 100 to 200% of its original strain and contract to 50% of its original strain. The foam sealant was seen to elongate more than the solid sealant before failure.
- The silicone foam has the capability of bonding to commonly used joint header materials (such as concrete, steel, and polymeric concrete) in bridge expansion joints.
- Tension tests show that the silicone foam sealant has a lower modulus (stress at 100% strain) than the commercially available solid sealant. The lower modulus of the foam applies a much lower stress to the interface at a given deformation, resulting in the majority of the foam test specimens failing cohesively (internal material failure) rather

than at the sealant-substrate bond interface (adhesive failure) as is the case with the solid sealant.

- After oven aging, the both the silicone foam and solid sealants were observed to exhibit a loss in stress after each cycle of freezing and elongation to 100% strain. The trends showed that both the solid and the foam sealants will ultimately achieve the minimum modulus and then will not continue to soften.
- Immersion of the foam and solid sealants in salt water resulted in no discernable negative effect on their bonding to asphalt. A negative effect was seen for both sealants when bonded to steel, however.
- If the foam sealant is damaged, either by tearing or separating from the substrate, it can be repaired by applying a new mixture of foam sealant to the affected area. When compared to a piece of damaged solid sealant repaired with new solid sealant, the repaired foam sealant has a higher ultimate strain.
- The strength of both sealants increases as it cures. Over time the rate of increase of the ultimate modulus will slow and plateau. While it appears that the rate of curing is slower for the foam sealant, the cure rates between the foam and solid sealants are not statistically different.
- The foam sealant, having been submersed in water after 1 and 2 hours of curing, was observed to have prevented leakage of water over the course of 7 days of ponding.

After the laboratory tests using specimens with a small quantity of sealant were conducted, a method to produce a larger quantity the foam sealant, which would allow for field application, was determined. Following this, an application procedure, consisting of the proper mixing and installation tools and step-by-step instructions, for installing the silicone foam into small movement bridge expansion joints in the field was developed. The installation process was practiced by sealing a prototype 7-ft long x 2-in wide joint in the laboratory. After successful practice of the application procedure in the laboratory, the procedure was used to seal expansion joints on four (4) bridges, one each in Connecticut, New Hampshire, Rhode Island, and New York. The Connecticut and New Hampshire bridge joints had concrete headers, where as the Rhode Island bridge had steel headers and the New York bridge the polymeric concrete headers. All four bridges were sealed with both the foam sealant and the commercially available solid sealant, for comparison. After the joints were sealed multiple trips were made to the bridge sites to evaluate the physical condition of the applied sealants over the course of approximately 20 months. Thus far, the foam sealant has suffered very minimal damage and has displayed resiliency in the bridge expansion joints in the four northeastern states. . At the Connecticut, New Hampshire, and Rhode Island the damage to the foam sealant was limited to slight peeling at the surface level of the joint header. The damage at the New York bridge was more significant at places, but this damage occurred at locations where the header was damaged. At all four bridges, the foam below the surface was observed to remain intact and attached to the header. While the solid sealant also displayed resiliency in most parts, it did not perform well as the foam. The solid was seen to be damaged by ripping (cohesive failure) and by completely peeling of the header (adhesive failure).

Through the laboratory tests, field installation and monitoring, it was observed that the silicone foam showed the ability to bond to various substrate materials, accommodated deformation well above that of typical small-movement expansion joints in bridges, was easy to install and it displayed durability over the course of 20 months applied to actual bridge expansion joints in the field. The foam sealant was seen to perform comparably to the commercially available solid sealant and in many of the lab and field tests, it performed better.

TABLE OF CONTENTS

LIST OF TABLES

LIST OF FIGURES

1.0 INTRODUCTION

This chapter discusses the motivation, objectives and scope for this research project, as well as presents the literature review on bridge expansion joints.

1.1 Background and Research Motivation

Expansion joints are a vital component to the design of a bridge. These joints accommodate movement of the road deck caused by temperature changes, vehicle loads, humidity, shrinkage, creep, seismic loading, and other factors. It is these factors that keep bridge components in a constant state of expansion and contraction. Bridge expansion joints are designed to allow the bridge to continue this constant movement while maintaining its structural integrity (Dornsife 1999). It is important, therefore, for the expansion joints to exhibit strong performance to ensure the health of the bridges.

There are a number of factors that can negatively influence the performance of the joints, including structural movements at the joint, the condition of the substrate, the weather or temperature during the installation of the expansion joint, and the design of the joint, itself. The traffic loads can influence the performance of the bearings, while the site preparation can affect the bond and anchorage (Price 1994). Aging and deterioration over time can also cause serious issues with the performance of the expansion joint. The gradual breakdown of the materials, which can drastically reduce the life of the bridge, that make up the joint scan be attributed to exposure to water, dirt, debris, and deicing chemicals. Constant exposure to traffic and snow plows, over time, can also have serious physical impacts on the heath of the expansion joint. The introduction of these external factors can result in damaged joint headers (e. g. cracks concrete headers or rusted steel headers), damaged steel plates and other metal bridge components, and misalignment or restriction of motion of the expansion joint (Guzaltan 1993). When these defects become present the worst-case scenario resulting from the damage is structural failure of the bridge. While joint sealants cannot prevent joint header damage, they can, when installed properly, prevent the water and corrosive deicing materials, discussed above, from interacting with and damaging the bridge components beneath the road deck. Sealants for bridge expansion joints, thus, become part of a necessary effort to deter external elements from negatively affecting the life span of newly constructed and existing bridges.

One of the important aspects of bridge expansion joints is the prevention of water and corrosive materials from leaking through the joint opening. These materials can cause serious damage to bridge substructure components, thereby shortening the lifespan of the bridge. There are a variety of joint sealing systems used for a wide range of bridge movements. A few commercial joint sealants specialized for bridges are available for use, including the Dow Corning 902 joint sealant (Dow Corning 2008) and the WABO two-part silicone sealant distributed by the Watson Bowman Acme Corporation (Watson Bowman 2008). These two materials are among a few different types of joint sealants. Applying these types of seals, however, does not always guarantee that leakage through the expansion joint will be prevented. Accumulation of debris, among other factors, can result in the loosening, splitting, and damaging of the joint seals.

A study was conducted in Phase 1 of this NETC project on the development of a silicone foam sealant with the ability to expand in volume as it cures (Malla et al. 2006, 2007, 2010; Shrestha et al. 2006). The expansion of the foam means that only certain, carefully calculated, amounts of sealant need to be poured into the expansion joint. As the sealant expands it gradually fills the joint volume and presses into the interstices of the header for optimal bonding. In this previous investigation, the sealant was subjected to various laboratory tests that evaluated its tensile strength, compressive strength, reaction to various temperatures, stress and creep behavior, and bonding capabilities to concrete.

The motivation behind the current (Phase 2) research endeavor was the need to determine whether the silicone foam can be effectively used to protect small-displacement bridge expansion joints with various bridge expansion joint headers used in practice. The project was also driven by the need to establish the ease of installation and durability of the foam sealant when applied to actual bridges in the field.

The research study discussed in this report covers the next phase of investigation which involved four major tasks. The first task was the evaluation of the foam sealant's bonding capabilities to various substrate materials. Concrete is a common bridge joint header material; however, other materials, such as steel and polymer concrete, are used as well. Polymer concrete, made by combining aggregate with a polymerizing monomer, is a high strength material that is also used as a joint header material on certain bridges (Vipulanandan 1993). Due to lack of resources, the scope of previous studies on the silicone foam sealant (Malla et al. 2006, 2007, 2010; Shrestha et al. 2006) were limited to the evaluation of its performance on concrete substrates. Investigations were still needed to test the performance of the sealant when bonded to other substrates available in practice. The second major task for this project was to develop an application procedure to install the foam sealant in bridge expansion joints. The challenge for this task was to develop a procedure that was efficient and quick to limit any traffic delay due to temporary lane closures. The third and fourth tasks involved the successful installation of the sealant in bridge expansion joints in the field and its subsequent monitoring.

1.2 Project Objectives

The main objective of this project is to test the behavior of the silicone foam sealant under various in-field conditions, make any necessary changes, and evaluate its performance while on an operating highway bridge in order to determine its cost effectiveness and durability. In particular the research involved the following steps:

- Pre-field laboratory evaluation of the silicone sealant's bonding and other characteristics with substrates other than the concrete, such as asphalt, steel, and polymer concrete used in practice (Tests on the concrete substrate were done in previous investigation, e.g. see Malla et al 2007).
- Development of an application procedure for field installation of the sealant in a bridge expansion joint
- Field application of the silicone foam sealant into bridge expansion joints in representative New England States.
- Post installation monitoring of sealant at the bridge site. This required regular visits to the bridge site to visually examine the health of the sealant and the collection of temperature, humidity, precipitation, and traffic count data.

1.3 Literature Review

This section presents a literature review of the different types of bridge expansion joints used and their sealing systems that are designed to prevent the leakage of water and corrosive materials through the joint opening.

1.3.1 Design Criteria for Bridge Expansion Joints

The 2007 AASHTO LRFD Bridge Design Specification covers the criteria needed to design bridge expansion joints. This specification requires that all joints and bearings are to be designed to accommodate movements and deformation of the road deck due to varying temperatures, creep, shrinkage, elastic shortening caused by prestressing, traffic loads, and other external factors (AASHTO 2007). In order to determine the appropriate type of expansion joint to use, a number of factors need to be considered. These factors include movement range, bridge span, type of bridge, joint performance, durability, maintenance requirements, bridge alignment, joint details at curbs, concrete barriers, or deck edges, initial costs, climate conditions, expected joint life, installation time, life-cycle costs, type of bridge supports, and the service level (Purvis 2003).

In designing expansion joints the effects of concrete shrinkage, thermal variation, and long-term creep need to be evaluated. These are the most common sources of movement. The effect of shrinkage is dictated by the concrete aggregate characteristics, aggregate proportions, average humidity, the W/C ratio, type of cure, volume of surface area ration number, and duration of the drying period (AASHTO 2007). According to the Washington State Department of Transportation, as of 2005, the shrinkage shortening of the deck is calculated with the following equation:

$$\Delta_{shrink} = \beta \cdot \mu \cdot L_{trib} \tag{1.1}$$

In this equation L_{trib} is the tributary length of the structure subject to shrinkage. β is the ultimate shrinkage strain after the joint has been installed. An assumed estimation of 0.0002 can be used for β. μ is the restraint factor that accounts for the restraining effect caused by superstructure elements installed before the concrete slab cast. This number can vary depending on the type of girder used. μ is 0.0 for steel girders, 0.5 for precast prestressed concrete girders, 0.8 for concrete box girders and T-beams, and 1.0 for concrete flat slabs (Washington State DOT 2005).

Thermal displacements are considered because there are many modes of heat transfer that affect the thermal gradient of the of the bridge superstructure. The modes of radiation, convection, and conduction all affect the bridge differently. Also, varying climactic conditions will result in a wide range of temperature variations. The movement range due to thermal effects can be calculated with the following equation:

$$\Delta_{temp} = \alpha \cdot L_{trib} \cdot \delta T \tag{1.2}$$

In this equation L_{trib} is the tributary length of the structure subject to thermal variation. α is the coefficient of thermal expansion, which is 0.000006 in./in./°F for concrete and 0.0000065 in./in./°F for steel. δT is the average temperature range of the bridge (Washington State DOT 2005).

1.3.2 Performance of Bridge Expansion Joints

There are a number of factors that can negatively influence the performance of the joints, including structural movements at the joint, the condition of the substrate, the weather or temperature during the installation of the expansion joint, and the design of the joint, itself. The traffic loads can influence the performance of the bearings, while the site preparation can affect the bond and anchorage (Price 1994). Aging and deterioration over time can also cause serious issues with the performance of the expansion joint. The gradual breakdown of the materials, which can drastically reduce the life of the bridge, that make up the joint scan be attributed to exposure to water, dirt, debris, and deicing chemicals. Constant exposure to traffic and snow plows, over time, can also have serious physical impacts on the heath of the expansion joint. The introduction of these external factors can result in damaged joint headers (cracks concrete headers or rusted steel headers), damaged steel plates and other metal bridge components, and misalignment or restriction of motion of the expansion joint (Guzaltan 1993). When these defects become present the worst-case scenario resulting from the damage is structural failure of the bridge.

The performance of the expansion joint depends on its ability to deter water and corrosive materials from leaking through the joint opening. The design of the expansion joints require some type of sealer to prevent corrosive materials from interacting with the internal components of the bridge substructure. If the joints are not sealed properly, the health of the bridge can be compromised. Figures 1 shows a collection of debris that has fallen through an open expansion joint that has not been sealed. Figures 2 and 3 show corrosion of the bridge steel diaphragms and the steel beam ends after exposure to damaging materials. Figure 4 is a frozen bearing and damaged bridge seat that has deteriorated due to a lack of a watertight seal (Purvis 2003). Sealants for bridge expansion joints, thus, become part of a necessary effort to deter external elements from negatively affecting the life span of newly constructed and existing bridges. Section 2.3 goes into greater detail the different types of bridge expansion joints and their systems of sealing.

Figure 1. Collection of Debris underneath the Bridge (Purvis 2003)

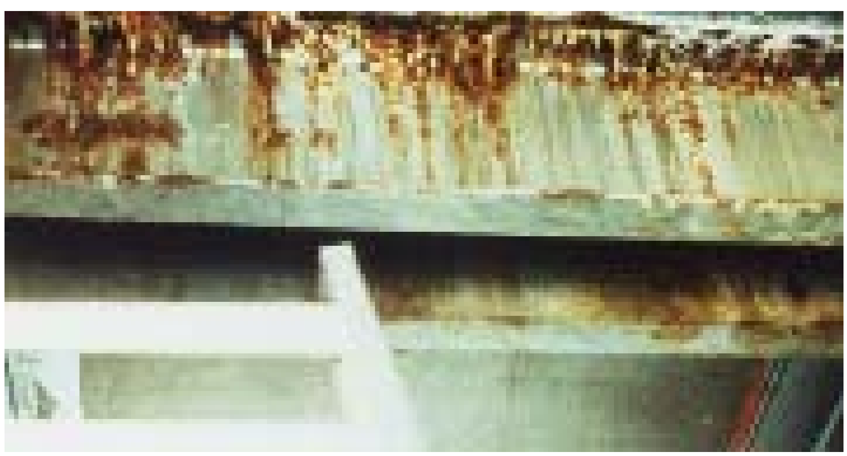

Figure 2. Corrosion of Steel Bridge Diaphragms (Purvis 2003)

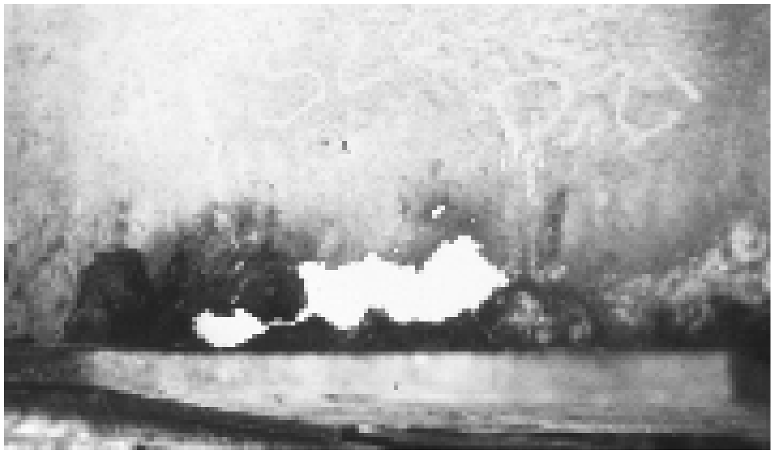

Figure 3. Corrosion at the end of Steel Beam (Purvis 2003)

Figure 4. Frozen Bearing and Damaged Bridge Seat (Purvis 2003)

1.3.3 Types of Bridge Expansion Joints

Bridge expansion joints can be placed into three categories: small movement, medium movement, and large movement. Small movement expansion joints are designed to accommodate bridge movements of up to 45 mm. Joints that fall under this category include compression seal joints, asphaltic plug joints, poured sealant joints, and butt joints. Medium movement joints are designed to accommodate bridge movements between 45 and 130 mm. Joints that full into this category include sliding plate joints, strip seal joints, and finger plate joints. Finally, large movement joints are designed to accommodate joint movements greater than 130 mm. Bolt-down panel joints and modular elastomeric seal joints would be considered large movement bridge expansion joints. The following describes, in more depth, the different types of bridge expansion joints. Table 1 displays the different types of bridge expansion joints, along with their advantages and disadvantages (Malla et al. 2006, Purvis 2003, Washington State DOT 2005, Chen and Duan 2000).

Table 1. Different Types of Bridge Expansion Joints

Joint Category	**Types of Joints**	**Advantages**	**Disadvantages**
Small Movement	Compression Seal Joint	1. Inexpensive 2. Minimal maintenance required 3. Reasonable lifespan 2. Easy to replace	1. Susceptible to damage from snowplows, debris, and traffic 2. Loss of adherence to the sides of the joint headers from varying joint widths
	Asphaltic Plug Joints	1. Easy to install and repair 2. Provides smooth and seamless roadway 3. Debris does not collect on top of seal 4. Avoids damage from snowplows	1. Not effective for vertical or skewed joints 2. Polymer modified asphalt can soften or creep in high temperatures and crack in cold temperatures
	Poured Sealant Joints	1. Durable 2. Self-leveling 3. Strong elastic performance for wide range of temperatures 4. Resistance to UV and ozone degradation 5. Rapid curing to limit traffic disruptions during lane closures as sealant is installed	1. Loss of bonding at the sealant-substrate interface 2. Collection of debris on top of sealant can result in cracking and splitting of material
	Butt Joint	1. The armor plates used can protect concrete from spalling or deteriorating because of continuous exposure from traffic flows	1. Do not prevent water and debris from entering the joint opening 2. Can only be used in certain geographical areas where deicing materials are not used 3. Joint armor can detach from concrete

Table 1. Different Types of Bridge Expansion Joints (continued)

Joint Category	Types of Joints	Advantages	Disadvantages
Medium Movement	Strip Seal Joint	1. Watertight 2. Demonstrated good performance 3. Damaged seal can be easily replaced with minimal traffic disruptions	1. Debris can collect on top of the seal, which can cause gland failure 2. Faulty installation can cause gland pullout
	Sliding Plate Joint	1. Constructed at reasonable cost 2. Prevents most debris from entering the expansion joint	1. Do not provide an effective seal against leakage of water and deicing materials 2. Plates can loosen over time 3. Improperly installed plates can bend and break 4. Plates need to be adjusted periodically to reduce noise levels
	Finger Plate Joint	1. Accommodate rotational movement and vertical Deflection 2. Built with drainage trough beneath the joint to stop water and debris from falling through the expansion joint	1. Fingers of the joint can bend upwards, creating a rough riding surface that can be noisy 2. If not maintained regularly, the troughs can clog and become ineffective
Large Movement	Plank Seal Joint	1. Durable, molded elastomeric panels 2. Accommodates movement ranges of 50 to 330 mm	1. Susceptible to snowplow damage 2. If damaged the entire seal needs to be replaced, making it an expensive repair. 3. The bolts and nuts that are part of the anchoring system can loosen and break in the presence of high speed traffic. This can result in anchor failure.
	Modular Joints	1. Provides watertight wheel load transfer across wide expansion joint openings 2. Accommodates movement ranges of 150 to 600 mm	1. High initial and maintenance cost 2. Fatigue cracking of welds 3. Damage to neoprene sealer material 4. Can be damaged by snowplow

Table 2 from Malla et al. 2006 gives a breakdown of the types of expansion joints used in New England bridges based on their survey. It is noted that for four out of the six New England States the asphaltic plug joint is the most used and preferred type of joint.

Table 2. Types of Bridge Expansion Joint used in New England (Malla et al. 2006, 2007)

State	Types of Joints	Experience with each Type	Comments
Connecticut	**a. Asphaltic Plug Joint** b. Silicone Sealant c. Neoprene Strip Seal d. Modular and Finger Plate	**a. First Preference**	**a. M.R. (< 40mm), Skew < 45** b. M.R. (40 - 80 mm) c. Elastomeric Concrete Header d. For Large Movement
Maine	**a. Compression Seal** b. Silicon Pour-in-Place c. Gland Seal d. Evazote Seal e. Asphaltic Plug Joint	**a. Most Preferred** b. Temporary, 8-10 yr c. Limited Success d. No Success, Failure in short period	**a. New Construction, Versatile, Cheap** b. Rehabilitation Project c. Large R. (> 100 mm) e. Small M.R. (< 50 mm)
New Hampshire	**a. Asphaltic Plug Joint** b. Silicone based Sealant c. Roadway Crack Sealer	**a. Good Results** b. Reasonable Success c. For short spans and on fixed end	**a. Short Spans (80 – 140 ft.)** b. Small M.R., 2-Part, Silicon c. Hot Applied, Petroleum Based
Rhode Island	**a. Asphaltic Plug Joint** b. Compression Seal c. Strip Seal d. Open Joints, Sliding Plate Joint	**a. Most Preferred** b. Poor c. Poor d. Poor	**a. Short Spans (< 100 ft.)** b. No more in use, Leakage, Loosening of Angles c. Large M.R., Leakage d. Exist in Old Construction
Massachusetts	Information Not Available		
Rhode Island	**a. Asphaltic Plug Joint** b. Compression Seal c. Strip Seal d. Open Joints, Sliding Plate Joint	**a. Most Preferred** b. Poor c. Poor d. Poor	**a. Short Spans (< 100 ft.)** b. No more in use, Leakage, Loosening of Angles c. Large M.R., Leakage d. Exist in Old Construction
Massachusetts	Information Not Available		
Vermont	**a. Asphaltic Plug Joint** b. Vermont Joint c. Finger Plate Joint d. Modular Joints	**a. Most Preferred for Short Spans (< 90 ft.)** b. For Spans > 90 ft.	**a. Small M.R. (< 50 – 75 mm)** b. Small M.R. (< 75 mm) c. Large M.R. (> 75 mm) d. Very Large M.R., Rarely Used

1.4 Structure of Report

Chapter 1 of this report covers the background information, literature review, and project objectives. Chapter 2 discusses the development of the silicone foam sealant and the laboratory methodology of the tests performed on the sealant while bonded to various substrate materials. The results of the laboratory tests are in Chapter 3. Chapters 4, 5, and 6 discuss the process of taking the silicone foam from the laboratory setting, applying to an actual bridge expansion joints. Topics, here, cover large scale mixing of the sealant, development of an application procedure, the actual field application of the sealants and finally post-installation monitoring. Chapter 7 covers the conclusions and recommendations for future research made based on the work performed in this phase of the project. Finally, all the references are displayed in Chapter 8.

2.0 LABORATORY EXPERIMENTAL STUDIES

This chapter discusses the development of the silicone foam sealant and describes the various laboratory tests conducted.

2.1 Silicone Foam Development

The silicone foam sealant investigated in this research is made from five ingredients: WABO two-part silicone sealant (Watson Bowman 2008), water, crosslinker (Momentive 2008, Gelest 2003), and a platinum catalyst (Gelest 2003) following the method and procedure developed in Malla et al. 2006, 2007, and 2010. Two parts of the WABO sealant, one white and one black, create a solid silicone sealant when mixed and cured. The addition of water (1.53% of total sealant mass), hydrosilane crosslinker (2.3% of total sealant mass) and a platinum catalyst (0.38% of total sealant mass) to the two part solid sealant creates the silicone foam. The foaming is the result of the reaction of water with hydrosilane, which produces silanol groups (–SiOH) and hydrogen gas. The silanol groups condense and thus aid the polymerization, while the hydrogen gas creates bubbles within the sealant, resulting in a foam material. Depending on conditions, the volume increase due to the foaming ranges between 50 and 70%. The chemical reaction is shown in Figure 5.

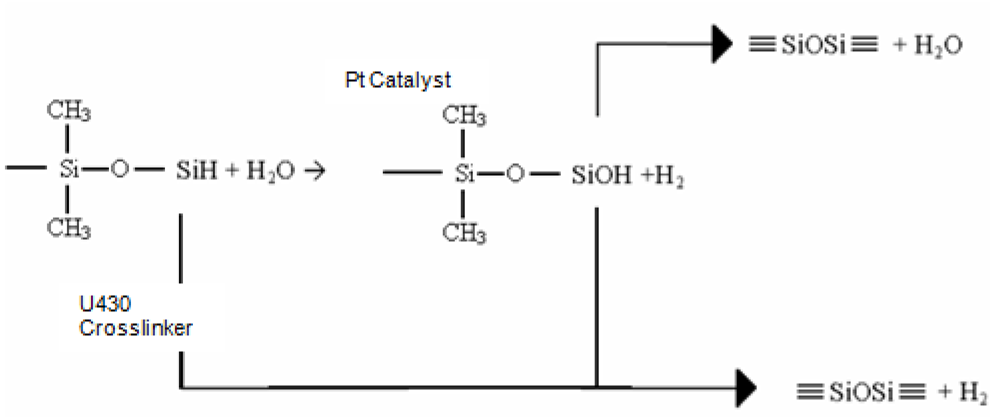

Figure 5. Schematic of Silicone Foam Reaction

Three different types of hydrosilane were used for specific laboratory tests, each of which had the same hydrogen content. The types of hydrosilane were produced by GE Bayer Silicones (GE Bayer 2003), Momentive Performance Materials (Momentive 2008), and Gelest, Inc. (Gelest 2008). Section 2.2 discusses which crosslinker was used in which laboratory test.

2.2 Laboratory Tests and Methodologies

To evaluate the performance of the silicone foam sealant several laboratory tests were conducted, including tensile properties, repair/retrofit, oven-aged bonding, salt water immersion, modulus over time, cure rate, freeze-thaw, and water ponding (Malla, Swanson, and Shaw 2010a, b; 2011). Some of these tests were performed using asphalt, steel, and polymer concrete as the bonding substrates and some using just the steel and asphalt substrates. These substrates were used to make test specimens depicted in a schematic in Figure 6. Each test specimen consisted of two blocks of the substrate material that are separated by a 1.27cm (0.5 in.) gap to be sealed. Each block had a length of 7.62 cm (3 in.), width of 5.08 cm (2 in.), and a depth of

1.27 cm (0.5 in.), except for the steel specimens which had a depth of 0.95 cm (0.375 in.). For comparison purposes, the tests were conducted using specimens with the silicone foam and the WABO two-part silicone sealant, which will be now, onward, called the “solid” sealant. Prior to the making of the test specimens, the substrates were cleaned with a lint-free cloth and secured to hold a gap of 1.27 cm (0.5 in.) between the pieces. The sealants were hand mixed and immediately poured into the gap between the substrates. For the foam sealant, the gap was partially filled to account for the expansion of the sealant as it cures. For the solid sealant the entire depth of 1.27 cm (0.5 in.) of the gap was sealed, as the material does not expand. The specimens, depending on which test was performed, were pulled at a specific crosshead velocity to a specific strain or until the sealant failed. Failure means either a complete tearing within the sealant (cohesive failure), a separation from the bonding substrate (adhesive failure), or a mixture of both. The various laboratory tests conducted using the test specimens are briefly described below.

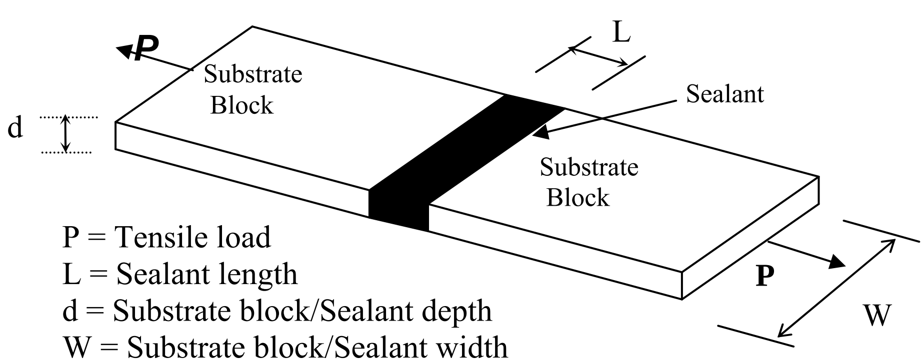

Figure 6. Laboratory Test Specimen

2.2.1 Tension Test

Two types of tension tests were performed: pull-to-fail and load/unload. Both tension tests used a hydrosilane called Baysilone U 430 Crosslinker produced by GE Bayer Silicones (GE Bayer 2003). This crosslinker has, since, become Silopren U Crosslinker 430 from Momentive Performance Materials (Momentive 2008). For these tests, 8 specimens - 4 using the foam and 4 using the solid - were made using each of the following substrates; asphalt, steel, and polymer concrete. For the pull-to-fail test each specimen was cured for 21 days at room temperature (23°C), after which they were placed in an Instron tensile tester, model 1011 (Instron 2008), which is shown in Figure 7. This machine was used to pull the two substrate blocks apart at a crosshead velocity of 10 mm/min until failure.

Figure 7. Instron Testing Machine (Model 1011) with Tension Specimen (Malla et al. 2006, 2007)

For the load/unload test the specimens were also cured for 21 days at room temperature (23°C). This time, however, the specimens were pulled at a crosshead velocity of 10 mm/min up to 300% strain and then unloaded until they reached zero strain. This loading and unloading process was repeated for another 4 cycles for a total of 5 cycles.

2.2.2 Repair/Retrofit Test

It is possible that the sealant could be damaged after it has been applied to a bridge expansion joint in the field. Thus, it is important to determine if a damaged sealant can be repaired simply by adding a fresh mixture of sealant to the damaged section. To evaluate this situation, a “repair” test was devised and performed. Test specimens were made where each of the samples had a cured sealant, foam (using the crosslinker from Gelest, Inc. 2008 or solid, on the surface of the bonding area. The specimens were then sealed with new (freshly made) sealant. The test units were made with the following characteristics: 4 samples of new foam sealed to old (previously cured/used) foam, 4 samples of new solid to old foam, 4 samples of new foam to old solid, 4 samples of new solid to old solid. A pull-to-fail tension test was performed on each sample at a crosshead velocity of 10 mm/min.

2.2.3 Oven-Aged Bond Test

An oven-aged bond test was performed on the sealants to evaluate the effects of extreme changes in temperature on the bonding capabilities of the sealant as it cures. Tests were done on specimens with steel, asphalt and polymer concrete substrates. For each bonding substrate, eight test specimens - four for the foam sealant (using the crosslinker from Gelest, Inc. 2008) and four for the solid sealant - were prepared. These specimens were cured for 7 days at room temperature (23°C), and then they were placed in an oven for 7 days at 70 °C. After the oven aging, the specimens were placed in an insulated box and held at −29 °C for 4 h using dry ice. After this cooling period, the test units were tested by loading them at a crosshead velocity of 6 mm/min until they reached 300% strain. The specimens were removed from the machine and left out on a table for 4 h to regain their original length. The specimens were then put in the dry ice at −29 °C for 4 h again, tested, and allowed to recover. The process of freezing, testing, and recovery was repeated for 5 cycles. This test procedure follows substantially the ASTM D 5893-96 standard (ASTM 1997).

2.2.4 Salt Water Immersion Test

A salt water immersion test was performed on test specimens to evaluate the effects of prolonged exposure to salt water on the material and bonding of the foam and solid sealants to different substrates. For this test also two types of substrates, asphalt and steel, were used. For each substrate 8 specimens were made, 4 with foam (using crosslinker from GE Bayer) and 4 with solid. The specimens were allowed to cure for 7 days at room temperature (23°C), and then placed in a bucket of saturated salt water for 14 days. During this time period, the salt water was kept at a temperature of 45°C. After the 2 weeks of submersion, the specimens were removed from the water, allowed to dry for 4 h, and tested. A pull-to-fail tension test was performed on the samples using a crosshead velocity of 10 mm/min.

2.2.5 Modulus over Time Test

The amount of time that the sealant has cured may have an effect on the strength of the sealant. To test this effect, laboratory specimens were made by bonding the foam and solid sealants to asphalt and steel substrates. For each type of substrates used, 8 specimens were made, 4 with the foam and 4 with the solid. The specimens were extended to 100% strain at 10 mm/min and then unloaded completely. The first was done on the sealants right after they were allowed to cure for 3 h. Subsequently, this loading and unloading was repeated on the same specimens at several other time intervals, including 6 hours, 18 hours, 24 hours, and then once every day for the next 42 days.

2.2.6 Freeze –Thaw Test

Tests were performed to evaluate how freezing the sealant will affect its performance. 3 sets of specimens were made with the foam, and 3 other sets were made with the solid sealant. Each set required the sealing of samples for multiple cure rate times: 1 hour, 2 hour, and 3 hour. For each of these curing times 4 samples were made with the foam sealant and 4 samples were made with the solid sealant (64 samples total for each set). A concrete substrate was used, but for this particular test the type of substrate used did not matter. After the samples were allowed to cure for their designated amount of time, each set was subjected to different tests. The first set of samples were soaked in water for 10 days, after which a pull to fail tension test was performed, extending the samples at 10mm/min (Submerse). The second set of samples were soaked in water for 7 days, placed in a freezer for 3 days at -20˚C, and pulled to failure in the Instron machine at 10mm/min (Submerse - Freeze). The third set were soaked for 7 days, placed in the freezer for 3 days, taken out of the freezer and allowed to thaw for 2 hours, and then pulled to failure at 10mm/min (Submerse - Freeze - Thaw).

2.2.7 Water Ponding Test

The foam sealant needs to be tested to see if during storm whether or not the material will permit water from leaking through to the underside of a bridge. To evaluate this, a ponding test was conducted. Taking plastic cylinders, each measuring 4 inches in diameter, Styrofoam stoppers were placed 5.5 inches below the top of the container. The foam was poured on top of the stoppers, which after foaming measured 1 inch in thickness. Finally, water was filled to the surface of the cylindrical container, creating a water depth of 4 inches. The surface of the water was 0.5 inches below the top of the cylinder. The top of the container was, then, covered. A major concern about using the sealant is how the sealant will react to external factors, like rain, during its initial stage of curing. Therefore, prior to adding water, the sealants were allowed to cure for just 1 hour or 2 hours. Four test units were made for the foam sealant cured for 1 hour prior to ponding, and four other units were made with foam cured for 2 hours prior to ponding. Over the course of the next 7 days the submersed sealant was monitored to see if water was leaking through to the bottom of the cylindrical container. Figure 8 is a schematic of the apparatus used in the water ponding test.

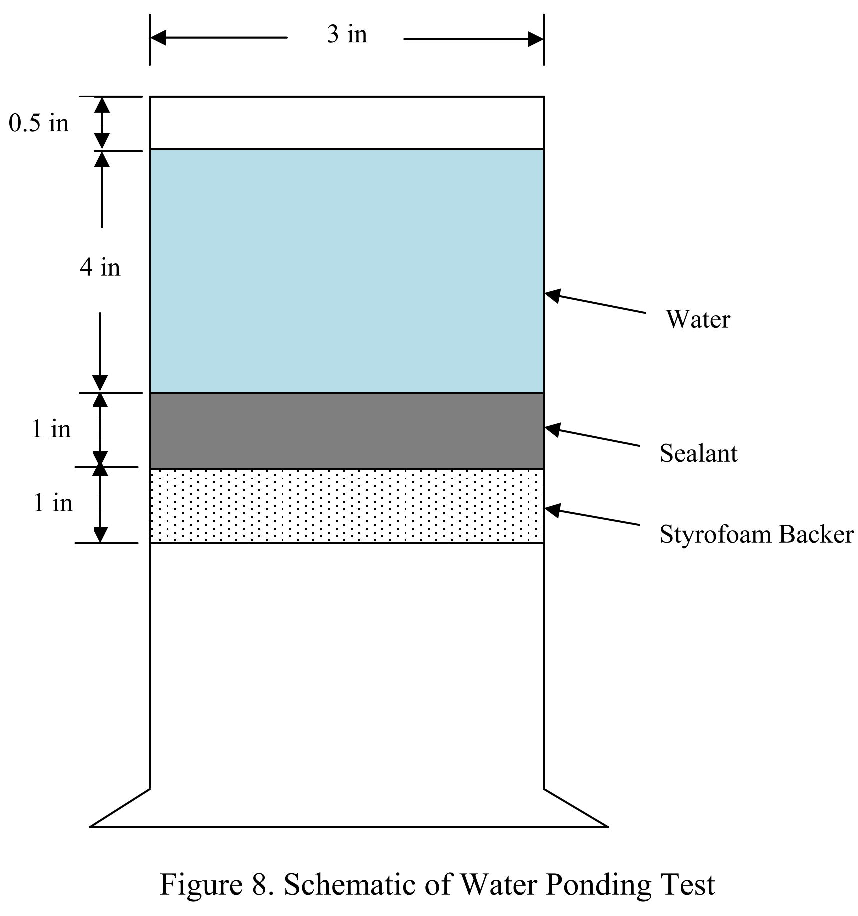

Figure 8. Schematic of Water Ponding Test

2.2.8 Cure Rate Test

For the cure rate test, a set of samples using asphalt and steel substrates were made with both the foam and solid sealants. Unlike the modulus over time test, where one set of samples were made and pulled to 100% strain at specific time intervals, the cure rate test required a set of samples to be made for each specified cure time. After a particular sample set reached its designated cure time, it was tested by pulling until the sealant failed internally or at the bonding interface with the substrate. Eight specimens - four using the foam and four using the solid - were made using asphalt and steel. Specimens were made with the following cure rate intervals: 3 days, 7 days, 10 days, 14 days, 21 days, 28 days, 35 days, and 42 days.

3.0 RESULTS AND DISCUSSIONS OF LABORATORY TESTS

Results obtained from the laboratory tests and brief discussions on them are presented below. These results have also been published in Malla, Swanson, and Shaw (2010a, b; 2011).

3.1 Tension Test Results

3.1.1 Tension Test – Pull to Fail

The results from the pull-to-fail tensile test are shown in Figures 9 (a, b, c) and Table 3. The data presented indicates that the solid sealant, when bonded to steel, asphalt, or polymer concrete, has a higher average 100% modulus than the foam sealant, which is expected. Because a difference is not expected to be seen in the 100% modulus from one substrate to another, the data using steel, asphalt, and polymer concrete was pooled together. A t-test comparing the average 100% modulus of the foam vs. solid sealant yielded a p-value of 5×10^{-9} ($t = 9.2$), which is much less than the threshold of 0.05. This result indicates that the difference between the average 100% modulus of the solid is statistically greater than that of the foam sealant.

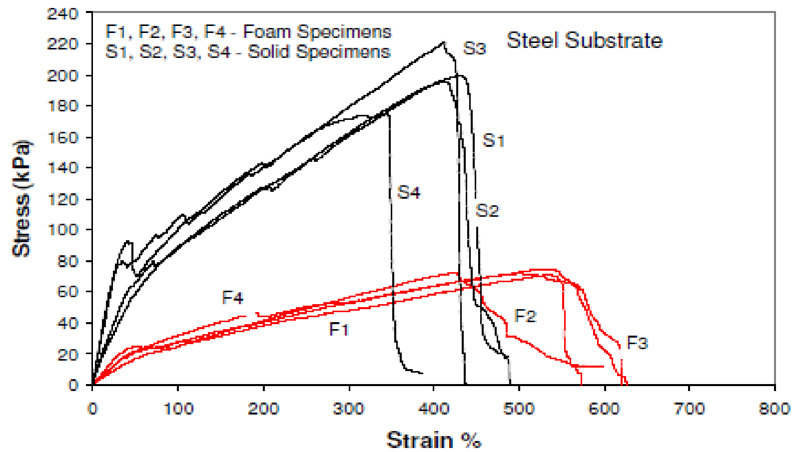

(a)

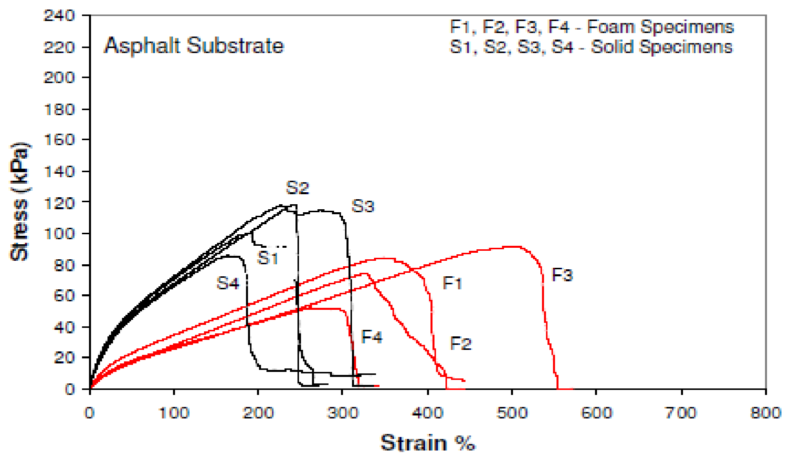

(b)

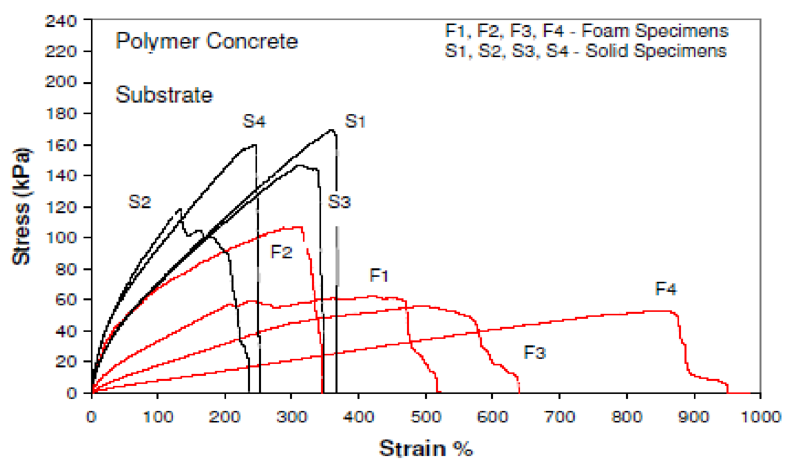

(c)

Figure 9. Tension Test - Pull to Failure using (a) Steel, (b) Asphalt, and (c) Polymer Concrete as Bonding Substrates.

Table 3. Tension Test - Pull to Failure using Steel, Asphalt, and Polymer Concrete Substrates and Comparison with Concrete Substrate

Substrate	Sealant Type	Sample	Average [a] Ultimate Stress (kPa)	Average Ultimate Strain (%)	Failure Modes
Steel	Foam	F1	71.2	534.8	Mixed
		F2	72.4	424.4	Cohesive
		F3	74.4	522.3	Mixed
		F4	72.0	502.0	Cohesive
		Average	72.5 ± 2 [b] (SE [c] = 0.68)	495.9 ± 79 (SE = 24.8)	
	Solid	S1	199.3	428.5	Cohesive
		S2	195.9	411.7	Cohesive
		S3	221.3	413.3	Adhesive
		S4	174.6	344.7	Cohesive
		Average	197.8 ± 30 (SE = 9.6)	399.6 ± 59 (SE = 18.7)	
Asphalt	Foam	F1	84.3	347.8	Cohesive
		F2	73.9	323.8	Cohesive
		F3	91.5	499.4	Cohesive
		F4	52.2	261.3	Cohesive
		Average	75.5 ± 27 (SE = 8.6)	358.0 ± 161 (SE = 24.8)	
	Solid	S1	100.7	190.4	Adhesive
		S2	118.5	242.3	Adhesive
		S3	118.1	227.6	Adhesive
		S4	85.9	164.2	Adhesive
		Average	94.6 ± 62 (SE = 7.8)	206.1 ± 56 (SE = 18.7)	
Polymer Concrete	Foam	F1	62.4	420.1	Cohesive
		F2	106.8	310.5	Cohesive
		F3	56.3	493.9	Adhesive
		F4	52.9	851.0	Cohesive
		Average	69.6 ± 40 (SE = 12.6)	518.9 ± 372 (SE = 116.7)	
	Solid	S1	169.4	360.2	Adhesive
		S2	118.4	133.9	Adhesive
		S3	146.8	309.8	Adhesive
		S4	160.2	244.5	Adhesive
		Average	148.7 ± 35 (SE = 11.1)	262.1 ± 155 (SE = 48.9)	
Concrete [d]	Foam	F1	103	597	Mixed
		F2	94	608	Cohesive
		F3	80	604	Cohesive
		Average	92 ± 30 (SE = 6.7)	603 ± 13 (SE = 3.2)	
	Solid	S1	210	444	Cohesive
		S2	186	374	Cohesive
		S3	251	607	Mixed
		Average	216 ± 81 (SE = 19.0)	475 ± 296 (SE = 69.1)	

[a] Average of the 4 test samples
[b] 95% Confidence interval for the averages
[c] SE = Standard error of the mean
[d] From Malla et al. 2007

Of more relevance is the strain at failure. This test yielded p-values of 0.02 (t = 3.69), 0.03 (t = 3.3), and 0.09 (t = 2.23), for foam vs. solid bonded to steel, asphalt, and polymer concrete, respectively. The comparison test reveals that, statistically, the average ultimate strain of the foam was higher than the solid sealant when bonded to steel or asphalt as the p-values calculated are less than 0.05. While the p-value calculated for foam vs. solid bonded to polymer concrete is very close to the threshold of 0.05, we cannot say, conclusively, that the average ultimate strain of the foam was not different from that of the solid sealant. Because of this borderline result, there is reason to believe that with further testing the data may show that the average ultimate strain of the foam will be higher than that of the solid when bonded to polymer concrete.

The raw observations of average values of the ultimate strain of the foam sealant for the various substrates followed the order (largest to smallest) concrete, polymer concrete, asphalt, and then steel. When the average ultimate strain of the foam sealant bonded to concrete (Malla et al. 2007, Malla et al. 2006, Shrestha et al. 2006) was compared to those using steel, asphalt, and polymer concrete using a t-test, the p-values were 0.02 (t = 4.1), 0.01 (t = 4.7), and 0.57 (t = 0.6), respectively. This implies that statistically, there is a difference in the average ultimate strain of the foam sealant between the concrete substrate and the asphalt and between the concrete and steel substrates. A difference in the average ultimate strains between the concrete and polymer concrete samples was not observed as the p-value is greater than 0.05. This finding is in accord with the fact that both sawn surfaces of the substrates are substantially the same, comprising mostly course and fine aggregate.

The average ultimate strain values of the solid sealant for the various substrates followed the order (largest to smallest) concrete, steel, polymer concrete, and finally asphalt. When the average ultimate strain values of the solid sealant bonded to concrete (Malla et al. 2006, 2007) were compared using a t-test to those using steel, asphalt, and polymer concrete, the p-values from the t-test were 0.28 ($t = 1.3$), 0.01 ($t = 5.1$), and 0.05 ($t = 2.8$), respectively. The results using concrete are statistically different from the results using asphalt and polymer concrete. The test specimens using concrete give similar results to the specimens using steel.

The lower modulus (stress at 100% strain) of the foam means that less stress is applied to the substrate when the sealant is strained, allowing the sealant to elongate to a higher strain than the solid. Because less stress is applied to the substrate, the foam tends not separate from the surface interface at failure, but fails internally (cohesive failure). In contrast, the higher stress applied by the solid sealant to the bonding area results in more frequent failure at the interface surface between the sealant and substrates (adhesive failure). An exception is seen when the steel substrate was used. In this situation, the solid sealant failed cohesively for 3 out of the 4 test samples, as shown in Table 1. The solid sealant seems to bond very well to the steel substrate.

The higher ultimate strain and cohesive failure mode for the foam are important results. The observations imply that seals made from foam, as opposed to the equivalent solid, are less likely to fail catastrophically. The foam will be more resilient than the solid in a situation where a stone, or other objects, will try to puncture the sealant. As the stone is pressed onto the sealant surface, the foam will deform and less stress will be created in comparison to the solid sealant. The low stress makes it unlikely that the sealant will rip from the substrate

3.1.2 Tension Test – Load and Unload

The results for the load and unload tensile test to 300% strain are displayed in Figures 10 (a) and (b) and in Table 4. Unless the sealant failed adhesively, there was no expectation to see a difference in the results from one type of substrate used to the next, as the fatigue of the material is a bulk characteristic. When the results from test specimens using steel and asphalt substrates are pooled together, the average slope of stress vs. cycle curves for the 8 test samples, with 95% confidence limit is -3.13 ± 1.8 and -2.6 ± 3.17 for foam and solid, respectively. A one-sided t-test (Volk 1956) comparing this average slope to a zero slope yields a t-value of -4.11 ($p = 0.006$) and -3.31 ($p = 0.08$) for foam and solid, respectively. This tells that statistically, slope of stress vs. cycle is different from the zero slope (critical t-value is 1.94 for $p = 0.10$). Practically, these results indicate that the probability is high that the stress of the foam and solid sealant decreases with cycle number. The 300% strain loading-unloading cycle did not induce adhesive or cohesive failure on any foam sealant attached to both steel and asphalt substrates and solid sealant attached to steel substrate. The only failure was the solid sealant bonded to asphalt. In this case, all four test samples failed on the first cycle at the bonding surface at an average strain of 123%.

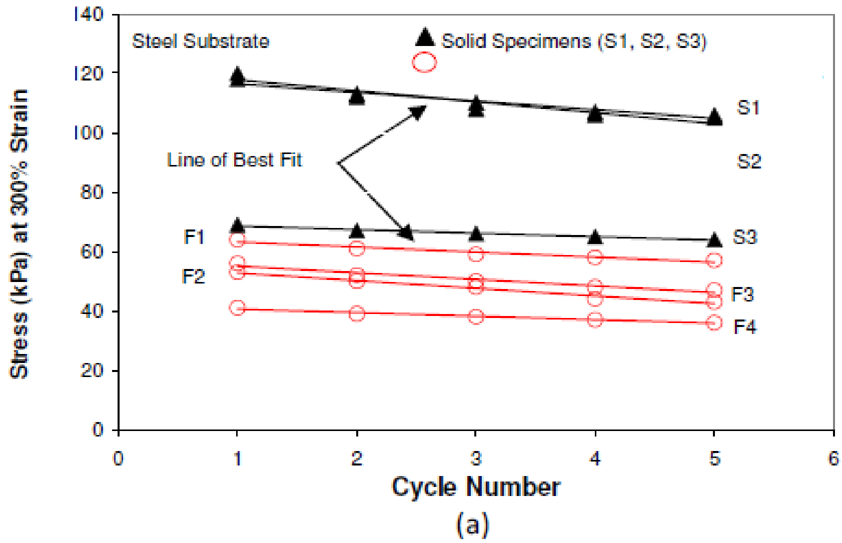

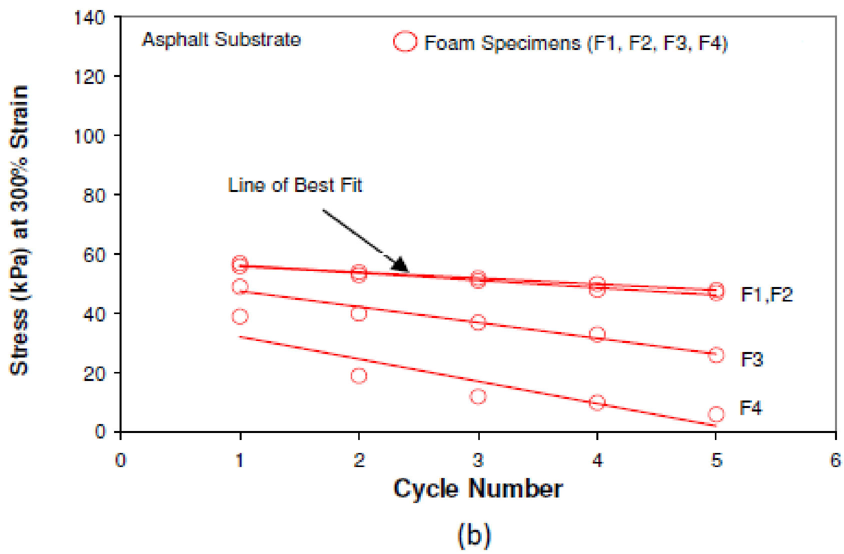

Figure 10. Loading/Unloading Tension Test – Stress at 300% Strain vs. Cycle Number – using (a) Steel and (b) Asphalt Substrates

Table 4. Loading/Unloading Tension Test – Average [a] Stress (kPa) at 300% Strain – Steel and Asphalt Substrates

Sealant Type		1st Extension	2nd Extension	3rd Extension	4th Extension	5th Extension
	Steel Substrate					
Foam	F1	53	50	48	44	43
	F2	41	39	38	37	36
	F3	64	61	59	58	57
	F4	56	52	50	48	47
	Average	53.5 ± 15 [b] (SE [c] = 4.8)	50.5 ± 14 (SE = 4.5)	48.8 ± 14 (SE = 4.3)	46.8 ± 14 (SE = 4.4)	45.8 ± 14 (SE = 4.4)
Solid	S1	69	67	66	65	64
	S2	118	112	110	107	106
	S3	120	113	108	-	-
	Average	102.3 ± 72 (SE = 14.5)	97.3 ± 65 (SE = 13.2)	94.6 ± 62 (SE = 12.4)	86.0 ± 267 (SE = 14.9)	85.0 ± 267 (SE = 14.9)
	Asphalt Substrate					
Foam	F1	56	54	52	50	48
	F2	49	40	37	33	26
	F3	39	19	12	10	6
	F4	57	53	51	48	47
	Average	50.3 ± 13 (SE = 4.5)	41.5 ± 26 (SE = 8.2)	38.0 ± 30 (SE = 9.3)	35.3 ± 29 (SE = 9.3)	31.8 ± 32 (SE = 10.0)
Solid	S1	94				
	S2	88				
	S3	71				
	S4	73				
	Average	81.5 ± 18 (SE = 5.7) [d]	- [d]	- [d]	- [d]	- [d]

[a] Average of the 4 test samples
[b] 95% confidence interval for the averages
[c] SE = Standard error of the mean
[d] The value reported is the average of stresses at the failure. All four solid sealant specimens bonded to the asphalt substrate failed well below 300% strain (at 161, 128, 101, or 103% strain) in the very first extension

Because the solid sealant failed prior to 300% strain when bonded to asphalt, this would indicate a possible difference in the data for stress vs. cycle. Further statistical analysis was conducted, this time taking into consideration the different substrates used. The average slopes of stress vs. cycle, with 95% confidence limits, for the foam sealant when bonded to steel (4 specimens) and asphalt (4 test samples) were -1.9 ± 0.97 and -4.33 ± 4.08, respectively. The average slope, with 95 % confidence limit, for the solid sealant bonded to steel (3 specimens) was -2.6 ± 3.17. The slopes for each line are negative, showing the loss of stiffness with loading and unloading. A one-sided t-test comparing the average slopes of stress vs. cycle for the foam sealant to a zero slope yielded t values of -6.33 ($p = 0.008$) and -3.37 ($p = 0.043$), for steel and asphalt substrates, respectively. As presented above, for the solid sealant bonded to steel, the t calculated was -3.31 ($p = 0.08$). These t-values are all less than the critical t-values (-2.92 for 2 degree of freedoms and -2.35 for 3 degree of freedoms at $p = 0.10$), which suggests that the slopes of stress vs. cycle for the foam and solid sealants are statistically different from a zero slope. Practically, this means that both the foam and solid sealant displayed a slight loss in stiffness after each extension to 300% strain. The tests, however, failed to find a difference between the foam and solid sealants for the average slopes of stress vs. cycle. This implies that more observations need to be performed to find any small differences between the two substrates.

A loss of stress of the foam and solid sealant due to repeated loading and unloading of elastomers is a result of the Mullin's Effect, where the loss in stress is primarily seen during the first extension (Drozdov 2008). With time, the sealant will heal and the loss in stress from one cycle to another will become less significant. When observing the effects of stress softening due to cyclical loading and unloading, the changes in maximum stress of the elastomers between the first cycle and the second cycle are the most critical (Cantournet 2008). This phenomenon was also observed in the sealants study here. The general trend of the hysteresis observed in this load and unload test is shown in Figure 11 (a) and (b). This chart displays the stress of the foam and solid sealants bonded to steel and asphalt as they are subjected to 5 cycles of loading and unloading to 300% strain.

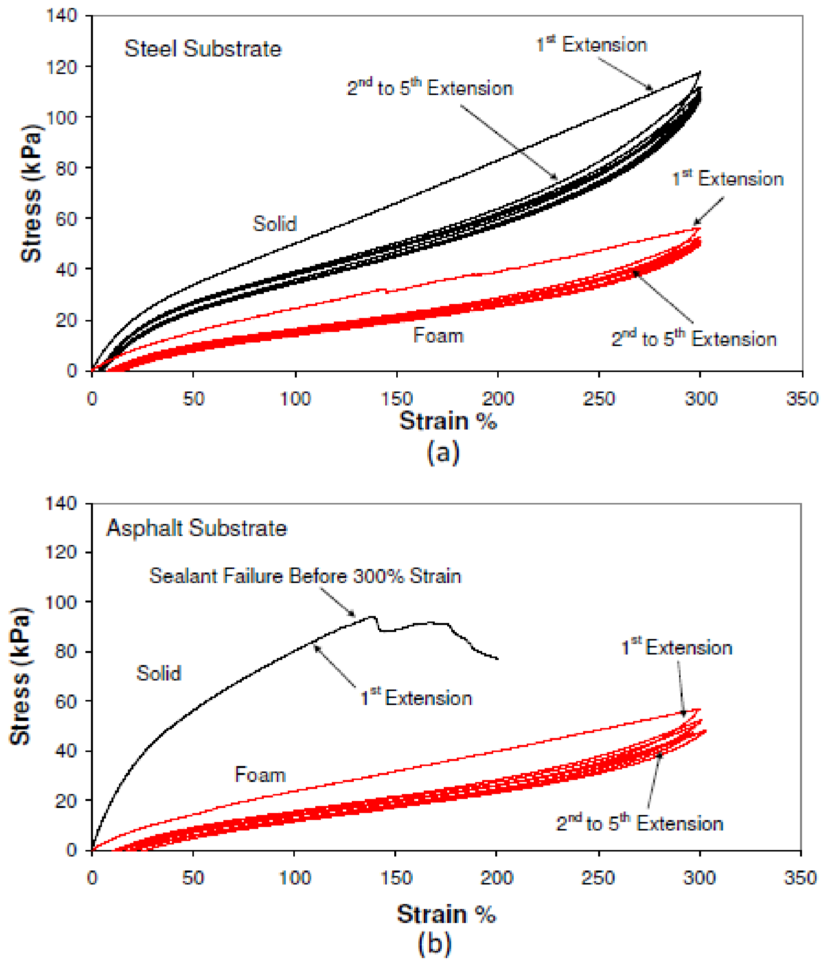

Figure 11. Representative Loading and Unloading Stress vs. Strain Curves up to 300% Strain using (a) Steel and (b) Asphalt Substrates

Because data could not be obtained for the solid sealant when bonded to asphalt the loading and unloading test was repeated. In this new tension loading/unloading test the samples were pulled to only 100% strain for five cycles. Figures 12 (a) and (b) and Table 5 display the results from this test. Figures 12 (a) and (b) display the trend lines of each sample tested. Again, since the expectation is that the substrates do not have an effect on the sealant characteristics, the entire foam and solid sealant specimens were considered ignoring the various substrates type. The average slopes, with 95% confidence limit, of the stress vs. cycle for the 8 foam test specimens and the 8 solid test specimens are -1.07 ± 0.5 and -2.56 ± 0.7, respectively. When these slopes are compared to a zero slope the t-values calculates for the foam and solid sealants are 5.37 ($p = 0.002$) and 8.77 ($p = 0.000$), respectively. Statistically, the slopes are different from a zero slope, meaning that the foam and solid sealant lose strength after each extension of 100% strain. When the foam and solid sealants are compared to each other, a two sided t-test of the average slopes yields a p-value of 0.0008 ($t = 4.23$). For the loading and unloading test to 300% strain, the p-value calculated, ignoring the differing substrates, was 0.76, indicating that the slopes of foam vs. solid were not statistically different. In the test to 100% strain, however, because the p-value is less than 0.05 the average slopes of stress vs. cycle for foam vs. solid are statistically different. The solid sealant, when loaded and unloaded to 100% strain, displays a greater loss of stress from the first to fifth extension compared to the foam sealant, as indicated by the larger, negative average slope of stress vs. cycle.

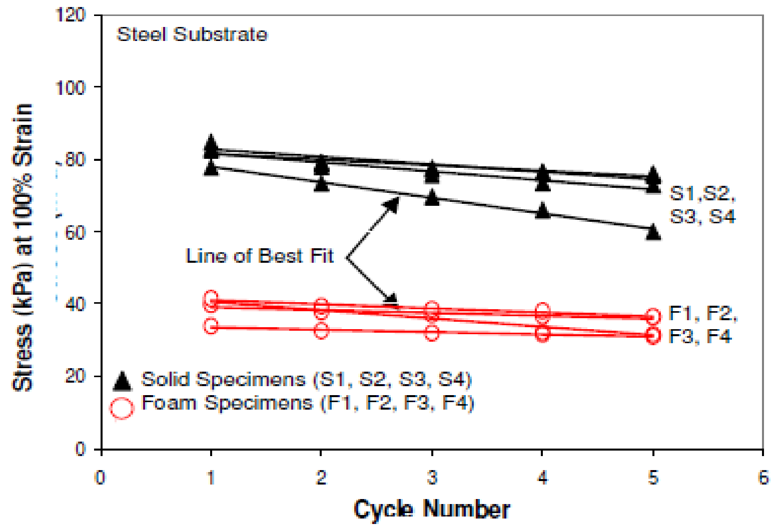

(a)

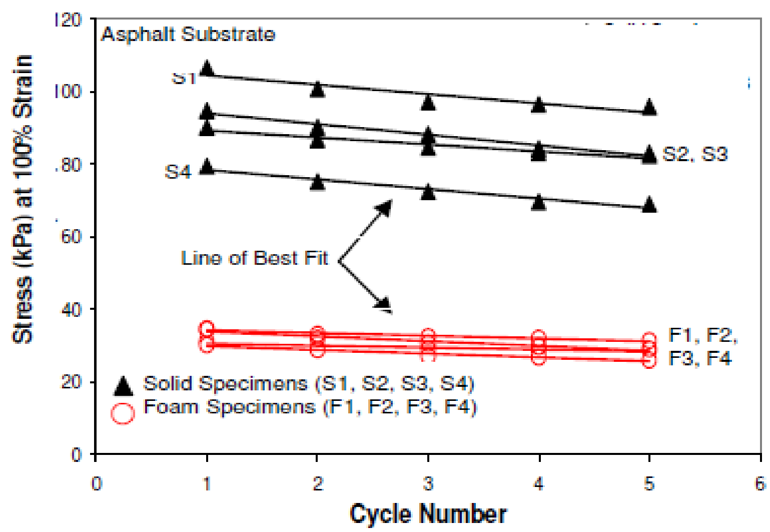

(b)

Figure 12. Loading/Unloading Tension Test – Stress at 100% Strain vs. Cycle Number – using (a) Steel and (b) Asphalt Substrates

Table 5. Loading/Unloading Tension Test – Average [a] Stress (kPa) at 100% Strain – Steel and Asphalt Substrates

Sealant Type	Sample	1st Extension	2nd Extension	3rd Extension	4th Extension	5th Extension
	Steel Substrate					
Foam	F1	31.1	29.5	29.1	28.9	28.7
	F2	34.5	33.2	32.5	32.0	31.4
	F3	30.2	28.8	27.1	26.8	26.0
	F4	34.6	32.0	30.7	29.8	29.1
	Average	32.6 ± 4 [b] (SD [c] = 2.3)	30.9 ± 3 (SD = 2.1)	29.9 ± 4 (SD = 2.3)	29.4 ± 3 (SD = 2.2)	28.8 ± 4 (SD = 2.2)
Solid	S1	79.5	75.2	72.5	69.7	69.0
	S2	94.8	90.3	88.3	84.3	83.1
	S3	106.6	100.8	97.2	96.5	95.9
	S4	90.3	86.8	84.7	83.2	82.5
	Average	92.8 ± 18 (SD = 11.2)	88.3 ± 17 (SD = 10.6)	85.7 ± 16 (SD = 10.2)	83.4 ± 17 (SD = 11.0)	82.6 ± 17 (SD = 11.0)
	Asphalt Substrate					
Foam	F1	40.0	38.4	37.7	32.2	31.6
	F2	39.8	37.9	37.1	36.7	36.4
	F3	41.5	39.4	38.5	38.1	36.5
	F4	33.9	32.6	32.0	31.6	31.1
	Average	38.8 ± 5 (SD = 3.4)	37.1 ± 5 (SD = 3.0)	36.6 ± 5 (SD = 2.9)	36.3 ± 5 (SD = 2.9)	33.9 ± 5 (SD = 3.0)
Solid	S1	77.8	73.4	69.6	66.1	60.0
	S2	84.8	79.0	77.3	76.3	75.7
	S3	82.6	79.2	77.5	76.6	76.1
	S4	83.1	78.1	75.8	73.6	72.9
	Average	82.1 ± 5 (SD = 3.0)	77.4 ± 4 (SD = 2.7)	75.2 ± 6 (SD = 3.8)	73.2 ± 8 (SD = 4.9)	71.2 ± 12 (SD = 7.6)

[a] Average of the 4 test samples
[b] 95% confidence interval for the averages
[c] SE = Standard error of the mean

There is a difference in the amount of stress lost between the first and second extension, depending on which substrate is used. As noted before, this could be due to a breaking in of the bonding interface. The slopes should be evaluated based on which substrate is used. When the differing substrates are considered, the average slopes, with 95% confidence limit, of stress vs. cycle for the foam sealant when bonded to steel and asphalt were -0.9 ± 0.5 and -1.2 ± 1.2, respectively. The average slopes, with 95 % confidence limit, for the solid sealant bonded to steel and asphalt were -2.5 ± 0.7 and -2.6 ± 1.9, respectively. As with the results from the tension loading/unloading test that extended the samples to 300% strain, the slopes from the loading and unloading to 100% strain were compared with a zero slope to determine if the differences are significant. The t-values calculated for the foam sealant bonded to steel and asphalt were 5.32 ($p = 0.013$) and 3.4 ($p = 0.042$), respectively. The t-values calculated for the solid sealant bonded to steel and asphalt were 11.7 ($p = 0.001$) and 4.4 ($p = 0.022$), respectively. These results imply that the loss in stress observed after 5 extensions of loading and unloading by the foam and solid sealant bonded to asphalt and steel is statistically significant (critical t values are 2.92 for 2 degree of freedoms and 2.35 for 3 degree of freedoms at $p = 0.10$). Even when they are elongated to just 100% strain, stress softening is observed in both the foam and solid sealants. The general trends of the stress softening observed are displayed in a representative graph shown in Figures 13 (a) and (b).

As with the test to 300% strain, a two sided t-test was conducted to compare the average slopes of stress vs. cycle for the foam sealant to that of the solid sealant. When the differing substrates are considered the foam vs. solid sealant comparison of the average stress vs. cycle slopes yields a p-values of 0.001 ($t = 5.9$) and 0.095 ($t = 2.0$) when bonded to steel and asphalt substrates, respectively. From the statistical analysis of the data collected, it can be determined that the average slopes of stress vs. cycle for the foam and solid sealants tested were statistically different from each other when bonded to steel as the p-values calculated from the t-test was greater than 0.05. On the other hand, the average slopes of stress vs. cycle for the foam and solid sealants do not differ, statistically. It can be determined, based on the given data, that the loss of stress displayed by both sealants followed different linear trends when bonded to steel. The solid sealant was observed to have a larger, negative trend from the first to fifth extension, indicating a greater loss of stress compared to the foam sealant. On the other hand, when bonded to asphalt, the foam and solid sealants display statistically similar negative trends.

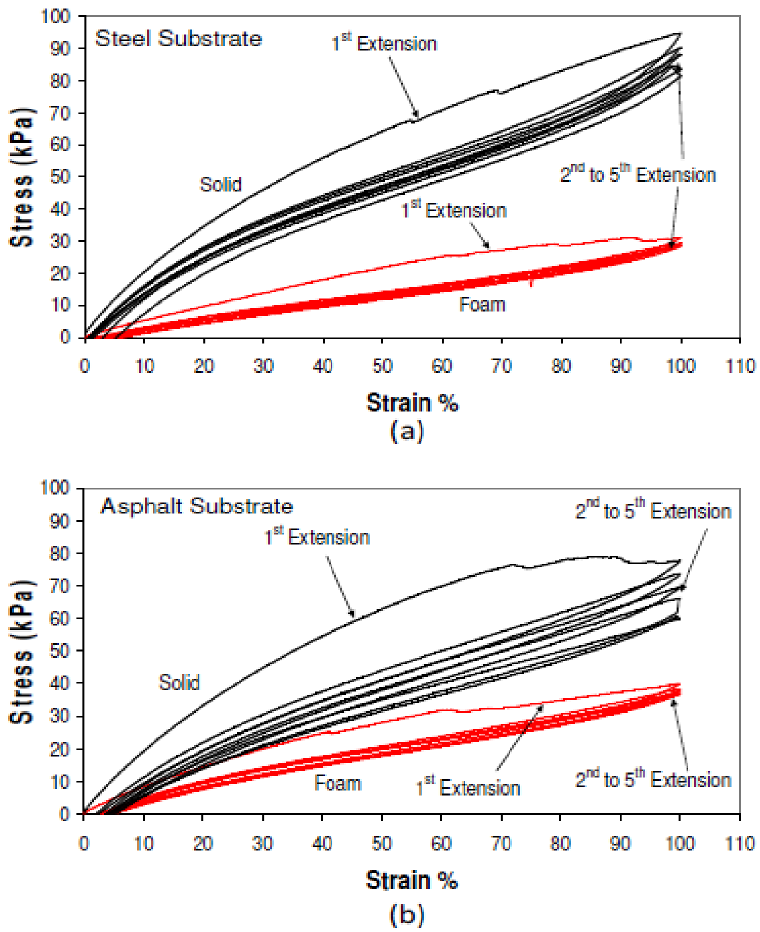

Figure 13. Representative Loading and Unloading Stress vs. Strain Curves up to 100% strain using (a) Steel and (b) Asphalt Substrates

3.2 Repair/Retrofit Test Results

The ultimate stresses of the sealants prior to failure are presented in Table 6. As expected, the solid sealant, either bonded to old (previously used) foam or old solid, exhibited a higher average ultimate strength compared to the foam sealant bonded to aged (old) foam or solid. The foam sealant bonded to older foam sealant performed the best with an average ultimate strain, with 95% confidence limit, of 433.6% ± 85. The results from a t-test show that the average ultimate strain of new foam/old foam test samples are not statistically different from new solid/old foam ($p = 0.14$, $t = 1.76$) or new foam/old solid ($p = 0.06$, $t = 2.34$). However, when the average ultimate strain from new foam/old foam test samples were compared to those of new solid/old solid, the t-test resulted in a p-value of 0.0006 and a t-value of 6.54. Since the p-value is significantly less than 0.05, it implies that there is a statistical difference in the average ultimate strain between new foam added to old foam and new solid added to old solid. Specimens with new foam added to old foam were observed to have a greater average ultimate strain compared to the specimens with new solid added to old solid.

The failure modes of the repaired test units were visually observed and are given in Table 6. For this particular test, adhesive failure is failure of the sealant at the repair interface between new sealant and old sealant. Cohesive failure is failure within the new sealant. For the new foam sealant, failure occurred cohesively (internal failure) for 3 out of the 4 test units when applied to old foam (the 4th one failed adhesively) and 2 out of 4 specimens when applied to old solid (one test unit failed adhesively and one displayed a mixed failure mode). Solid sealant when bonded to old foam failed adhesively for 2 out 3 samples (the 3rd one had a mixed failure). New solid bonded to old solid failed adhesively for all 4 test samples.

Table 6. Repair/Retrofit Test - Ultimate Stress (kPa) and Ultimate Strain

Sample	New Foam To Old Foam			New Wabo To Old Foam		
	Ultimate Stress (kPa)	Ultimate Strain (%)	Failure Mode	Ultimate Stress (kPa)	Ultimate Strain (%)	Failure Mode
1	60.2	418.4	Adhesive	121.7	329.0	Mixed
2	80.1	512.3	Cohesive	110.6	375.5	Adhesive
3	62.2	409.4	Cohesive	126.5	403.7	Adhesive
4	91.2	394.1	Cohesive			
Average [b]	73.4 ± 24 [b] (SE [c] = 7.4)	433.6 ± 85 (SE = 26.7)		119.6 ± 20 (SE = 4.1)	369.4 ± 94 (SE = 21.8)	
Sample	New Foam To Old Wabo			New Wabo To Old Wabo		
	Ultimate Stress (kPa)	Ultimate Strain (%)	Failure Mode	Ultimate Stress (kPa)	Ultimate Strain (%)	Failure Mode
1	61.9	375.6	Adhesive	114.5	208.5	Adhesive
2	48.2	291.0	Cohesive	66.5	125.9	Adhesive
3	60.3	278.0	Mixed	88.1	131.8	Adhesive
4	70.5	405.1	Cohesive	132.5	242.2	Adhesive
Average [b]	60.2 ± 15 (SE = 4.6)	337.4 ± 99 (SE = 31.3)		100.4 ± 46 (SE = 14.5)	177.1 ± 91 (SE = 28.7)	

[a] 95% Confidence Interval for the Averages
[b] Average of the Samples

The results from the repair test indicate that the foam sealant can be safely used to repair itself in the event that the old sealant has been damaged. The challenge in this test was determining whether or not the sealants failed at the interface with the old, cured sealants. For future repair tests, the old sealant needs to clearly marked prior to the addition of new sealant. When the pull to fail test is performed it will be clearer as to whether or not failure occurred at the sealant interface.

3.3 Oven-Aged Bond Test Results

The average 100% modulus (stress at 100% strain) values for each specimen after the 5th extension to 100% strain for the oven-aged bond test are shown in Figures 14 (a, b, c). The vertical bars indicate the standard error of the mean of 100% modulus values. There is a higher standard error for the solid sealant than that for the foam sealant.

Table 7 shows the variances in modulus of foam as well as solid sealants for each of the 5 loading cycles/extensions for each substrate (steel, asphalt, and polymer concrete). An f test analyzing the equality of these variances in modulus of foam vs. solid sealant when the data were pooled together for the 5 cycles for each sealant type yields f values of 37.6 ($p = <0.0001$), 2.601 ($p = 0.0369$), and 4.675 (0.0038) for sealants bonded to steel, asphalt, and polymer concrete, respectively. If the probability is taken to be 0.05 for all 3 cases, the f values come to be 37.6 ($f_{critical} = 2.403$), 2.601 ($f_{critical} = 2.403$), and 7.0244 ($f_{critical} = 2.544$) for sealants bonded to steel, asphalt, and polymer concrete respectively. When the variances for each sealant type (foam or solid) are pooled together for all 3 substrates and for all 5 cycles, the f test yields an f value of 6.85 ($p = <0.0001$, $f_{critical} = 1.66$).

Each of these calculated f values are greater than the critical f values. Therefore, the variances in the modulus of the test specimens using the solid sealant are significantly different from those using the foam sealant. The variances in the modulus values of the solid sealant are judged to be higher than those of the foam sealant. It is quite evident from the observations that the solid was exhibiting more scatter in its secant modulus than the foam. The analysis using the f statistic supports this conclusion for all substrates. Thus, the higher scatter appears to be a characteristic of the solid sealant. The reason for this is not clear; in fact, with its more complex formulation, the foam might be expected to exhibit higher stiffness variability. While stiffness variability is not in itself a problem, it could lead to a corresponding variability in performance.

The standard error of the mean of the 100% modulus for the foam sealant decreases after each consecutive extension to 100% strain. Combining data for all substrates, the foam sealant, was observed to have lost, on average, 21.5 % in the average 100% modulus from the first to fifth extension. Likewise, the solid sealant displayed an average loss of 18.3% in average value of 100% modulus between the first and fifth extension. When steel, asphalt, and polymer concrete are used, a Student's t-test comparison of the percent loss of stress from the first to fifth extension for the foam versus the solid sealant yields a p-value of 0.18 ($t = 1.4$). Therefore, statistically, the percent loss in strength from the first to fifth extension for the foam sealant could not be distinguished from that of the solid sealant.

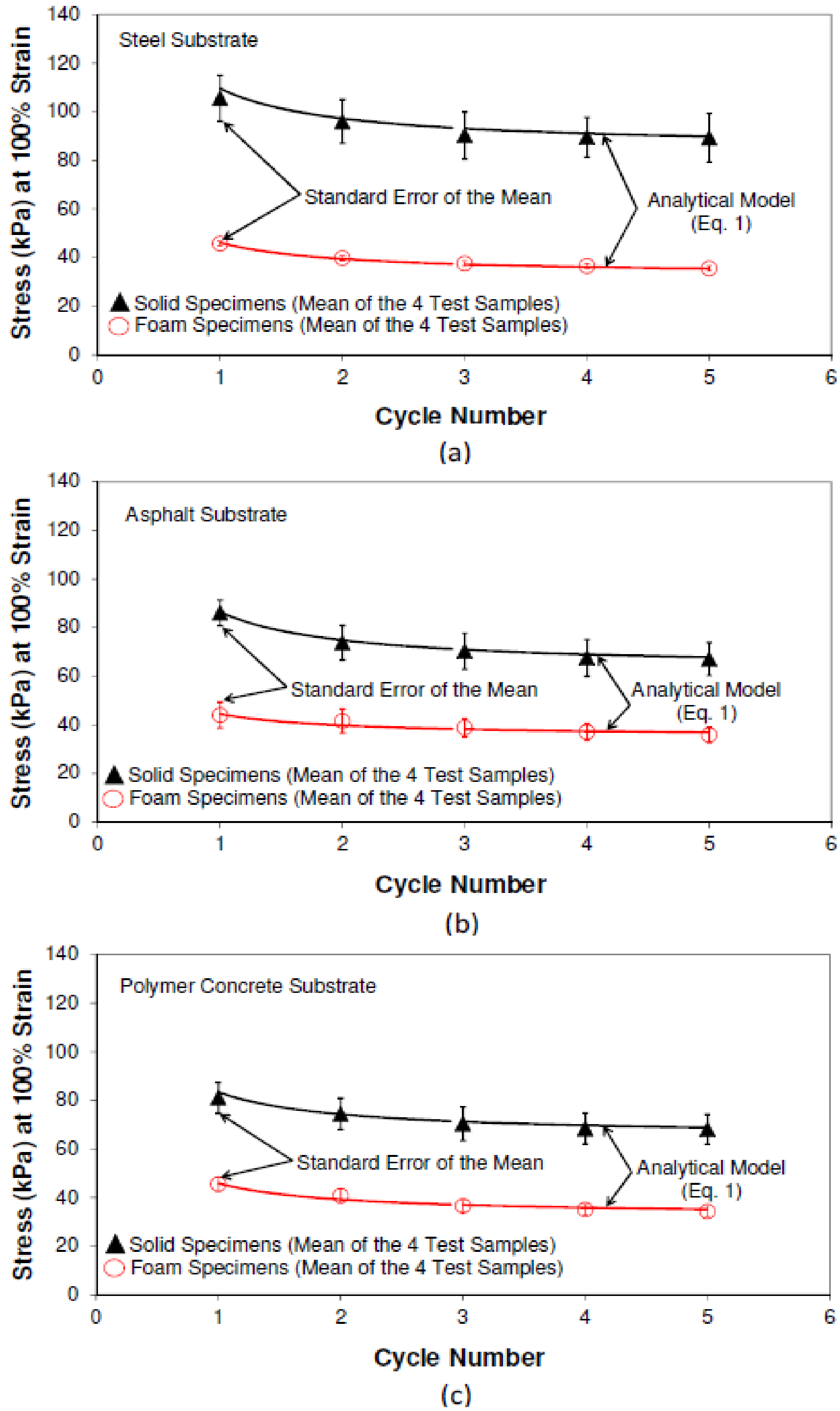

Figure 14. Oven Aged Bond Test - 100% Modulus with Cycle Number using (a) Steel, (b) Asphalt, and (c) Polymer Concrete Substrates with Standard Error Bars

Table 7. Variances of Modulus (in kPa^2) of the Sealant Samples for Oven-Aged Bond Test

Sealant Type	1st Extension	2nd Extension	3rd Extension	4th Extension	5th Extension
	Steel Substrate				
Foam	15.6 [a]	24.9	1.7	1.7	1.7
Solid	355	320.7	374.9	265.7	398.3
	Asphalt Substrate				
Foam	116.7	97.7	57.6	48.0	38.9
Solid	112.7	200.9	214.9	225.7	179.3
	Polymer Concrete Substrate				
Foam	13.3	9.3	19.0	13.0	9.3
Solid	108.0	80.3	80.3	37.0	69.3

[a] Variance of the 4 observations

The following empirical equation has been used to develop a curve-fit model displaying the trend of the 100% modulus versus cycle number for the foam and solid sealant:

$$E(n) = \mathrm{E}_{\infty}\left[1+\left(\frac{\alpha}{n}\right)\right] \tag{3.1}$$

In this equation *E(n)* is the 100% modulus at a specific cycle of loading n, E_{∞} is the modulus after an infinite number of cycles, n is the cycle number, and α is the decay parameter. This decay parameter is the number of cycles for E to reach a value of 2 E_{∞}. The trend of the decaying 100% modulus after each extension is displayed in Figures 14 (a, b, and c). By conducting a nonlinear regression analysis using commercially available software, Polymath (Polymath 2010) values for α and E_{∞} have been computed. These values are presented in Table 8.

Table 8. Decay Parameter and Modulus at Infinite Number of Cycles for Oven-Aged Bond Test

Substrate	**Sealant**	**Sample**	**Decay Parameter, α, (Number of Cycles)**	**Modulus at Infinite Number of Cycles, E_∞, kPa**
Steel	Foam	F1	0.44	34.6
		F2	0.50	33.1
		F3	0.33	32.7
		F4	0.25	32.5
		Average	0.41 ± 0.09 [a]	32.7 ± 1.3
	Solid	S1	0.22	103.7
		S2	0.23	94.6
		S3	0.17	77.6
		S4	0.41	62.8
		Average	0.26 ± 0.09	84.9 ± 3.8
Asphalt	Foam	F1	0.41	42.6
		F2	0.31	34.7
		F3	0.17	33.6
		F4	0.18	28.9
		Average	0.27 ± 0.21	35.0 ± 3.5
	Solid	S1	0.18	85.6
		S2	0.51	56.0
		S3	0.36	52.5
		S4	0.41	53.6
		Average	0.37 ± 0.05	63.1 ± 1.3
Polymer Concrete	Foam	F1	0.36	38.5
		F2	0.59	31.3
		F3	0.40	29.8
		F4	0.44	28.1
		Average	0.41 ± 0.15	32.5 ± 2.2
	Solid	F1	0.20	78.2
		F2	0.40	57.8
		F3	0.20	58.5
		Average	0.28 ± 0.08	65.1 ± 2.4
[a] 95% Confidence Interval for the Averages				

As expected, the solid sealant was observed to have a greater modulus at infinite time than the foam sealant. With the exception of the test units using asphalt substrates, the foam sealant bonded to steel and polymer concrete appears to achieve 2 E_∞ at a slower rate than that of the solid sealant. The solid sealant was observed to have decayed quicker than the foam sealant. This observation is the opposite when the test specimens using asphalt are considered. In this case the solid sealant achieves 2 E_∞ at a slower rate than that of the foam sealant.

When the data from the test samples using steel, asphalt, and polymer concrete are pooled together, a comparison of foam vs. solid for α yielded a p-value of 0.40 (t = 0.9). This result implies that the decay parameters for the foam and solid sealants are not statistically different. However, there is an indication that the decay parameters for the foam and solid sealant when bonded to steel and polymer concrete are different from that of the test units using asphalt. A comparison of the α values for foam vs. solid bonded to steel and polymer concrete together yields a p-value of 0.01 (t = 2.9), suggesting that the decay parameter for solid and foam are different. Asphalt was not considered in this analysis because the decay parameter for the foam is less than that of the solid, which is the opposite of what was observed with the steel and polymer concrete substrates. As a matter of fact, decay parameters for foam vs. solid when bonded to asphalt are not statistically different as their comparison results in a p-value of 0.18 (t = 1.5). It is conceivable that during the 7 days when the samples were placed at 70 °C, components of the asphalt could creep into the foam and solid sealants, slightly changing the characteristics of the sealants. However, further investigation needs to be conducted as there is no direct evidence for this possible reaction of the sealants when placed in an oven while bonded to asphalt.

3.4 Salt Water Immersion Test Results

The results from the salt-water immersion test are shown in Figures 15 (a & b) and Table 9. When bonded to asphalt, 3 out of 4 foam test units failed cohesively (1 test specimen had mixed failure), whereas all 4 solid sealant test sampled failed adhesively, i.e. failed at sealant-substrate interface. When bonded to steel, 3 out of 4 foam test units failed cohesively (1 test specimen had mixed failure) whereas all 4 solid sealant test specimens failed adhesively.

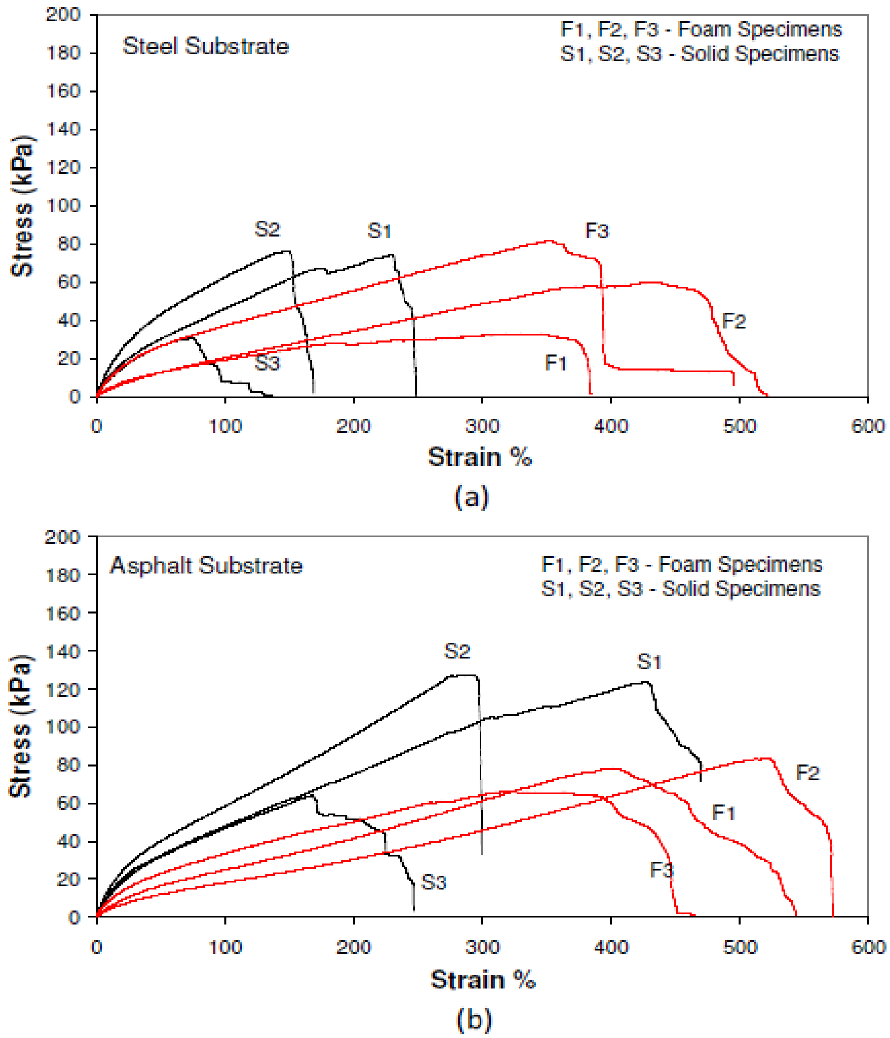

Figure 15. Salt Water Immersion Test - Pull to Failure using (a) Steel and (b) Asphalt Substrates

As presented in the Tension Test section, results from the tension pull-to-fail tests on the dry specimens, cured and tested at room temperature, show that both the foam and the solid sealants have better bonding capabilities to the steel substrate than to the asphalt substrate. However, this is not the case with the salt water immersion test case. An unpaired t-test was conducted to determine whether or not the differences in average ultimate strain between the dry and immersed specimens were statistically different. The comparison of dry vs. immersed for foam applied to steel and asphalt resulted in p-values of 0.02 ($t = 3.30$) and 0.37 ($t = 0.99$), respectively. The comparison of dry vs. immersed for solid sealant applied to steel and asphalt resulted in p-values of 0.002 ($t = 5.71$) and 0.25 ($t = 1.3$), respectively. The p-values for the foam and solid sealants bonded to steel are less than 0.05. This indicates that statistically, the average ultimate strains for the immersed sealants, both foam and solid, were different from that of dry sealants when bonded to steel. This implies that the immersion of the sealants in salt water was observed to have a deleterious effect on both the foam and solid sealant bonded to steel, but not asphalt.

Table 9. Salt Water Immersion Test - Dry vs. Immersed Sealants using Asphalt and Steel Substrates

Sealant Type	Sealant Condition	Sample	Asphalt Substrate: Average [a] Ultimate Stress (kPa)	Asphalt Substrate: Average Ultimate Strain (%)	Asphalt Substrate: Failure Modes	Steel Substrate: Average Ultimate Stress (kPa)	Steel Substrate: Average Ultimate Strain (%)	Steel Substrate: Failure Modes
Foam	Dry	F1	84.3	347.8	Cohesive	71.2	534.8	Mixed
		F2	73.9	323.8	Cohesive	72.4	424.4	Cohesive
		F3	91.5	499.4	Cohesive	74.4	522.3	Mixed
		F4	52.2	261.3	Cohesive	72.0	502.0	Cohesive
		Average	75.5 ± 27 [b] (SE [c] = 8.6)	358.0 ± 161 (SE = 50.5)		72.5 ± 2 (SE = 0.68)	495.9 ± 79 (SE = 24.8)	
	Immersed	S1	78	403	Cohesive	33	334	Cohesive
		S2	83	520	Cohesive	60	427	Mixed
		S3	65	363	Cohesive	82	354	Cohesive
		S4	-	-	-	-	-	-
		Average	75.3 ± 23 (SE = 4.7)	428.7 ± 202 (SE = 40.8)		58.3 ± 61 (SE = 12.3)	371.7 ± 122 (SE = 24.5)	
Solid	Dry	F1	100.7	190.4	Adhesive	199.3	428.5	Cohesive
		F2	118.5	242.3	Adhesive	195.9	411.7	Cohesive
		F3	118.1	227.6	Adhesive	221.3	413.3	Adhesive
		F4	85.9	164.2	Adhesive	174.6	344.7	Cohesive
		Average	105.8 ± 25 (SE = 7.8)	206.1 ± 56 (SE = 17.8)		197.8 ± 30 (SE = 9.6)	399.6 ± 59 (SE = 18.7)	
	Immersed	S1	123	428	Adhesive	74	229	Adhesive
		S2	127	282	Adhesive	76	148	Adhesive
		S3	64	168	Adhesive	82	73	Adhesive
		S4	-	-		-	-	
		Average	104.7 ± 88 (SE = 17.7)	292.7 ± 324 (SE = 65.2)		77.3 ± 10 (SE = 2.1)	150.0 ± 194 (SE = 39.0)	

[a] Average of the 4 Test Samples
[b] 95% Confidence Interval for the Averages
[c] SE = Standard error of the mean

The salt water appears to affect the solid sealant's ability to bond to steel. As stated in previous paragraph, each of the solid sealant test units bonded to steel failed at the interface after immersion. However, the dry solid sealant test specimens bonded to steel failed cohesively for 3 out of the 4 test units that were evaluated. Upon close inspection the steel accumulated rust on the outer portion of the steel up to the bonding surface, an expected result when immersed in salt water. Very little, if any, rusting was seen on the bonding substrate for the test specimens that displayed adhesive failure. While no rust was present on the sealant-substrate bonding interface surface, the rust along the edge of the surface may have caused the solid sealant to separate at the corners of the steel pieces. Because steel has a high surface-energy and silicone has a very low surface energy, it is possible that these differences encouraged water to seep into the bonding interface between the substrate and the sealant. This could negatively affect the bonding of the solid to the steel. It was observed that in tensile pull-to-fail tests with the solid sealant, any slight imperfection on the bonding area of the substrate or the sealant resulted in a quick failure.

3.5 Modulus over Time Test Results

The results for the modulus over time test using asphalt and steel as substrates are displayed in Figures 16 (a) and (b) and Table 10. The vertical bars in the figures are the standard errors of the mean of 100% modulus values. The trend that the modulus takes in Figures 16 (a) and (b) can be described using the equation below:

$$E(t) = E_{\infty} \frac{\beta t}{1+\beta t} \tag{3.2}$$

$E(t)$ is the modulus at a specific time, β is the cure-rate parameter (reciprocal of the time to get to 0.5 E_{∞}), E_{∞} is the modulus at infinite time, and t is the curing time in days. Equation (3.2) can be derived using sealant material kinetics in terms of rate of silanol concentration change with time (Fogler 1992). This is displayed, below:

$$-\frac{d[\text{SiOH}]}{dt} = \frac{d(N/2)}{dt} = k_2[\text{SiOH}]^2 \tag{3.3}$$

where [SiOH] is the silanol concentration (mol/L), k_2 is the second-order rate constant (L/mol s), N is the concentration of network chains (mol/L), and t is time.

The above equation takes into account the following assumptions:

1. Two silanols react irreversibly to form a new network chain, $2SiOH \rightarrow SiOSi + H_2O$, where [SiOSi] is the siloxane bond concentration (mol/L) (Stevens 1999).
2. Each network chain is elastically active and contributes to the modulus
3. Silanol reaction is rate limiting, and there are no side reactions.
4. Ideal rubber elasticity (Shaw 2005), e.g.,

$$E = 3NRT \tag{3.4}$$

where E is Young's modulus, R is the gas constant (8.315 Pa m^3 /mol), and T is temperature

Using Equation (3.3) along with the above assumptions will create the curve fit equation for the modulus over time test. Solving Equation (3.3) gives the following relation:

$$[\mathrm{SiOH}] = \frac{[\mathrm{SiOH}]_0}{1 + k_2[\mathrm{SiOH}]_0 t} \tag{3.5}$$

Here, $[\mathrm{SiOH}]_0$ is the original silanol concentration. Using Equation (3.5), a relation for N can be established.

$$N = [\mathrm{SiOSi}] = \{[\mathrm{SiOH}]_0 - [\mathrm{SiOH}]\}/2 = [\mathrm{SiOH}]_0\left[1 - \frac{1}{1 + [\mathrm{SiOH}]_0 k_2 t}\right]/2 \tag{3.6}$$

Equation (3.4) given in assumption 4 allows the following equation to be derived:

$$E(t) = \frac{3}{2} RT[\mathrm{SiOH}]_0\left[\frac{[\mathrm{SiOH}]_0 k_2 t}{1 + [\mathrm{SiOH}]_0 k_2 t}\right] \tag{3.7}$$

Equation (3.7) is of the form:

$$E(t) = E_\infty \frac{\beta t}{1+\beta t} \tag{3.8}$$

Where:

$$\beta = [\mathrm{SiOH}]_0 k_2 \tag{3.9}$$

$$E_\infty = \frac{3}{2} RT[\mathrm{SiOH}]_0 \tag{3.10}$$

E_∞ represents the modulus at infinite time and α is the rate parameter. The parameters β and E_∞ can be calculated through nonlinear regression and the least squares method. Once these parameters are calculated, *E(t)* can be determined at each time, *t*.

The values for β and E_∞ for each sealant bonded to asphalt and steel are shown in Table 11. Superficially, the foam, when bonded to both steel and asphalt, is observed to have a lower modulus and a slower cure rate (lower value of β) compared to the solid sealant. Comparing foam versus solid statistically, the t-test gives a p-value for the β and E_∞ values of 0.15 (t = -2.2) and 0.002 (t = 24), respectively. As expected, the statistical analysis also shows that the solid sealant has a greater modulus at infinite time (E_∞) than the foam sealant (p = 0.002). While there is an indication that the solid sealant cures faster than the foam, based on the statistical analysis of the available data, the cure-rate parameter of the solid could not be distinguished from that of the foam sealant (p = 0.15). From the point of view of application, the foam and solid sealants, for each of the substrates (steel and asphalt) considered, were observed to obtain 60 to 63% of their average 3-week strength within the first 3 days of curing. As the foam has a more complex reaction involving diffusion of water and gas, the expectation is that the cure of the foam will be slower than that of the solid sealant. However, there are also some mitigating factors such as the better insulating properties of the foam. This factor keeps the material warmer and, thus, reacting faster.

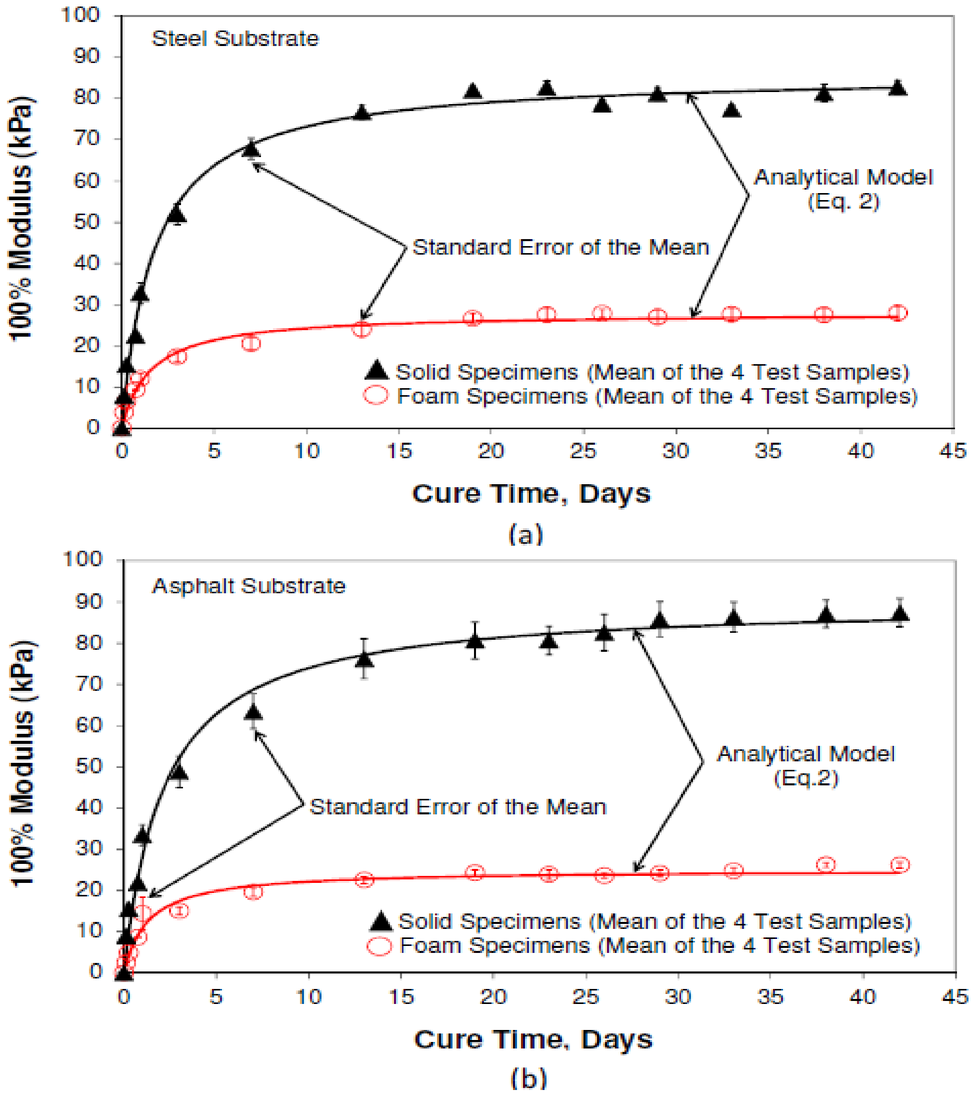

Figure 16. Modulus over Time Test Results using (a) Steel and (b) Asphalt Substrates with Standard Error Bars

Table 10. Modulus over Time Test Results

Substrate	Curing Hours	Foam Sealant Stress(kPa) At 100% Strain	Solid Sealant Stress(kPa) At 100% Strain	Curing Hours (Days)	Foam Sealant Stress(kPa) At 100% Strain	Solid Sealant Stress(kPa) At 100% Strain	Curing Hours (Days)	Foam Sealant Stress(kPa) At 100% Strain	Sealant Stress(kPa) At 100% Strain
Steel	3	3.8 ± 3 [a]	7.9 ± 3	72 (3)	17.4 ± 4	51.9 ± 8	624 (26)	27.9 ± 3	78.6 ± 4
	6	6.5 ± 2	15.4 ± 2	168 (7)	20.5 ± 5	67.8 ± 8	696 (29)	27.0 ± 6	81.1 ± 5
	18	9.3 ± 4	22.4 ± 9	336 (14)	24.0 ± 6	76.7 ± 6	792 (33)	27.6 ± 5	77.3 ± 3
	24	12 ± 4	32.7 ± 8	456 (19)	26.6 ± 4	81.9 ± 3	912 (38)	27.5 ± 5	81.3 ± 7
				552 (23)	27.6 ± 5	82.6 ± 5	1008 (42)	28.0 ± 5	82.1 ± 4
Asphalt	3	2.37 ± 0.4 [b]	9.0 ± 13 [b]	72 (3)	15.0 ± 3	48.7 ± 12	624 (26)	23.6 ± 2	82.5 ± 14
	6	4.33 ± 2	15.5 ± 4	168 (7)	19.6 ± 3	63.5 ± 13	696 (29)	24.1 ± 3	85.8 ± 14
	18	8.6 ± 4	21.8 ± 7	336 (14)	22.5 ± 3	76.2 ± 15	792 (33)	27.3 ± 7	86.3 ± 12
	24	14.4 ± 13	33.7 ± 8	456 (19)	24.3 ± 3	80.6 ± 14	912 (38)	26.2 ± 2	87.1 ± 11
				552 (23)	23.9 ± 4	80.6 ± 11	1008 (42)	26.2 ± 2	87.3 ± 11

[a] Average of the 4 Test Samples
[b] 95% Confidence Interval for the Averages

Table 11. Rate Parameter and Modulus at Infinite Time for Curve Fitting Modulus over Time

Substrate	**Sealant**	**Rate parameter, 1/day, (β)**	**Ultimate Modulus, E_∞, kPa**
Asphalt	Foam	0.77 ± 0.28 [a]	25 ± 1.5
	Solid	0.46 ± 0.11	90 ± 3.7
Steel	Foam	0.64 ± 0.09	28 ± 1.3
	Solid	0.57 ± 0.12	86 ± 2.8

[a] 95% confidence interval based on the data and model. As the data are a time series, this interval will generally be smaller than that derived from independent repetitions.

3.6 Freeze-Thaw Test Results

The samples for the freeze – thaw test, when adding together the total amount of time submersed in water and frozen, were cured for 10 days. To compare the results of this test a control set of samples were made using concrete substrates; four samples using the foam sealant and four using the solid sealant. These samples were allowed to cure for 10 days at room temperature without exposing them to water submersion or freezing conditions. After the 10 days the samples were pulled to failure. Table 12 shows the ultimate stress, ultimate strain, stress at 100% strain, and failure modes for the control samples. The results from this test were compared to the freeze – thaw test results seen in Tables 13 and 14. The graphs for all the results are displayed in Figures 17, 18 (a-c), 19 (a-c), and 20 (a-c).

For both the control samples and the freeze thaw test samples the foam exhibits a lower ultimate strength than the solid sealant, but it elongates farther prior to failure. As discussed in the Tension Test, Pull-to-Fail Results section, the lower strength of the foam results in less stress applied at the bonding substrate, generally resulting in cohesive failure of the sealant. The same is seen with the 10 day cured control test samples. The foam sealant fails cohesively, while the solid sealant, as it applies much more stress to the bonding interface, fails adhesively.

For all three types of freeze thaw tests (submersed-freeze, submersed-freeze-thaw, and submersed) the solid sealant tends to fail by separating from the bonding substrate, while the foam sealant fails internally, with a rare exception where the failure is a mixture of adhesive and cohesive. The submersion in water within the first 3 hours of curing, based on the test results, does not affect the bonding of the foam sealant to the concrete bonding substrate.

From the data there is no visible trend that displays a clear difference between the differing initial curing times prior to water submersion. To compare the results from each test performed (submersed-freeze, submersed-freeze-thaw, and submersed), the test data were not grouped by initial curing time prior to submersion, but only by the type of sealant used (solid or foam). An unpaired t test was conducted to compare the ultimate stress and strain values for each treatment with the corresponding control test results.

Comparing the ultimate stresses for the foam sealant against the control, the t values for the submersed-freeze, submersed-freeze-thaw, and submersed tests were 0.10 ($p = 0.92$), 0.56 ($p = 0.58$), and 1.27 ($p = 0.22$), respectively (the results for 1, 2, and 3 hours of curing time were pooled together). These values are less than the critical t value of 1.76, which is based on 14 degrees of freedom and 95% confidence. This suggests that the observed differences between the foam samples of all three freeze thaw tests and the control foam samples were not significant. For the solid sealant the t values were 2.28 ($p = 0.04$), 3.13 ($p = 0.01$), and 1.28 ($p = 0.22$), respectively. Based on a comparison to the critical t value of 1.76, there is a likely difference between the solid sealant results in the submersed-freeze and control test as well as the submersed-freeze-thaw and control tests. On the other hand, the differences observed between the submersed and control tests were not statistically significant. Based on the data available, it appears that placing the solid sealant in −20˚C (−4˚F) temperature after submersion in water has a negative effect on the sealant's ultimate strength.

For the ultimate strain, the t values for the submersed-freeze, submersed-freeze-thaw, and submersed tests were 0.08 ($p = 0.94$), 0.39 ($p = 0.7$), and 0.47 ($p = 0.65$), respectively, for the foam sealant and 1.3 ($p = 0.21$), 1.9 ($p = 0.07$), and 0.02 ($p = 0.99$), respectively, for the solid sealant. The results show that only the solid sealant samples for only the submersed-freeze-thaw test were statistically different from the solid control samples (t value greater than critical t value of 1.76). However, further laboratory testing may be necessary to confirm this conclusion because the calculated t value is just slightly greater than the critical t value.

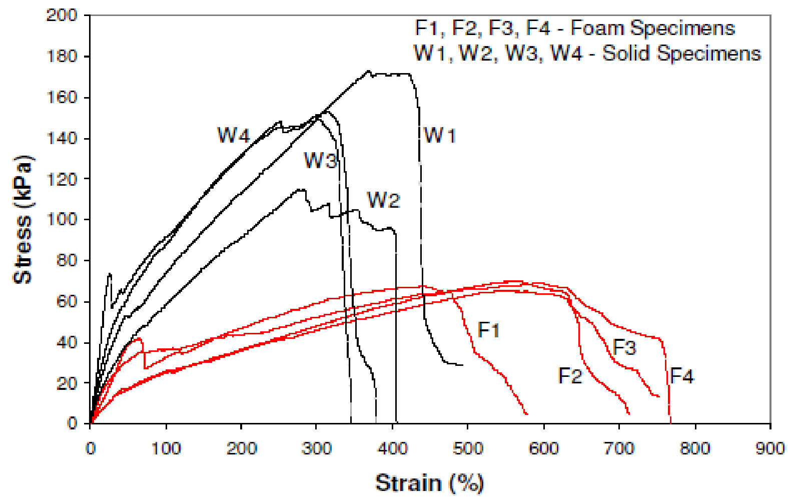

Figure 17. Ultimate Tensile Stress-Strain of Control Samples (10 Day Curing, Concrete Substrate)

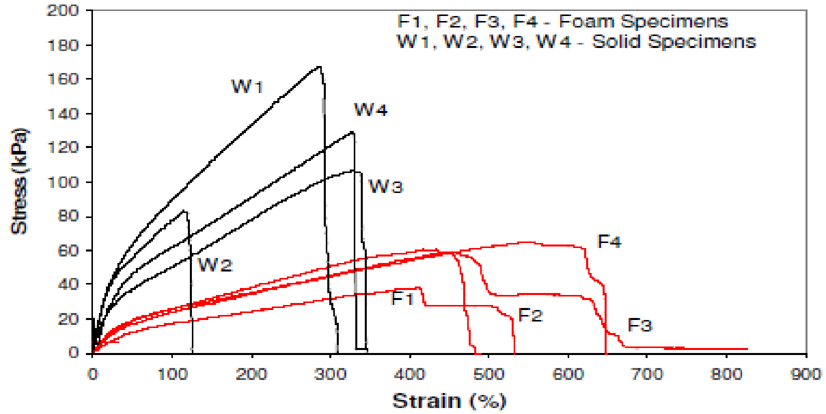

(a)

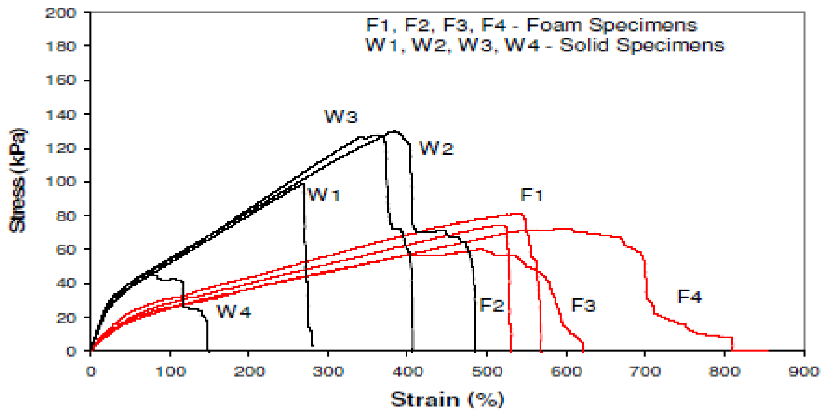

(b)

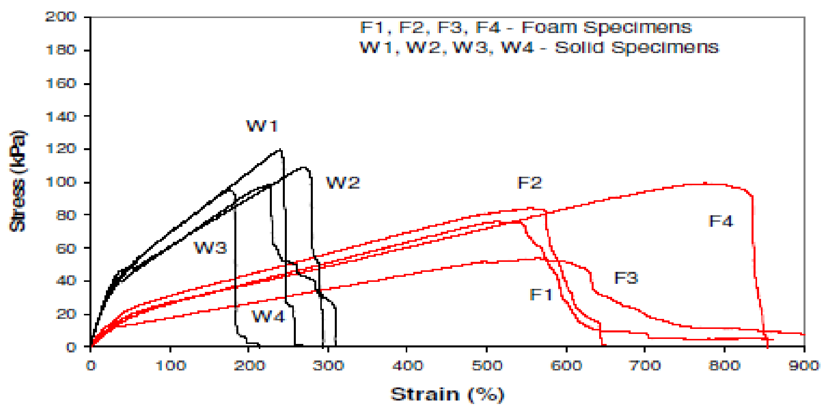

(c)

Figure 18. Ultimate Tensile Stress-Strain Results from Submersed - Freeze Test for (a) 1 Hour of Curing Prior to Submersion, (b) 2 Hours of Curing Prior to Submersion, and (c) 3 Hours of Curing Prior to Submersion (Concrete Substrate)

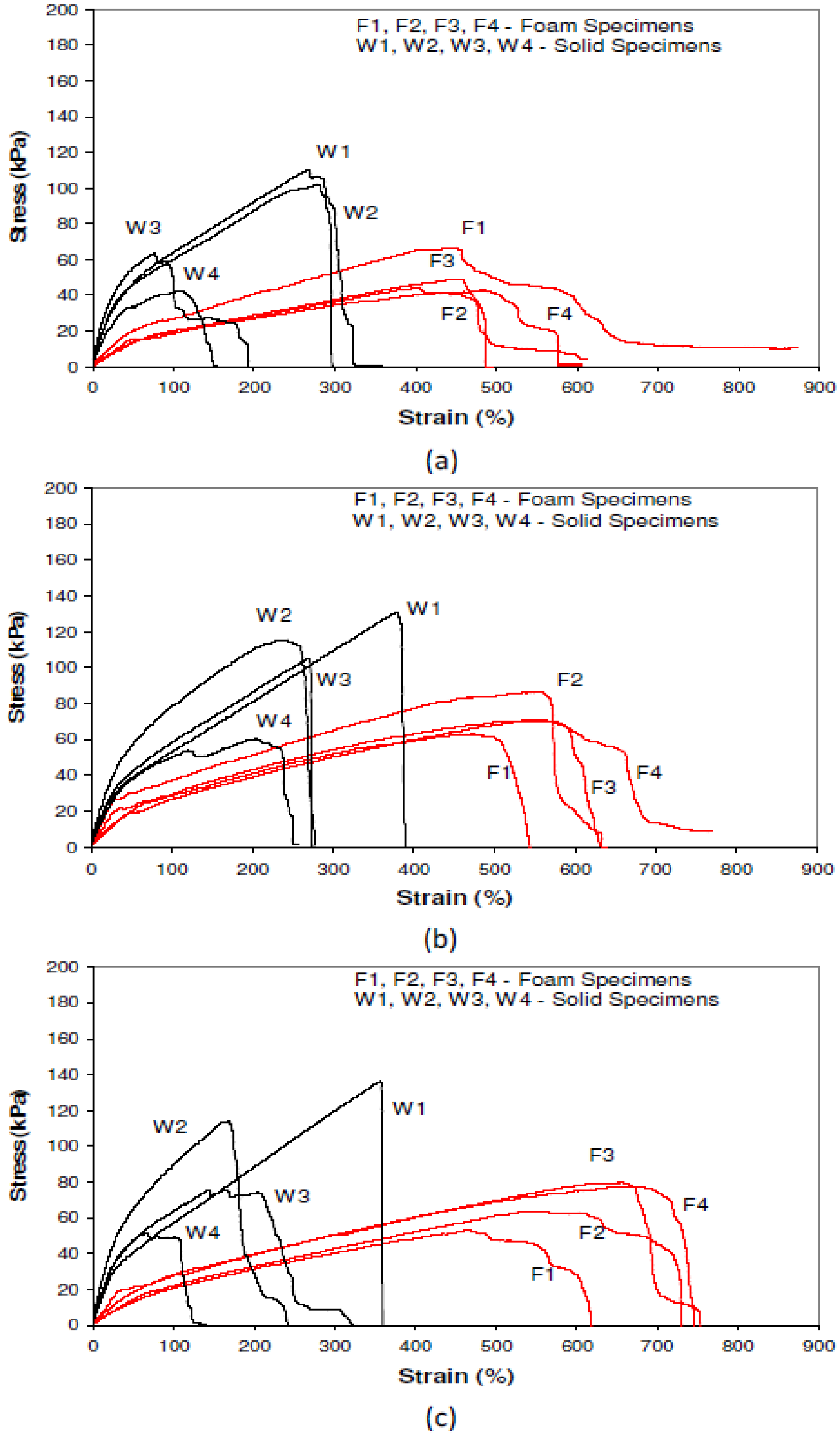

Figure 19. Ultimate Tensile Stress-Strain Results from Submersed – Freeze - Thaw Test for (a) 1 Hour of Curing Prior to Submersion, (b) 2 Hours of Curing Prior to Submersion, and (c) 3 Hours of Curing Prior to Submersion (Concrete Substrate)

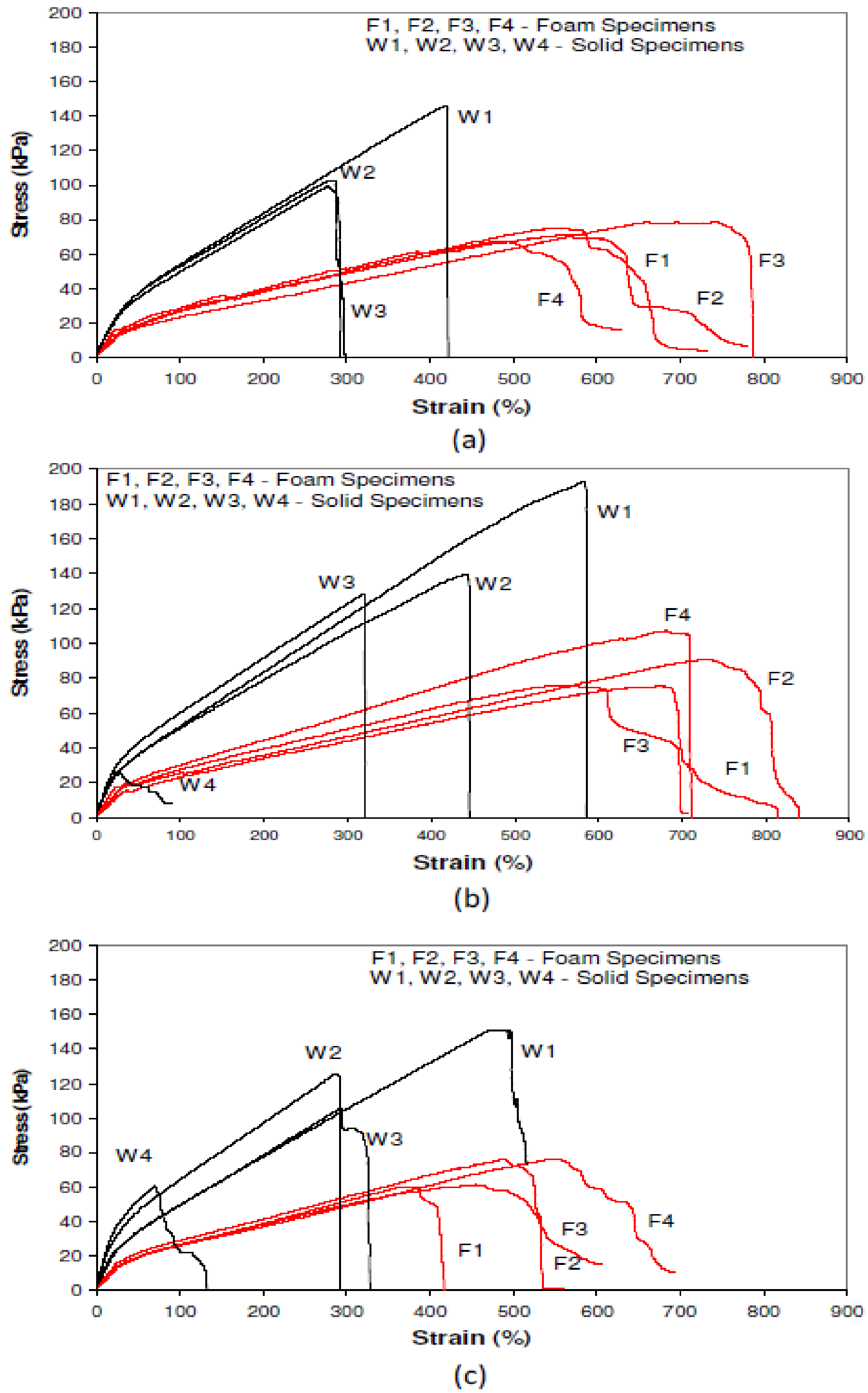

Figure 20. Ultimate Tensile Stress-Strain Results from Submersed Test for (a) 1 Hour of Curing Prior to Submersion, (b) 2 Hours of Prior to Submersion, and (c) 3 Hours of Curing Prior to Submersion (Concrete Substrate)

Table 12. Ultimate Tensile Stress-Strain Results of Control Samples (10 Day Curing, Concrete Substrate)

Sealant Type	Average [a] Ultimate Stress (kPa)	Average Ultimate Strain (%)	Failure Modes
Foam	67.9 ± 3 [b] (SD [c] 1.9)	536.9 ± 102 (SD 64.7)	4 Cohesive
Solid	147.1 ± 38 (SD 24.0)	316.7 ± 58 (SD 36.4)	3 Adhesive 1 Cohesive

[a] Average of the 4 Test Samples
[b] 95% Confidence Interval for the Averages
[c] Standard Deviation

Table 13. Ultimate Tensile Stress-Strain Results for the Freeze – Thaw Test using Concrete Substrates

Curing Time (Hours) Prior to Submersion	Sealant Type	Submersed Freeze		Submersed Freeze Thaw		Submersed	
		Average [a] Ultimate Stress (kPa)	Average Ultimate Strain %	Average Ultimate Stress (kPa)	Average Ultimate Strain %	Average Ultimate Stress (kPa)	Average Ultimate Strain %
1	Foam	55.7 ± 19 [b] (SD [c] 11.9)	460.7 ± 91 (SD 57.4)	50.6 ± 17 (SD 11.0)	447.4 ± 54 (SD 33.7)	73.0 ± 8 (SD 5.1)	567.0 ± 112 (SD 70.3)
	Solid	99.1 ± 38 (SD 23.6)	245.8 ± 164 (SD 103.3)	79.5 ± 51 (SD 31.8)	181.4 ± 167 (SD 105.1)	115.9 ± 64 (SD 25.9)	327.6 ± 198 (SD 79.5)
2	Foam	72.1 ± 14 (SD 9.0)	537.4 ± 76 (SD 47.5)	72.6 ± 16 (SD 9.8)	530.9 ± 61 (SD 38.2)	87.5 ± 24 (SD 15.0)	660.8 ± 114 (SD 71.6)
	Solid	100.6 ± 63 (SD 39.6)	245.8 ± 164 (SD 103.3)	101.5 ± 53 (SD 33.1)	270.6 ± 124 (SD 77.9)	121.9 ± 111 (SD 69.7)	342.2 ± 378 (SD 237.3)
3	Foam	78.8 ± 32 (SD 19.8)	601.8 ± 188 (SD 118.1)	68.2 ± 20 (SD 12.5)	580.1 ± 146 (SD 91.4)	68.3 ± 14 (SD 8.8)	463.9 ± 121 (SD 75.9)
	Solid	105.3 ± 17 (SD 10.5)	227.6 ± 63 (SD 39.9)	94.3 ± 60 (SD 37.8)	188.2 ± 196 (SD 123.2)	110.5 ± 61 (SD 38.2)	286.0 ± 274 (SD 172.4)

[a] Average of the 4 Test Samples
[b] 95% Confidence Interval for the Averages
[c] Standard Deviation

Table 14. Freeze – Thaw Tension Test Failure Modes

Curing Time (Hours) Prior to Submersion	Sealant Type	Submersed Freeze	Submersed Freeze Thaw	Submersed
1	Foam	1 Cohesive 3 Adhesive	3 Cohesive 1 Mix	3 Cohesive 1 Mix
	Solid	1 Cohesive 3 Adhesive	4 Adhesive	4 Adhesive
2	Foam	1 Cohesive 2 Adhesive 1 Mix	4 Cohesive	4 Cohesive
	Solid	4 Adhesive	4 Adhesive	4 Adhesive
3	Foam	3 Cohesive 1 Mix	4 Cohesive	3 Cohesive 1 Adhesive
	Solid	4 Adhesive	4 Adhesive	4 Adhesive

3.7 Ponding Test Results

After observing the foam sealant for 7 days it could be determined that water had not leaked through to the underside of the sealant. For the foam sealant cured for 1 hour prior to ponding the drop in water depth was 0.45, 0.3, 0.15, and 0.1 inches. It should be noted that the sample that lost 0.45 inches in water depth was slightly damaged prior to ponding. There was a small gap between the sealant and the bonding surface. For the first day water slightly dripped to the underside of the sealant. After the first day this leaking stopped as the sealant cured. Of the 3 samples this was the only one that displayed leaking of water. For the foam sealant cured for 2 hours prior to ponding the drop in water depth was 0.55, 0.3, 0.3, and 0.25 inches. None of the samples displayed any leakage of water. While the sealant, based on this test, seemed to me impervious to leakage, the depth of the water did drop, albeit slightly, over the course of 7 days. This can be attributed to a combination of evaporation and the foam soaking up some of the water. It should be noted that the stopper supporting the sealant was left in throughout the duration of the test. This stopper did not deter any potential leaking of water as the plug was not sealed in any way to the inner wall of the plastic cylinder. The sealant did not exhibit any signs of deformation, perhaps because the stopper (plug) was helping to support the sealant.

3.8 Cure Rate Test Results

The results for the cure rate test are displayed in Table 15. This table displays the 100 % modulus for each sample tested. It was expected that the 100% modulus value would increase when the cure time is increased, which was depicted in the modulus over time test. Unfortunately, the data gathered does not show a clear trend as the cure time is increased. This could be due, in large part, to the fact that all the samples were not made on the same day. Due to limitations in resources, many samples were made at different parts of the year. It is recommended that for any possible repetition of this test that all the samples should be made on the same day to ensure that they cure under the same conditions.

Table 15. Modulus (Stress at 100% Strain) for Cure Rate Test

Substrate	Sealant Type	Sample	3 Days	7 Days	10 Days	14 Days
Steel	Foam	F1	12.3	19.5	18.9	14.7
		F2	11.3	19.1	20.7	14.9
		F3	13.6	24.5	18.1	15.0
		F4	12.5	-	17.4	20.0
		Average	12.4 ± 1 [b] (SE [c] = 0.41)	21.0 ± 3 (SE = 1.4)	18.8 ± 1 [b] (SE [c] = 0.6)	16.2 ± 2 [b] (SE [c] = 1.1)
	Solid	S1	41.2	62.6	75.5	29.2
		S2	44.6	64.5	71.6	28.4
		S3	91.0	53.9	56.9	36.2
		S4	57.4	-	55.8	60.8
		Average	58.6 ± 19 (SE = 9.8)	60.3 ± 5 (SE = 2.7)	65.0 ± 9 (SE = 4.4)	38.7 ± 13 (SE = 9.6)

Table 15. Modulus (Stress at 100% Strain) for Cure Rate Test (Continued)

Substrate	Sealant Type	Sample	3 Days	7 Days	10 Days	14 Days
Asphalt	Foam	F1	7.6	15.8	20.4	16.4
		F2	9.5	20.5	16.5	10.9
		F3	10.1	16.8	18.8	8.6
		F4	10.0	15.7	31.6	13.9
		Average	9.3 ± 1 [b] (SE [c] = 0.5)	17.2 ± 2 (SE = 1.0)	21.8 ± 7 (SE = 2.9)	12.5 ± 3 (SE = 1.5)
	Solid	S1	54.1	72.0	54.4	28.5
		S2	28.4	68.5	100.4	36.5
		S3	50.4	67.9	76.8	45.2
		S4	-	-	-	59.2
		Average	44.3 ± 13 (SE = 6.5)	69.5 ± 2 (SE = 1.0)	77.2 ± 21 (SE = 10.8)	42.4 ± 11 (SE = 5.7)
Substrate	**Sealant Type**	**Sample**	**21 Days**	**28 Days**	**35 Days**	**42 Days**
Steel	Foam	F1	31.1	28.7	20.1	25.0
		F2	27.6	28.0	15.3	20.6
		F3	27.8	22.5	16.4	20.6
		F4	21.2	30.5	-	-
		Average	26.9 ± 4 [b] (SE [c] = 1.8)	27.4 ± 3 (SE [c] = 1.5)	17.3 ± 2 (SE [c] = 0.68)	22.1 ± 2 (SE [c] = 1.2)
	Solid	S1	80.7	77.0	60.9	48.1
		S2	80.9	77.2	46.0	14.7
		S3	95.4	93.3	43.7	3.7
		S4	104.6	85.0		-
		Average	90.4 ± 10 (SE = 5.1)	83.1 ± 7 (SE = 3.4)	50.2 ± 9 (SE = 4.4)	22.2 ± 21 (SE = 10.9)
Asphalt	Foam	F1	25.6	23.9	21.7	19.1
		F2	26.1	19.6	25.0	17.3
		F3	29.1	16.2	46.0	18.7
		F4	35.1	16.4	-	-
		Average	29.0 ± 4 (SE = 1.9)	19.0 ± 3 (SE = 1.6)	30.9 ± 12 (SE = 6.2)	18.4 ± 1 (SE = 0.4)
	Solid	S1	60.8	60.7	46.1	66.3
		S2	61.2	60.8	56.2	67.9
		S3	71.2	49.9	-	48.5
		S4	72.0	-	-	-
		Average	66.3 ± 5 (SE = 2.7)	57.1 ± 6 (SE = 3.0)	51.2 ± 7 (SE = 3.6)	60.9 ± 10 (SE = 5.1)

[a] Average of the 4 test samples
[b] 95% Confidence interval for the averages
[c] SE = Standard error of the mean

4.0 APPLICATION PROCEDURE FOR SEALANT

While the laboratory tests were conducted, an application procedure for field installation of the silicone foam was developed. This process involved 4 major steps: mixing and preparing a large batch of silicone foam, determining the proper tools to pour the sealant, developing a step-by-step application procedure, and rehearsal of the sealing process prior to field installation.

The first challenge in the process to develop an application procedure was mixing together the necessary materials and preparing large quantities of the silicone foam sealant. Prior to developing an application procedure, only small volumes of sealant were created to make the laboratory test specimens. For a real world application, however, larger quantities of the foam sealant needed to be mixed. The specifications to mix the sealant for the laboratory tests, shown in Table 16 under “Mass of Material for Laboratory Sample,” were used to help determine the amount of sealant needed to fill an expansion joint. Conversions were made to show each material’s percent volume. When mixing large amounts of the sealant it is much easier to measure based on volume than by mass, which was used to measure the materials to make the small laboratory samples. Table 16 shows the mass and density of each material needed to calculate the percent volume.

Table 16. Conversion of Material Mass to Percent Volume

Materials	Specific Gravity	Density (g/cm^3)	Mass of Material for Laboratory Sample (g)	Volume (cm^3)	Percent Volume (%)
WABO White	1.08	1.08	3.5	3.24	54.43
WABO Black	1.45	1.45	3.5	2.41	40.54
Crosslinker	0.98	0.98	0.1615	0.16	2.77
Water	1.0	1.0	0.107	0.11	1.80
Platinum Catalyst	0.98	0.98	0.027	0.03	0.46

Using these percentages the volumes for each material can be measured given the desired amount of joint volume that needs to be filled. For example, a joint with a length of 12 feet, depth of 0.75 in, and an opening of 2 in has a volume of 3539.61 mL. Considering that the sealant, conservatively, increases in volume by 50%, the amount of sealant used to seal the joint is 2359.74 mL. Using this amount, the breakdown of the material volumes as shown in Table 17 can be used.

Table 17. Volume of Each Sealant Material to fill 12' Joint Length

Materials	Material Volume (mL)
WABO White	1284.4
WABO Black	956.7
Crosslinker	65.3
Water	42.4
Platinum Catalyst	10.9

The next step was to test the effectiveness of these materials when mixed in such large volumes. To do this a simulated expansion joint was setup in the laboratory. This setup, displayed in Figure 21, consisted of two, 7 foot long steel I-beams set 2 inches apart from each other. This gap was used as the "joint." A closed cell backer rod was placed in the joint 1 inch below the surface to stop the sealant from flowing underneath the beams.

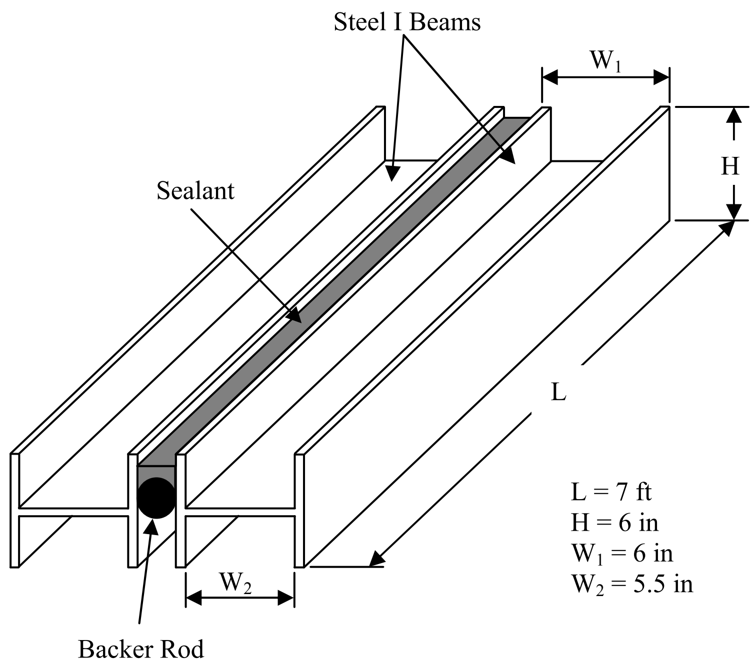

Figure 21. Schematic of Simulated Expansion Joint

With a simulated joint in place, mixing and pouring of a large volume of sealant could commence. The materials were gathered to accommodate a 7 foot joint length, mixed in a container, and finally poured into the joint. Figure 22 (a-d), below, shows the pouring of the foam sealant into the simulated expansion joint, the foaming of the sealant, and dry sample of the poured material that was allowed to cure for 1 day. The pictures in this figure show that the higher volumes of materials, in comparison to those used to make the small laboratory samples, does not change the process of foaming.

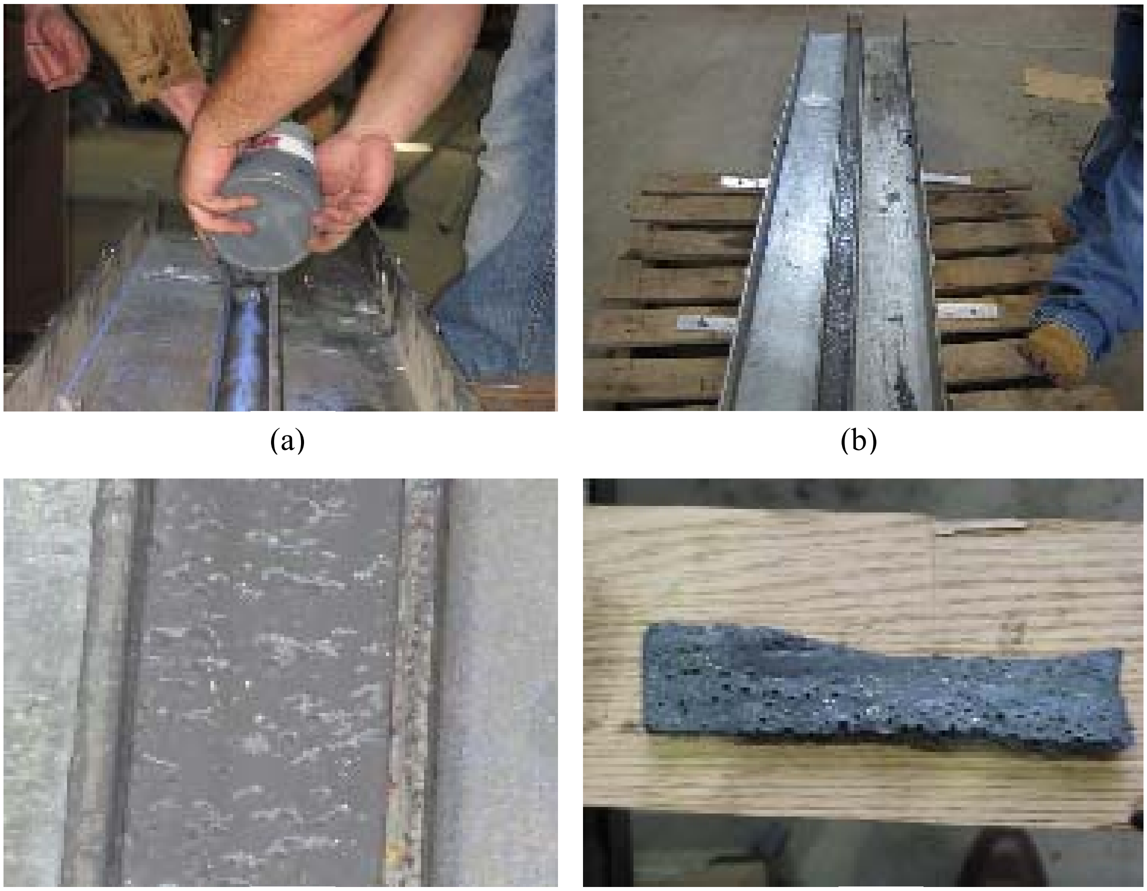

(a) (b)

(c) (d)

Figure 22. (a) Pouring of the Foam in Simulated Expansion Joint, (b) Sealed Joint, (c) Foaming of Sealant, and (d) Foam Material Specimen

The next step was the development of a procedure to apply the foam sealant into a bridge expansion joint. This involved developing an applicator tool, a list of items that could help in the sealing process, and a detailed procedure mapping out each essential step (i.e. what order to mix the materials). The challenge behind determining the best course of action to applying the sealant was making sure it is installed in the expansion joint in a very small amount of time. While the tack free time of the foam sealant in the laboratory setting was measured to be approximately 80 minutes, the sealant, still, needs to be applied within a matter of a couple minutes. The reason for this is because the sealant will begin to gel, limiting its ability to flow freely from the applicator tool. Therefore, time is the most crucial factor that could slow the sealing process.

Many different types of applicator tools were considered. The first tool that was looked at was the applicator gun used by Watson Bowman Acme Co. to apply their two part silicone sealant (the “solid” sealant). This is a pressurized gun that houses the two separate WABO cartridges. Using air pressure from an external source, two plungers press the two parts in a mixing spiral which, then, dispenses the mixed solid sealant into the expansion joint. While this would be an effective tool, the problem is that 5 separate materials are needed to make the foam sealant. Pre-mixing the materials into two containers could be an option. The crosslinker can be mixed with the WABO white because the white already contains some hydrosilane. The water cannot be mixed with the white because it will react with the hydrosilane. However, the water, along with the platinum, can be mixed with the WABO black. Unfortunately, there are a few issues that develop with this option. The WABO white and black come in sealed cartridges. Once the container holding the WABO white is opened, the contact with the air causes the material to begin to cure. Bubbles can be seen forming within the material. At the same time, the water cannot be thoroughly mixed into the WABO black. The best option would be to mix all the materials at once, on site, and then immediately pour the mixture into the expansion joint.

The second type of applicator tool considered looked at taking a batch of sealant that was mixed in a container, pouring it into an applicator tool, and then using a pressurized plunger-like device to squeeze the sealant into the expansion joint. This type of tool would be comparable to a grease gun a type of tool that used a plunger to press the sealant out of the housing container, as seen in Figure 23 (a) and (b), below. The problem with these types of applicator tools is that a lot of time is wasted mixing the sealant in a separate container, pouring it into the applicator tool, and then finally applying it into the joint. Plus, a portion of the mixed sealant is left behind in the mixing container when it is transferred into the applicator tool. The sealant could be mixed in the applicator tool, itself, however the small confines of the container raises the possibility that the materials will not be thoroughly mixed. The sealant needs to be mixed in a large enough container.

(a) (b)

Figure 23. Sealant Applicator Options Consisting of (a) a Grease Gun and (b) a Modified Pressure Applicator

The option that was eventually chosen as was simply a mixing bucket. Instead of transferring the sealant from the mixing bucket into a tool, the sealant can be poured straight from the bucket. Within the first couple of minutes after mixing, the sealant flows very well before it begins gel. A bucket made of thin plastic will allow the user to deform the top into a thin opening to control the rate at which the sealant flows into the joint. A spatula can be used to help guide the sealant out of the bucket.

With the applicator tool established a step-by-step application procedure can be developed. The following list describes the process developed in the laboratory:

1. Obtain the necessary materials
    a. Chemicals (WABO white, WABO black, crosslinker, distilled water, and platinum catalyst
    b. Syringes to hold crosslinker, distilled water, and platinum catalyst
    c. Closed Cell Backer Rod
    d. Tool to adjust depth of backer rod
    e. Tool to level poured sealant at a specific depth
    f. Plastic mixing container
    g. Battery powered drill
    h. Mixer to attach to drill
    i. Spatula
    j. Cooler with ice
2. Pre-measure the volume of each material given the known dimensions of the expansion joint to be filled (Fig. 24 a-b).

(a)

(b)

Figure 24. (a) Measuring of the Materials and (b) Pouring of the Materials in Mixing Bucket

3. Pack all the chemicals in a cooler with ice. When the materials are mixed while cool the reaction is slowed. For every decrease of 10˚C the reaction of the chemicals when mixed together decreases by one half. This will give more time to apply the sealant before the major foaming reaction takes place. This is especially important when the application of the sealant is performed in hot temperatures.
4. On site, place the closed cell backer rod into the expansion joint. Press the backer rod down to a specific depth below the bridge surface using a tool specifically designed for this process. For this particular procedure, the top of the backer rod was placed 1 inch below the surface.
5. Pour the WABO white, WABO black, distilled water, and platinum catalyst into the plastic mixing bucket (Fig. 25). Using the drill and attached mixer thoroughly mix these four materials together. The crosslinker is left out of this step because of its high

reactivity to the water. It would be best that the water is dispersed evenly throughout the entire mixture before the crosslinker is added.

(a) (b)

Figure 25. Pouring of Materials in Mixing Bucket

6. Add the crosslinker. Mix all the materials one last time (Fig 26).

Figure 26. Mixing of the Materials

7. Pour the mixed sealant material into the expansion joint (Fig. 27).

Figure 27. Pouring of the Mixed Sealant in the Simulated Expansion Joint

8. To ensure the sealant is it the proper depth before it begins to foam, another person needs to follow behind the person applying the silicone foam with a leveling tool (Fig. 28).

Figure 28. Leveling of the Sealant to a Specific Depth Prior to Foaming

It is important to understand that the entire procedure, from start of mixing to sealant leveling, needs to take place during a reasonably short time (in the order about 10 minutes) so that the sealant installation is complete before the main foaming reaction takes place. Time is a factor as the reaction of the chemicals, when mixed together, is immediate. By controlling and shortening the reaction rate, careful attention can be made to establishing a thoroughly mixed sealant prior to application.

The next step was to practice the joint sealing procedure outside of a laboratory setting. To rehearse the sealing procedure in an exposed environment, two driveway cracks were chosen, as seen in Figure 29 (a-d). Crack 1 (Fig. 29a) was 11 feet long, 2 inches deep, and had a crack opening of 1.75 inches. Crack 2 (Fig. 29b) was 13.5 feet long, 2 inches deep, and had a crack opening of 1.5 inches. The foam sealant was successfully applied to both cracks; however with Crack 2 the decision was made to see what would happen if the platinum catalyst was excluded. The reason for not using the platinum in one of the sealant mixtures was because, as seen in Table 18 below, the platinum is the most costly item of all 5 material components needed to make the foam. Removing the platinum catalyst would dramatically decrease the price of sealing an expansion joint. Unfortunately, without the platinum the sealant does not foam properly. As a consequence, the sealant does not increase in volume as it cures. With that said, it is clear that the platinum, while the smallest component of all the materials, plays a very essential role in the foaming process of the sealant. In the end, the practicing of sealing these cracks proved to be very beneficial as this was perfect preparation for sealing an actual bridge expansion joint.

(a) (b)

(c) (d)

Figure 29. Sealing of Driveway Cracks: (a) Driveway Crack 1, (b) Driveway Crack 2, (c) Sealed Driveway Crack 1, (d) Sealed Driveway Crack 2

Table 18. Tentative Estimate of Price Breakdown of Silicone Foam Materials

Materials	Material Price Per Volume ($/mL)	Price of Each Material for 12' Lane
WABO White	0.03	$17.00
WABO Black	0.03	$12.66
Crosslinker	0.15	$4.32
Platinum Catalyst	6.35	$30.61
Water	-	-
		Total Price = $64.59

5.0 FIELD INSTALLATION OF SEALANT IN BRIDGE EXPANSION JOINTS

With the help of the NETC Project Technical Committee members, four bridges located throughout New England were chosen for field installation of the silicone foam sealant. For each joint sealed, the WABO two-part silicone sealant (termed here solid sealant) was installed next to and in the same joint as the foam for comparison purposes. The sealants were placed in such a way so as to ensure that both would experience the same amount of traffic flow. The following is a list of bridge locations and the sealing application dates [Malla, Swanson, and Shaw 2010b].

- August 17, 2009 – Connecticut Bridge spanning Route 6, west bound, in Mansfield, CT
- September 16, 2009 – New Hampshire Bridge on E. Thetford Rd. spanning the Connecticut River in Lyme, NH
- October 21 & 22, 2009 – Pascoag River Bridge on Route 102 in Burrillville, RI
- November 6, 2009 – New York Bridge on Route 22 in Dover Plains, NY

5.1 Connecticut Bridge

The candidate bridge in Connecticut (Fig. 30) was a 140 foot long bridge in Mansfield, CT spanning Route 6, west bound. The joint that was sealed was located on the south side of the bridge. It is 41 feet in length and is skewed 12˚. Figure 31 below is a schematic diagram showing the dimensions of the bridge.

Figure 30. Connecticut Bridge in Mansfield, CT

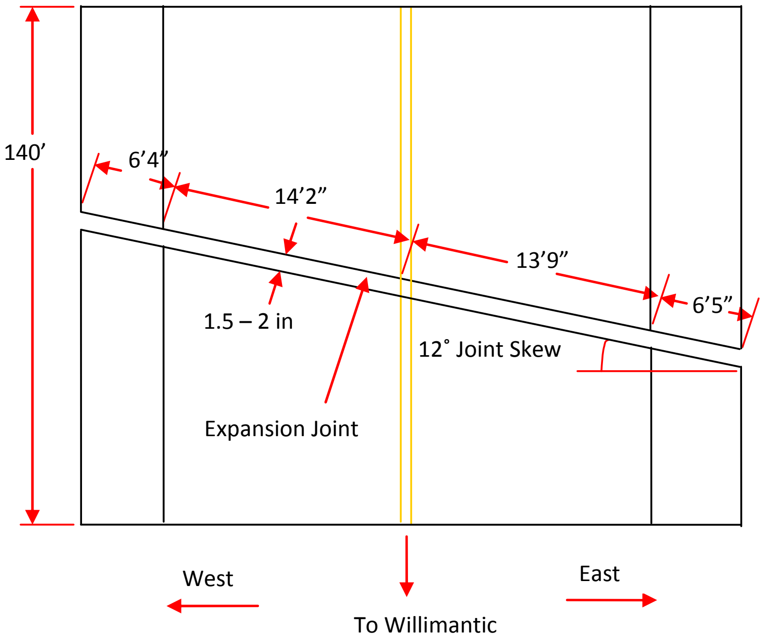

Figure 31. Dimensions of the Connecticut Bridge

As stated before, both the silicone foam and the solid sealant were used in the field application for comparison purposes. The sealants were set up in a way so as to ensure that each would experience the same traffic flow on each lane. Thus, the sealants were staggered every 10.2', as seen in Figure 32 below.

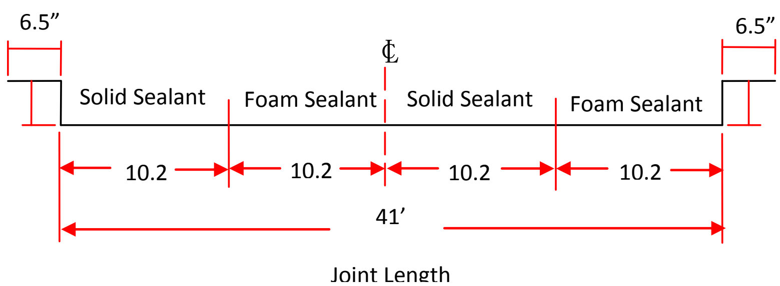

Figure 32. Schematic of the Staggering of the Foam and Solid Sealants

With the help of the Connecticut DOT directing traffic, the expansion joint was filled on August 17, 2009 starting around 11 am and ending around 2 pm. The conditions at that time consisted of an average temperature of 87˚F and an average humidity of 55%. Figure 33 displays a couple of pictures showing the bridge joint sealing application in progress using the foam and solid.

(a) (b)

Figure 33. Pouring of the Sealant into the Connecticut Bridge Expansion Joint

5.2 New Hampshire Bridge

The bridge in New Hampshire (Fig. 34) is a 471 foot bridge spanning the Connecticut River in Lyme, NH. The bridge consists of 3 expansion joints, one on the Vermont side two on the New Hampshire side. The two joints on the New Hampshire side, both 21 feet in length from curb to curb, were sealed. Figure 35 displays the dimensions of the bridge along with the locations of each type of sealant used. The sealing installation was conducted on September 16, 2009, beginning at around 8 am and ending at around 11 am. The testing environmental conditions consisted of an average temperature of 56˚F and an average humidity of 78%. Figure 36 displays a couple pictures showing the joints after the sealants have been applied.

Figure 34. New Hampshire Bridge in Lyme, NH

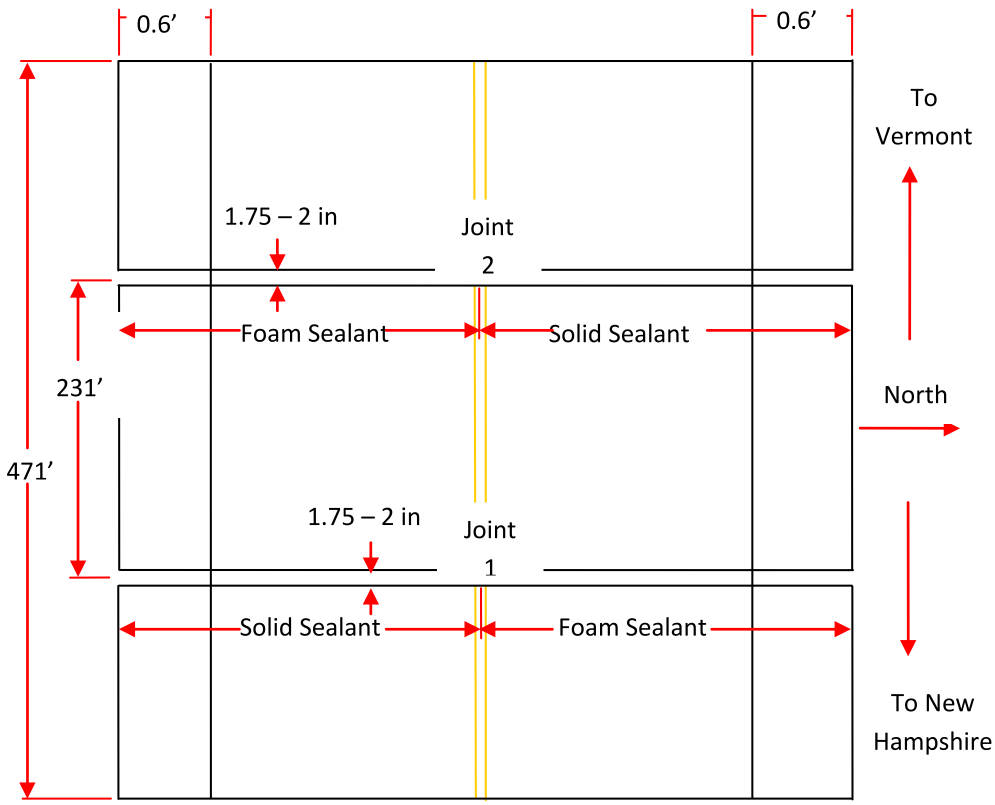

Figure 35. Dimensions of the New Hampshire Bridge

(a)

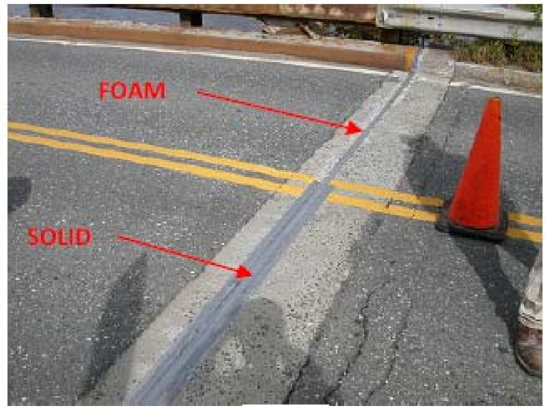

(b)

Figure 36. New Hampshire Expansion Joints after Sealant Application

5.3 Rhode Island Bridge

The Pascoag River Bridge in Burrillville, RI (Fig. 37), sealed on October 21 & 22, 2009, has an expansion joint of 56 feet in length. The southern half of the joint was sealed on October 21, beginning at about 12 pm and ending about 2 pm. The northern half of the joint was sealed on October 22, beginning at 11 am and ending at 1 am. Over the course of two days the expansion joint, with the help of the Rhode Island DOT crew, was filled. During day 1, from 12 pm to 2 pm, the average temperature was 87˚F and the average humidity was 41%. During day 2, from 11 am to 1 pm, the average temperature was 71˚F and the average humidity was 75%. Figure 38 is a schematic of the bridge, and Figure 39 displays the staggering of the sealant over the length of the joint. The staggering consists of 6 zones where the two zones on either side of the bridge are all 10 feet in length. The remaining two zones in the middle of the bridge are both 8 feet in length.

Figure 37. Rhode Island Bridge in Burrillville, RI

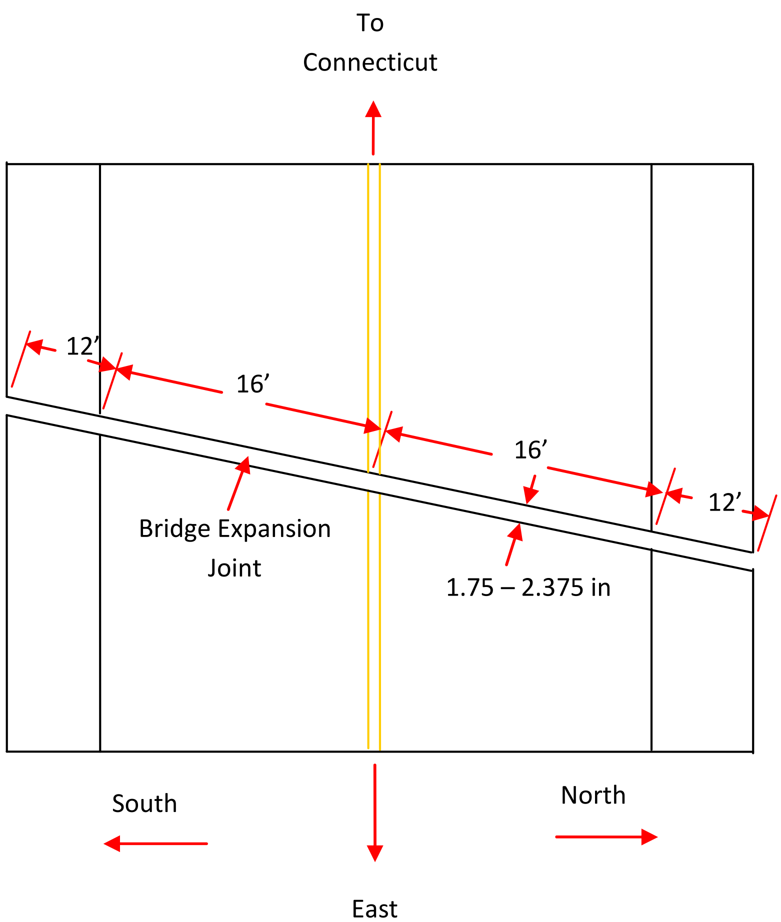

Figure 38. Dimensions of the Rhode Island Bridge

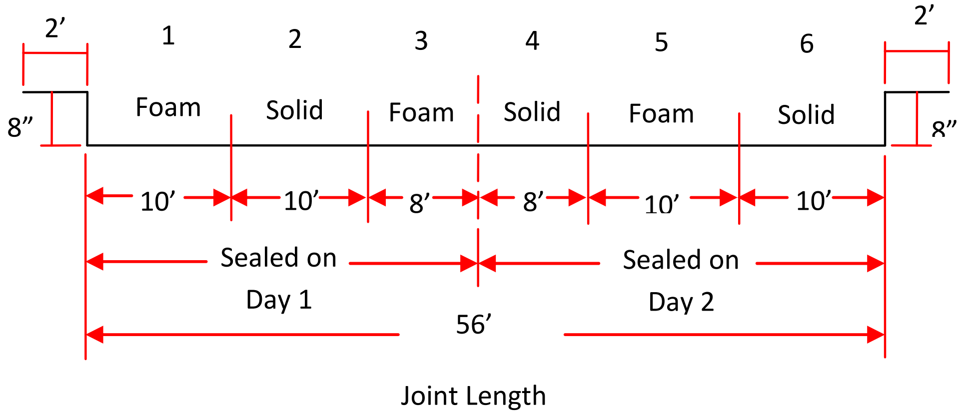

Figure 39. Schematic of the Staggering of the Foam and Solid Sealants

5.4 New York Bridge

The sealing in New York was conducted on a 207 foot long bridge on Route 22 in Dover Plains, NY (Fig. 40) on November 6, 2009. The sealing operation began about 12 pm and ended at around 3:30 pm. The expansion joint, which is on a 60˚ skew, covers 97 feet in length from curb to curb. Between 12 pm and 3:30 pm the average temperature was 52˚F and the average humidity was 43%. Figure 41 and 42 display the dimensions of the bridge and the staggering of the sealant locations. Due to the late start time the lane closest to the curb on the east side of the bridge was filled with the solid sealant the following Monday, November 9, 2010. During this bridge sealing the temperature became an issue as the cooler temperatures slowed the curing process of the foam sealant. In the laboratory setting at room temperature the tack free time for the foam is approximately 80 minutes. After this time the foam sealant can be touched without damaging it. Because the cooler temperatures slowed the reaction of the mixed materials, traffic needed to be directed away from the foam section for much longer than expected. Figure 43 (a-

c) displays a few pictures showing the cleaning of the joint prior to sealing and the application of the foam.

Figure 40. New York Bridge in Dover Plains, NY

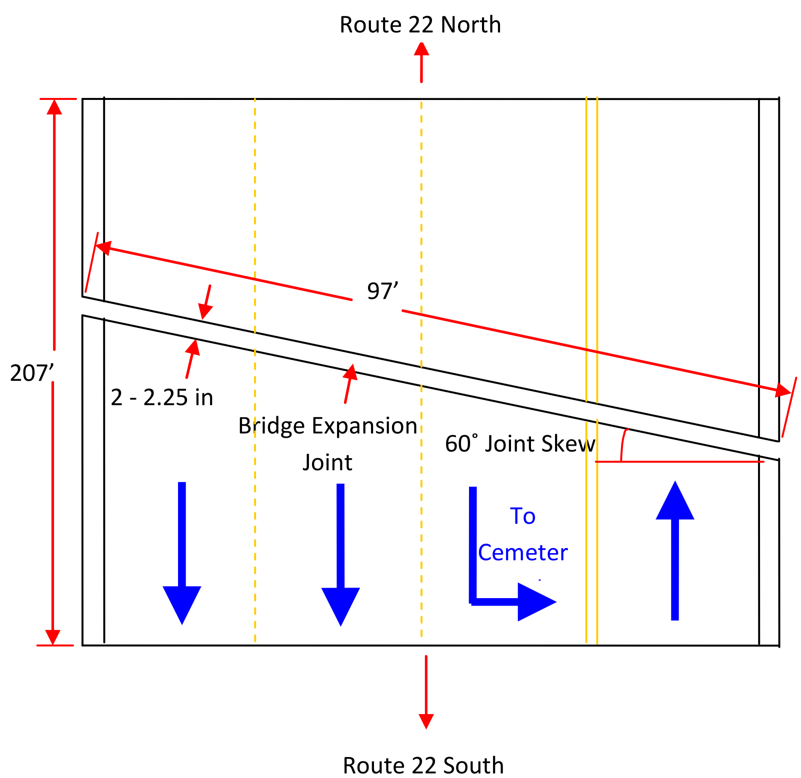

Figure 41. Dimensions of New York Bridge

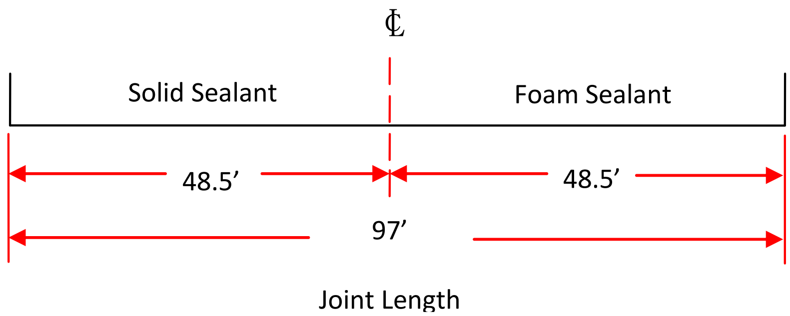

Figure 42. Schematic of the Staggering of the Foam and Solid Sealants

Figure 43. (a) Removal of Old Sealant, (b) Cleaning of the Joint Prior to Application, and (c) Sealing of the Expansion Joint

6.0 POST-INSTALLATION MONITORING OF SILICONE FOAM SEALANT

With the expansion joints on the four bridges sealed with both the silicone foam and solid sealant, the next step was monitoring of the expansion joints. For the bridges in Connecticut, New Hampshire, Rhode Island, and New York, the temperature, humidity, and precipitation data were collected. A temperature and relative humidity data logger from Omega Engineers, Inc. was placed at each bridge site to continuously measure the temperature and humidity (Omega 2009). The precipitation data for each bridge site was gathered from Weather Underground (Weather Underground 2009), a web site which displays temperature, humidity, and precipitation data collected by the National Weather Service (National Weather Service 2009). Traffic volume data was available for each bridge, but was also measured again in the Connecticut and Rhode Island bridges. Unfortunately, the joint movement of the expansion joints was not monitored on each bridge as there was no available power source at any of the locations to attach a measuring device.

6.1 Connecticut Bridge

The data for temperature, humidity, and precipitation over a 22 month span are displayed below in Figure 44 and Table 19. Table 19 displays, for each month, the average of daily average temperatures, the average of daily maximum temperatures, the average of daily minimum temperatures, the average of daily humidities, the average of daily maximum humidities, the average of daily minimum humidities, and the total precipitation for a month. A traffic counter, which was placed on the bridge after the completion of the sealant application, collected traffic volume data starting on August 17, 2009 and ending on September 10, 2009.

The data, shown in Table 20, shows that over the course of this 25 day period 27509 vehicles traveled on the bridge. These volumes result in an average daily traffic volume (ADT) of 1148 vehicles and an annual average daily traffic volume (AADT) of 1148 vehicles. Tables 21 and 22 display the breakdown of vehicle speeds and classifications. The majority of the vehicles, which happen to be cars, pickups, or vans with or without 1 to 2 axle trailers (see FHWA Vehicle Classification Figure 45) travel between 30 and 50 miles per hour.

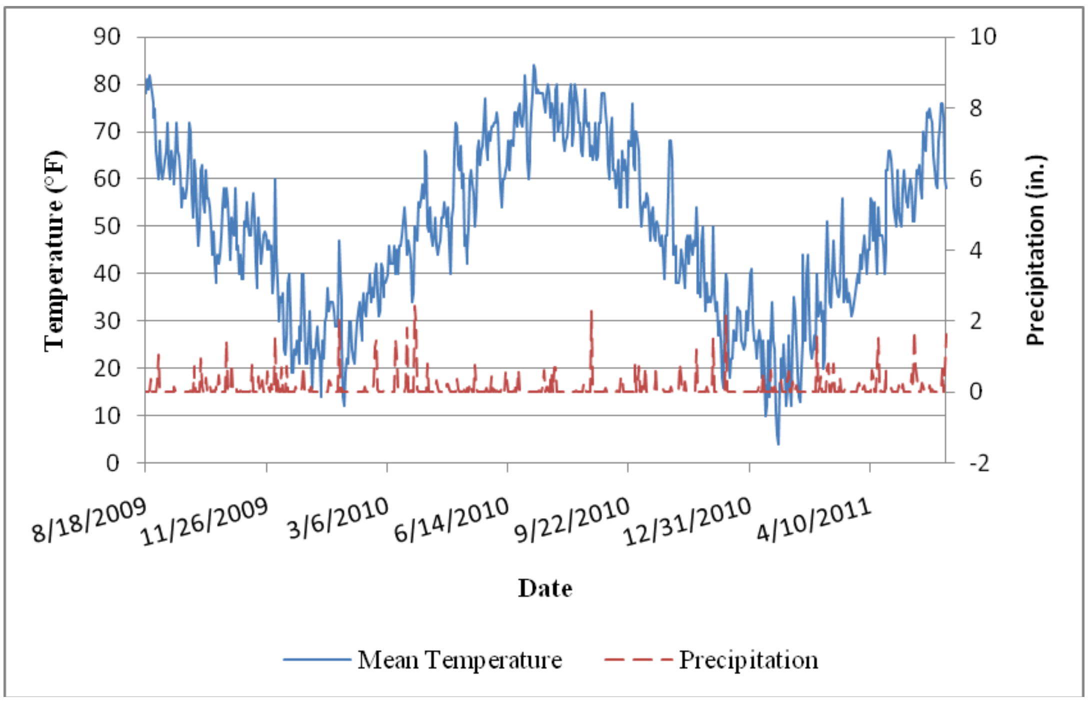

Figure 44. Average Daily Temperature and Total Daily Precipitation Data Collected in Mansfield, CT for the Period Starting August 18, 2009 and Ending June 12, 2011.

Table 19. Post - Installation Monitoring: Temperature, Humidity and Precipitation Data

Collected in Mansfield, CT for the Period Starting August 18, 2009 and Ending June 12, 2011

Month	Monthly Average of Daily Temperatures (˚F)	Monthly Average of Daily Maximum Temperatures (˚F)	Monthly Average of Daily Minimum Temperatures (˚F)	Monthly Average of Daily Humidities (%)	Monthly Average of Daily Maximum Humidities (%)	Monthly Average of Daily Minimum Humidities (%)	Total Monthly Precipitation (in.)
August, 2009	73.4	82.5	64.7	78.6	95.2	52.6	1.79
September, 2009	61.8	73.3	50.5	77.9	95.4	48.4	1.47
October, 2009	50.9	60.8	41.0	75.5	93.4	50.6	4.91
November, 2009	46.8	55.4	37.9	74.9	91.1	52.7	2.74
December, 2009	30.9	38.4	23.2	67.8	84.5	49.4	4.62
January, 2010	27.1	34.9	19.5	68.4	84.4	51.2	2.6
February, 2010	31.3	37.6	24.8	65.1	78.1	51.1	3.19
March, 2010	43.8	53.1	33.8	63.2	86.4	41.8	9.26
April, 2010	52.0	65.6	38.9	61.8	90.9	31.3	1.78
May, 2010	61.5	74.1	49.5	68.7	93.0	39.7	2.25
June, 2010	38.8	79.4	58.7	77.6	97.4	50.7	2.78
July, 2010	74.1	86.2	64.2	74.6	97.0	47.0	3.31
August, 2010	71.1	81.9	60.7	76.5	97.3	48.8	2.93
September, 2010	65.4	75.9	55.1	77.6	96.9	49.8	2.06
October, 2010	51.9	62.3	42.3	76.1	95.6	50.5	3.07
November, 2010	41.4	51.0	31.8	70.2	89.6	46.0	2.97
December, 2010	28.8	36.2	21.1	67.9	83.0	29.9	3.79
January, 2011	21.8	31.1	12.2	73.2	89.9	52.1	2.23
February, 2011	26.9	38.3	14.9	67.0	84.6	43.6	3.70
March, 2011	37.0	46.4	27.5	64.6	86.4	42.2	3.28
April, 2011	49.9	59.7	40.6	71.9	94.3	45.5	4.80
May, 2011	60.2	70.4	50.5	78.0	96.1	54.8	4.80
June, 2011	66.5	77.8	55.5	72.8	95.8	46.1	3.10

Table 20. Connecticut Bridge Traffic Data

Date	Lane 1 Total	Lane 2 Total	Lane 1 AM Peak Volume	Lane 2 AM Peak Volume	Lane 1 PM Peak Volume	Lane 2 PM Peak Volume
8/17/2009 [a]	272	272	-	-	48 (16:00)	48 (15:00)
8/18/2009	562	555	47 (10:00)	44 (11:00)	54 (13:00)	64 (17:00)
8/19/2009	576	562	43 (10:00)	45 (10:00)	53 (15:00)	57 (17:00)
8/20/2009	594	551	47 (10:00)	45 (11:00)	59 (14:00)	58 (17:00)
8/21/2009	553	564	41 (10:00)	38 (10:00)	55 (15:00)	58 (17:00)
8/22/2009	495	513	54 (10:00)	47 (11:00)	40 (13:00)	48 (13:00)
8/23/2009	435	429	34 (10:00)	44 (11:00)	43 (14:00)	41 (14:00)
8/24/2009	581	583	50 (7:00)	51 (11:00)	48 (15:00)	63 (17:00)
8/25/2009	579	598	38 (8:00)	44(11:00)	58 (16:00)	77 (16:00)
8/26/2009	625	588	51 (7:00)	45 (11:00)	52 (17:00)	67 (14:00)
8/27/2009	662	700	51 (7:00)	55 (11:00)	53 (18:00)	66 (17:00)
8/28/2009	593	613	48 (6:00)	40 (10:00)	45 (14:00)	71 (14:00)
8/29/2009	392	439	42 (11:00)	32 (11:00)	40 (13:00)	47 (14:00)
8/30/2009	452	471	40 (11:00)	46 (11:00)	60 (14:00)	57 (15:00)
8/31/2009	653	670	55 (6:00)	51 (11:00)	68 (16:00)	78 (16:00)
9/1/2009	666	650	57 (6:00)	45 (11:00)	57 (15:00)	67 (16:00)
9/2/2009	688	700	54 (6:00)	46 (11:00)	57 (14:00)	66 (14:00)
9/3/2009	677	679	67 (6:00)	47 (11:00)	60 (14:00)	64 (14:00)
9/4/2009	622	726	48 (6:00)	47 (11:00)	49 (15:00)	82 (15:00)
9/5/2009	512	547	48 (10:00)	47 (11:00)	47 (12:00)	52 (14:00)
9/6/2009	428	434	38 (10:00)	41 (11:00)	39 (12:00)	40 (15:00)
9/7/2009	383	422	30 (10:00)	31 (10:00)	42 (14:00)	46 (16:00)
9/8/2009	656	711	54 (6:00)	46 (11:00)	60 (15:00)	73 (15:00)
9/9/2009	660	671	55 (6:00)	51 (11:00)	60 (14:00)	64 (15:00)
9/10/2009 [b]	307	235	54 (6:00)	52 (11:00)	40 (12:00)	42 (12:00)

[a] Data collection began at 14:00
[b] Data collection ended at 12:00

Table 21. Connecticut Bridge Vehicle Speeds

Speed (mph)	0 – 15	16 - 20	21 - 25	26 - 30	31 – 35	36 - 40	41 - 45
Vehicle Count	94	68	254	1801	5820	9394	6576
Speed (mph)	46 – 50	51 - 55	56 - 60	61 - 65	66 - 70	71 - 75	76 - 9999
Vehicle Count	2456	654	197	66	30	21	78

Table 22. Connecticut Bridge Vehicle Classification

Classification	1	2	3	4	5	6	7
Vehicle Count	487	23219	3010	119	304	8	6
Classification	8	9	10	11	12	13	14
Vehicle Count	69	6	2	0	0	2	277

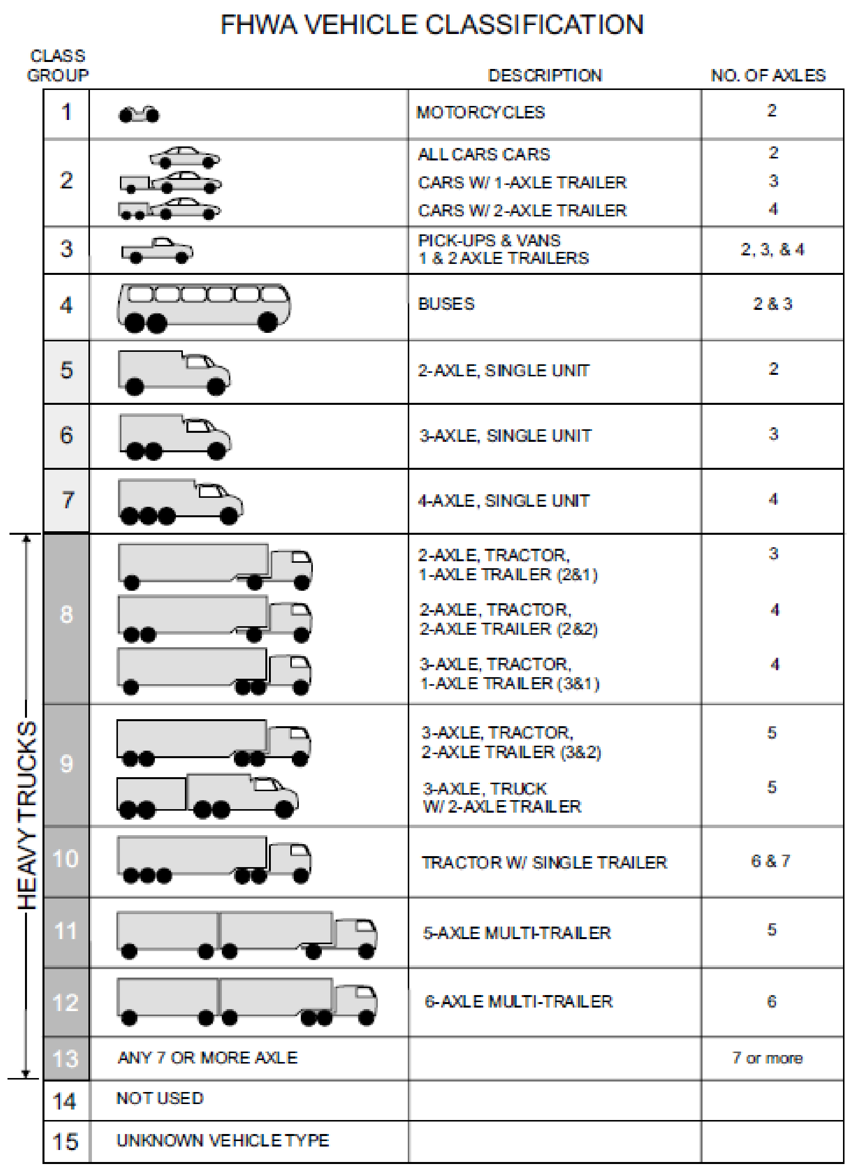

Figure 45. FHWA Vehicle Classification (Federal Highway Administration 2010)

The sealed joints on the Connecticut bridge were visually monitored and inspected on May 18, 2010, October 7, 2010, and May 25, 2011. The sealants were examined for possible tearing or detaching from the bonding surface. On May 18, 2010, no damage was seen to either sealant.

Figures 46 and 47 display the pictures of the sealants on October 7, 2010. No significant damage was observed to either sealant. Some slight peeling of the foam and solid were observed towards the surface of the road. This was, most likely, due to the constant traffic continuously pulling on the sealants as they crossed over the expansion joint. However, the peeling was minor, and the sealants remained attached to the bonding substrate.

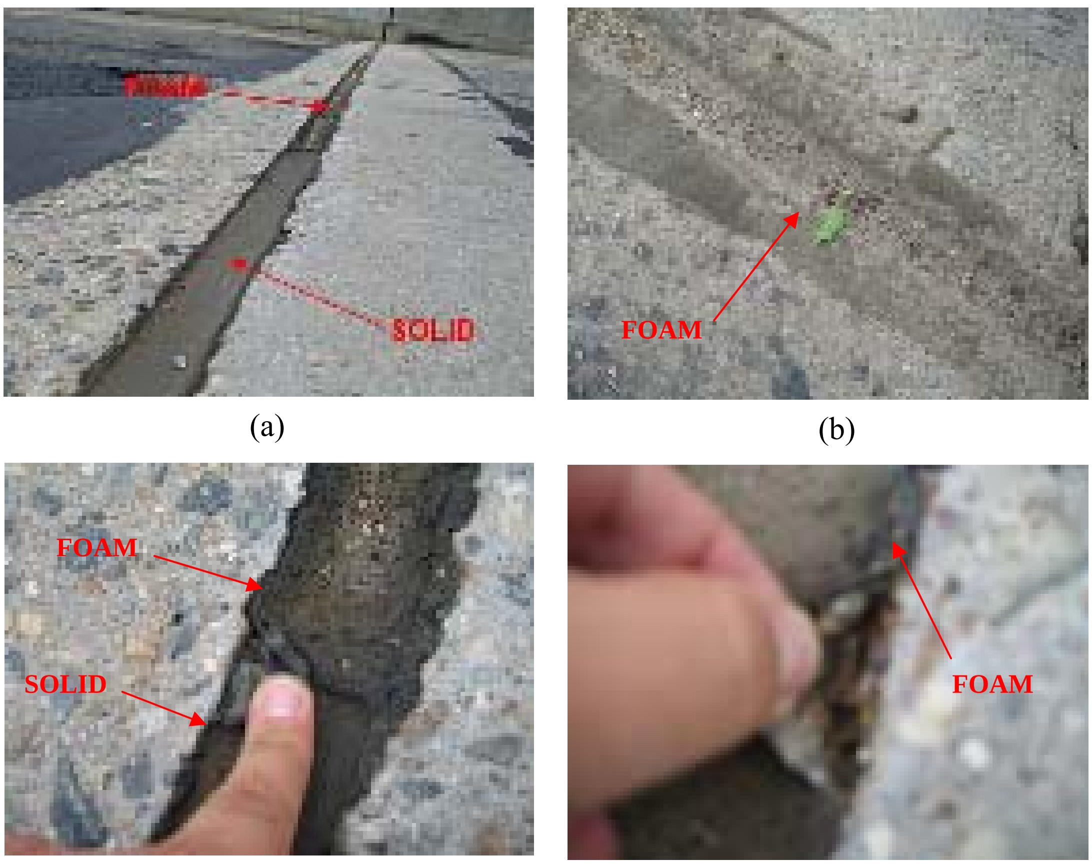

(a) (b) (c) (d)

Figure 46. Monitoring: Pictures of Sealants in Connecticut on October 7, 2010

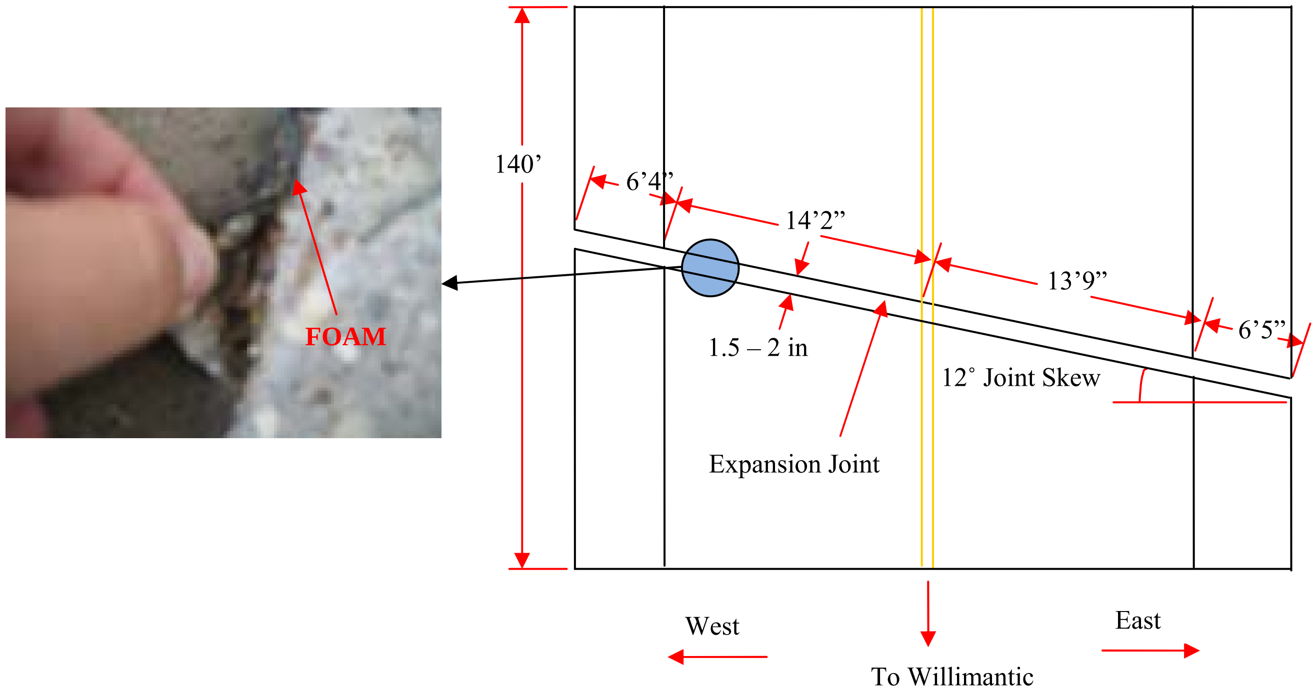

Figure 47. Monitoring: Damage to Connecticut Bridge, October 7, 2010

Figure 48 is pictures of the sealants on May 25, 2011. During this visit, the damage to the sealant was seen to be more significant than before, but it still was not extensive. Minor peeling was seen by both the solid and foam sealants, but the sealants still remained bonded to the header. It should be noted that one of the points of peeling occurred at portion of the header which had been damaged before the expansion-joint was sealed.

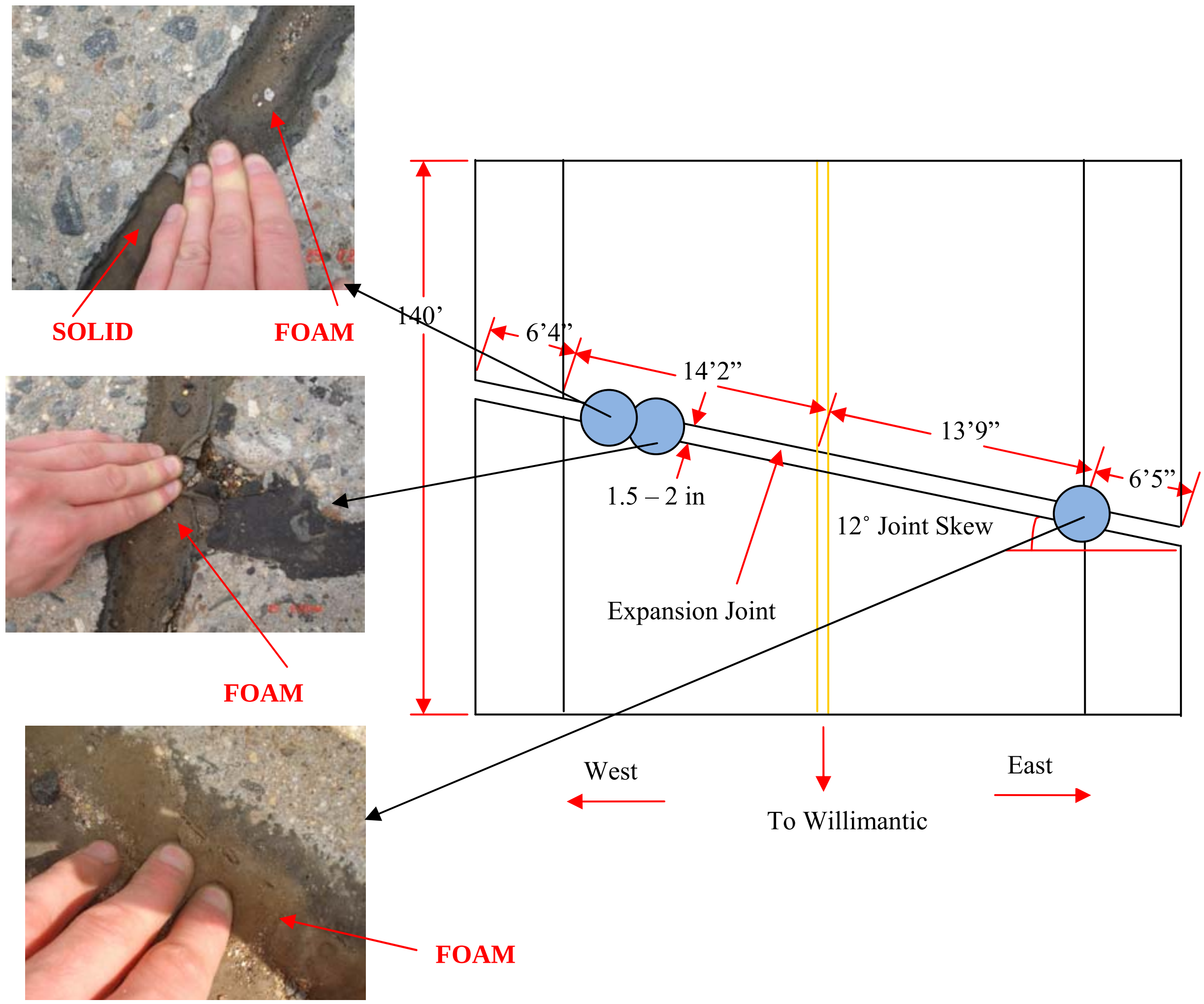

Figure 48. Monitoring: Damage to Connecticut Bridge, May 25, 2011

6.2 New Hampshire Bridge

The data for temperature, humidity, and precipitation are displayed, below, in Figure 49 and Table 23. Table 23 displays, for each month, the average of daily average temperatures, the average of daily maximum temperatures, the average of daily minimum temperatures, the average of daily humidities, the average of daily maximum humidities, the average of daily minimum humidities, and the total precipitation for a month. No traffic data was collected after the installation of the foam and solid sealants, however data collected in 2004 and 2007 shows that the bridge sees, on average, 2500 and 2300 vehicles per day, respectively (New Hampshire DOT 2010).

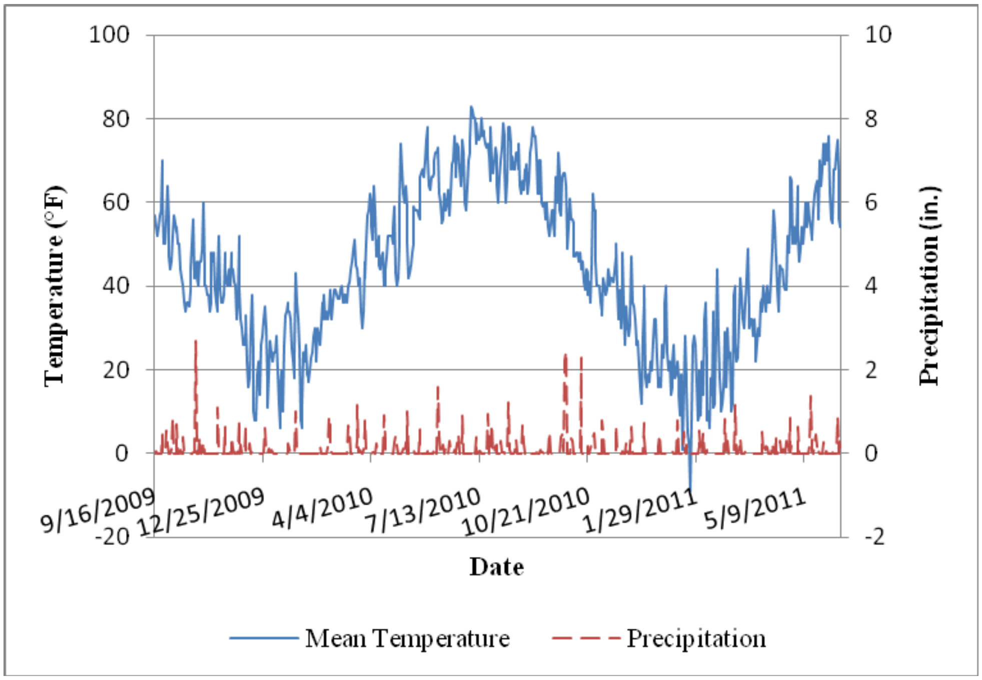

Figure 49. Average Daily Temperature and Total Daily Precipitation Data Collected in Lyme, NH for the Period Starting September 16, 2009 and Ending June 12, 2011

Table 23. Post-Installation Monitoring: Temperature, Humidity and Precipitation Data Collected in Lyme, NH for the Period Starting September 16, 2009 and Ending June 12, 2011

Month	Monthly Average of Daily Temperatures (˚F)	Monthly Average of Daily Maximum Temperatures (˚F)	Monthly Average of Daily Minimum Temperatures (˚F)	Monthly Average of Daily Humidities (%)	Monthly Average of Daily Maximum Humidities (%)	Monthly Average of Daily Minimum Humidities (%)	Total Monthly Precipitation (in.)
September, 2009	58.6	70.1	47.1	80.2	94.8	49.9	1.66
October, 2009	45.5	55.2	36.1	77.5	91.6	52.9	5.80
November, 2009	41.3	50.8	31.5	74.6	89.1	51.5	2.34
December, 2009	25.1	32.8	17.5	69.7	82.3	55.8	2.92
January, 2010	23.8	31.1	16.3	69.4	81.1	54.8	1.50
February, 2010	28.4	35.0	22.1	64.7	78.3	49.1	2.08
March, 2010	40.5	51.6	29.4	61.3	81.1	38.7	4.35
April, 2010	50.4	64.4	37.0	61.3	84.9	31.5	2.40
May, 2010	61.0	75.4	46.9	63.2	85.5	32.0	2.20
June, 2010	65.8	77.5	54.6	74.8	91.3	46.6	5.14
July, 2010	73.0	86.1	60.4	72.3	92.0	42.1	2.74
August, 2010	69.5	81.3	58.0	73.7	91.5	44.3	3.04
September, 2010	62.8	74.4	51.2	73.2	90.5	46.2	4.13
October, 2010	48.3	59.1	37.5	73.1	89.6	46.6	6.97
November, 2010	38.0	46.6	29.3	69.4	83.2	48.2	2.63
December, 2010	25.2	31.9	18.2	69.8	81.1	56.8	2.42
January, 2011	17.9	28.3	7.3	68.7	83.5	48.9	1.63
February, 2011	19.5	32.5	6.6	66.2	84.6	42.1	2.69
March, 2011	30.7	40.7	20.8	66.0	85.1	44.9	2.83
April, 2011	44.9	55.0	34.8	69.4	90.4	40.6	3.64
May, 2011	59.4	70.8	48.7	70.6	90.2	48.8	3.71
June, 2011	63.8	76.5	51.8	70.3	90.3	40.9	1.46

The bridge on East Thetford Rd. in Lyme, NH was visited on May 16, 2010 (8 months after joint sealing), October 8, 2010 (13 months after joint sealing), and May 24, 2011 (20 months after joint sealing). During the first trip to the bridge, the middle joint (Joint 2 in Figure 35) displayed no damage in either the foam or solid sealant. As with the Connecticut bridge, slight peeling of the sealants was seen due to continuous use of the bridge. The foam section on the end joint, Joint 1, also displayed no visible damage. However, the solid sealant section on Joint 1 suffered some tearing from the joint header on two sections. Towards the middle of the road, there is a 2 inch rip within the solid sealant. 2 feet from the curb there is a detaching, spanning 4 inches in length, of the solid sealant from the concrete joint header. Another detaching from the substrate is seen 4 feet from the curb. In the sections where the sealant has detached from the substrate, it appeared as though the solid had separated from the concrete all the way through to the backer rod, underneath. Figure 50 displays pictures of the damaged sealant. It should be noted that during the sealing application the section of solid sealant in Joint 1 was the last section to be sealed on the bridge. When the solid was being mixed the battery in the drill used to mix the sealant ran out of power, and the materials needed to be mixed by hand. Because such a large amount of sealant was being mixed by it cannot by assured that the materials were mixed thoroughly. This means that the solid may not have been mixed properly, possibly explaining the bad performance.

The second trip to the bridge site saw new damage to the solid sealant in Joint 1. A second tear in the middle of the sealant is now seen about 2 feet from the curb, as well as another detaching from the bonding substrate. Figure 51 shows the damage seen from the second trip to New Hampshire. Figure 52 shows the location of the damaged sections.

When the sealant were examined on May 24, 2011, new damage was seen to both the solid and foam sealants. The damage and location is shown in Figure 53. The foam sealant was seen to be peeling off the header at two locations (one in each joint). The foam was detaching at the roadway surface, but had not completely separated from the header down to the backer rod. The solid sealant was seen to be in much worse shape than the foam. In two locations of Joint 1, the solid had completely detached from the substrate down the backer rod (these detachments were about 1 and 3 in. long). In Joint 2, four rips were seen within the solid sealant of about lengths 1, 4, 4.5, and 5 in. None of the three shorter rips went through the entire thickness of the solid sealant. However, the longest rip in the solid sealant did penetrate through the entire depth of the sealant to the backer rod.

The recommendation, here, is to repair the damaged sealant with a new mix of the solid sealant. Also, the vertical joints need to be re-sealed. The verticals were filled during the sealant installation, however, the sealants did not remain attached to the substrate in the vertical portion of the joint. The New Hampshire DOT has tried to fix this problem with a different sealant, but to no avail. The procedure to successfully fill a vertical joint must be derived.

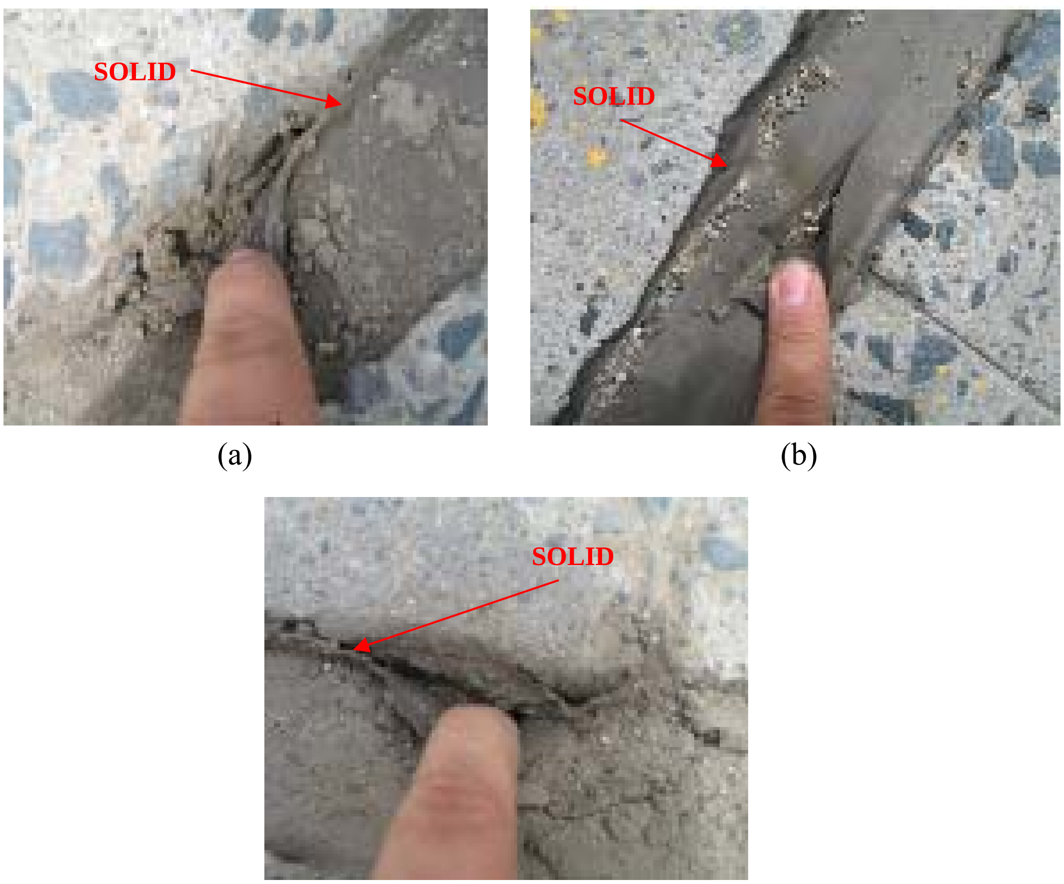

(a) (b)

(c)

Figure 50. Monitoring: Damage to the Solid Sealant in NH Bridge, May 16, 2010

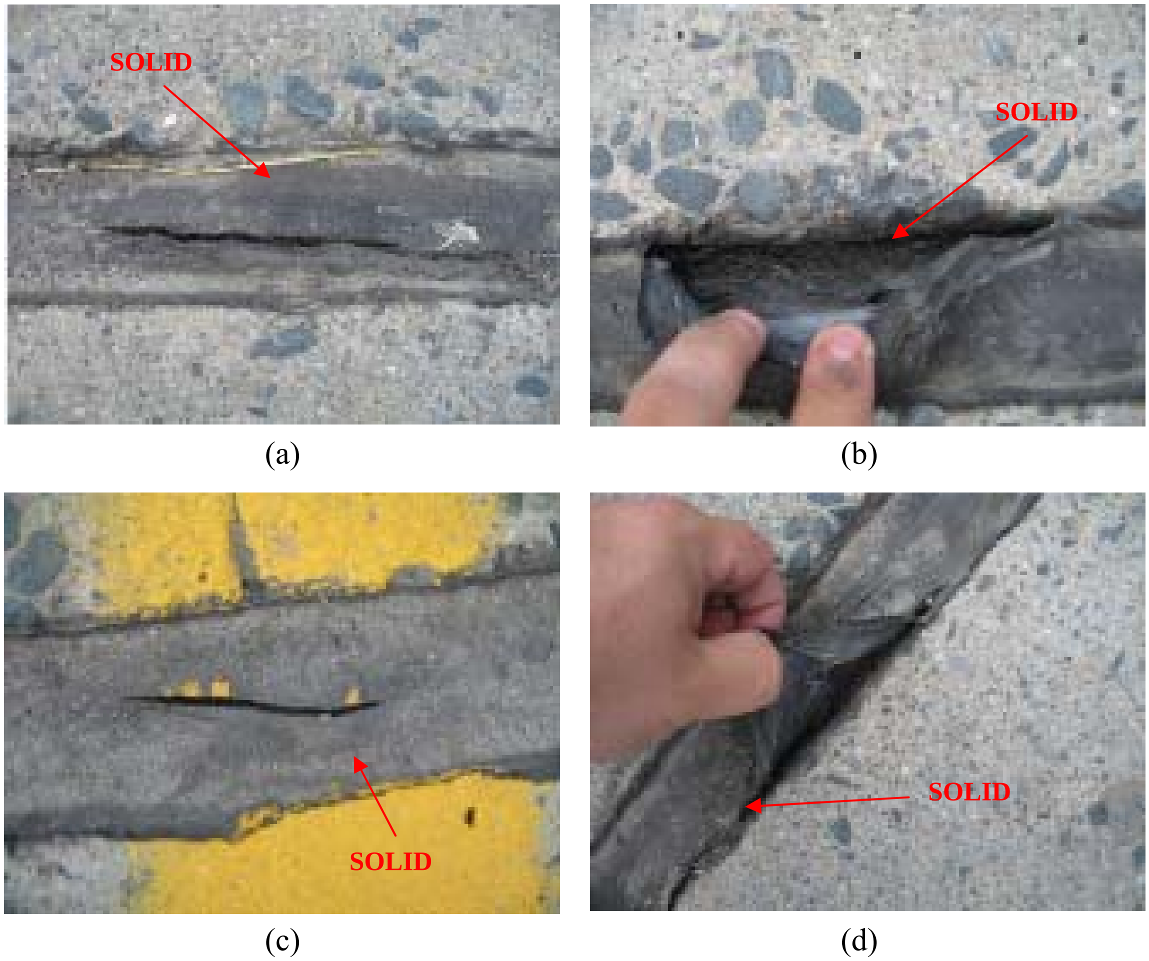

Figure 51. Monitoring: Damage to the Solid Sealant in NH Bridge, October 8, 2010

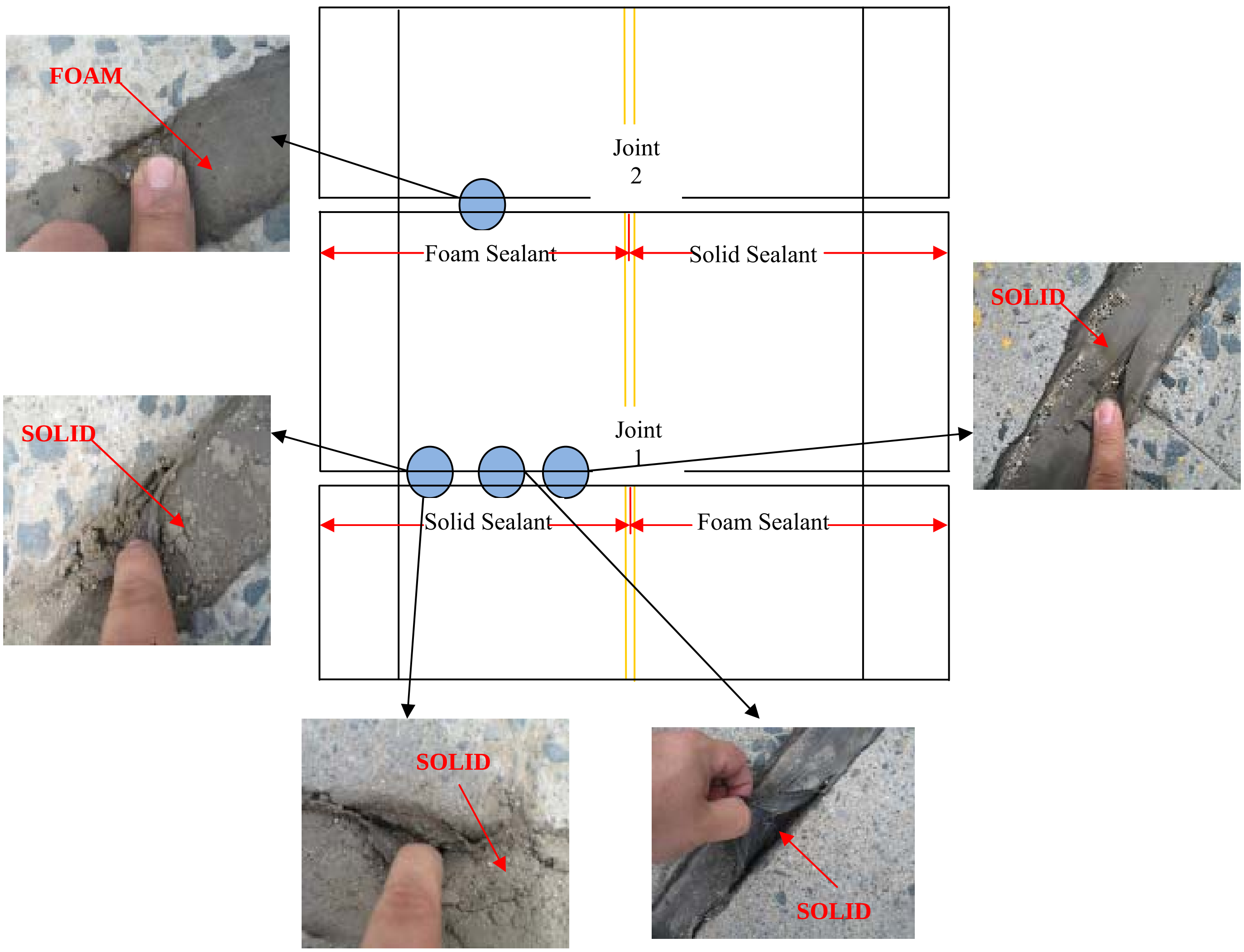

Figure 52. Monitoring: Damage at the New Hampshire Bridge on May 16, 2009 and October 8, 2010

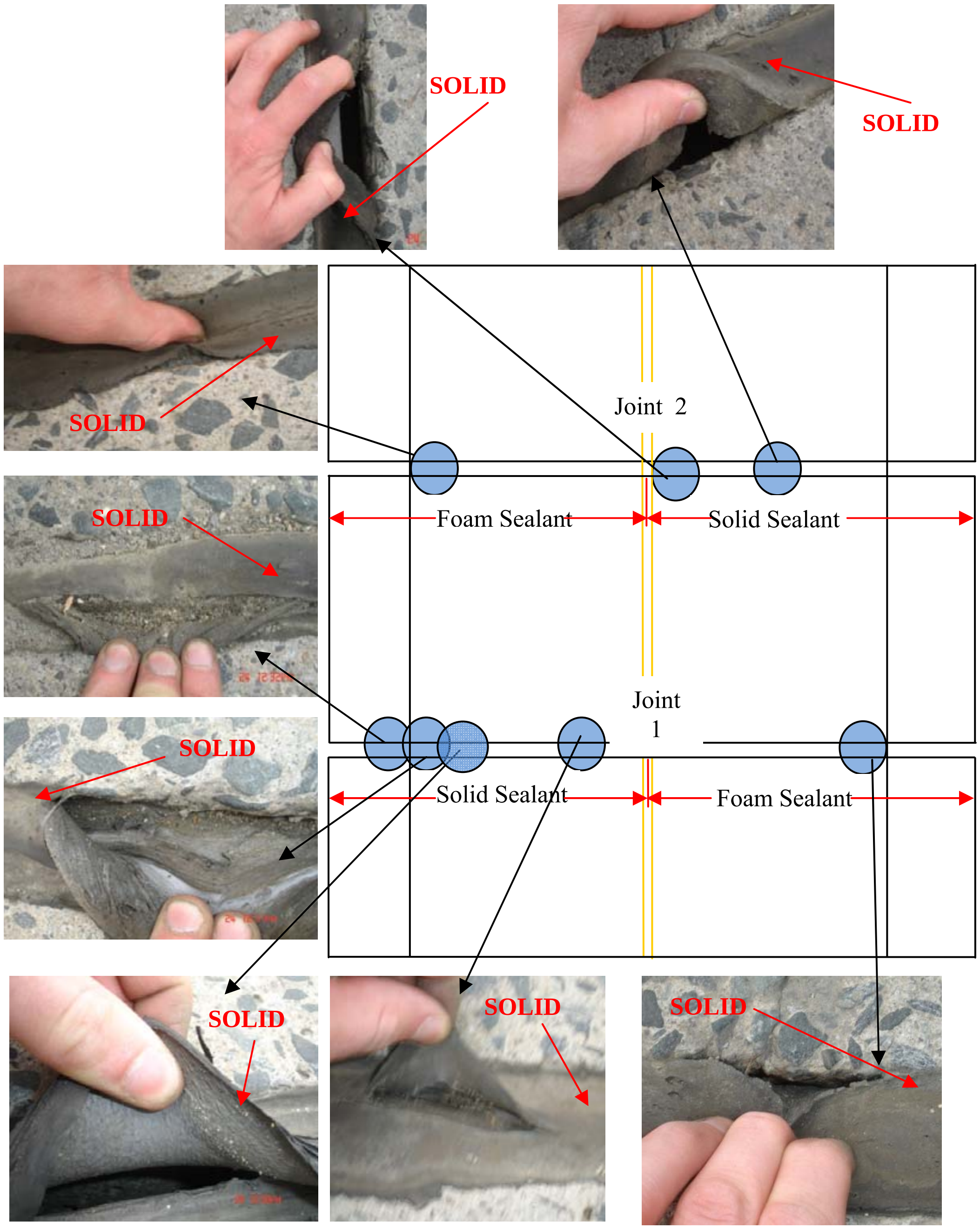

Figure 53. Monitoring: Damage at the New Hampshire Bridge on May 25, 2011

6.3 Rhode Island Bridge

The data for temperature, humidity, and precipitation are displayed, below, in Figure 54 and Table 24. Table 24 displays, for each month, the average of daily average temperatures, the average of daily maximum temperatures, the average of daily minimum temperatures, the average of daily humidities, the average of daily maximum humidities, the average of daily minimum humidities, and the total precipitation for a month. Traffic data collected over the course of 2 days results in and ADT of Route 102 of 8293 and 7998 vehicles for October 27 and 28, 2009, respectively.

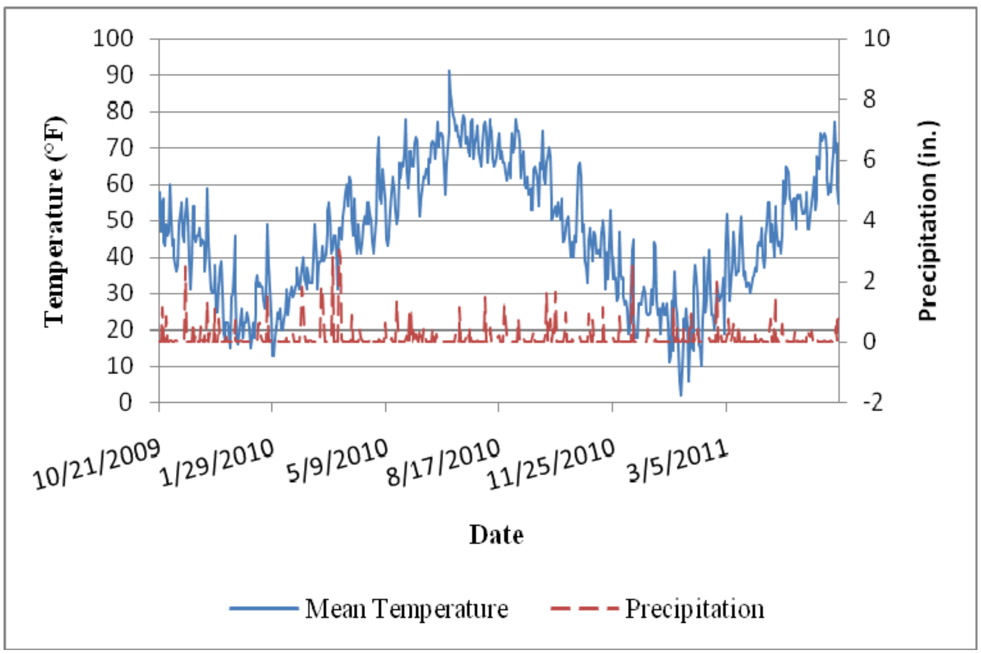

Figure 54. Average Daily Temperature and Total Daily Precipitation Data Collected in Burrillville, RI for the Period Starting October 21, 2009 and Ending June 12, 2011

Table 24. Post – Installation Monitoring: Temperature, Humidity and Precipitation Data Collected in Burrillville, RI for the Period Starting October 21, 2009 and Ending June 12, 2011

Month	Monthly Average of Daily Temperatures (˚F)	Monthly Average of Daily Maximum Temperatures (˚F)	Monthly Average of Daily Minimum Temperatures (˚F)	Monthly Average of Daily Humidities (%)	Monthly Average of Daily Maximum Humidities (%)	Monthly Average of Daily Minimum Humidities (%)	Total Monthly Precipitation (in.)
October, 2009	52.0	61.3	42.8	74.9	91.4	56.8	1.38
November, 2009	46.6	53.1	40.2	74.6	91.7	57.3	4.73
December, 2009	30.6	36.8	23.8	67.7	84.7	51.5	5.07
January, 2010	26.8	33.4	20.4	69.5	86.0	53.8	3.08
February, 2010	30.0	36.1	23.6	86.7	80.8	50.9	5.23
March, 2010	42.7	49.6	34.9	63.5	79.7	46.6	12.11
April, 2010	52.2	62.3	41.6	59.7	80.4	38.2	1.07
May, 2010	61.1	71.0	51.4	62.3	82.7	41.9	1.57
June, 2010	68.1	77.3	59.0	74.7	92.7	53.4	2.71
July, 2010	73.8	83.2	64.4	74.1	93.6	51.7	3.31
August, 2010	70.2	79.0	61.2	76.0	96.5	53.5	2.83
September, 2010	64.9	73.2	56.4	76.1	94.9	54.6	2.29
October, 2010	51.0	58.0	45.0	81.6	93.4	64.7	4.59
November, 2010	40.5	46.9	34.4	75.0	87.6	58.9	3.40
December, 2010	28.7	35.0	22.3	77.9	89.8	65.0	3.98
January, 2011	22.0	29.7	13.5	82.0	93.9	65.8	2.41
February, 2011	26.0	35.2	16.6	76.1	88.2	60.2	5.14
March, 2011	36.4	43.9	29.5	71.0	87.4	52.3	3.06
April, 2011	48.6	56.9	41.4	75.0	92.1	51.0	4.31
May, 2011	58.4	68.5	51.2	82.5	96.5	61.8	2.46
June, 2011	64.1	75.4	56.0	80.6	95.6	55.4	2.19

The bridge in Burrillville, RI was visited on May 7, 2010 (8 months after joint sealing), October 1, 2010 (13 months after joint sealing), and May 19, 2011 (20 months after joint sealing) for joint inspection and monitoring purpose. Little damage was seen in either sealant during the first trip to the bridge in May 2010. Pictures from the trip on May 7, 2010 are displayed in Figure 55. The only major damage was in the foam sealant on the shoulder line on the north side of the bridge. Here, the foam sealant has significant peeling from the steel header, as seen in Figure 56. However, upon inspection the steel header is damaged where the foam is peeling. It is possible that the dip in the steel helped the slight detaching of the foam.

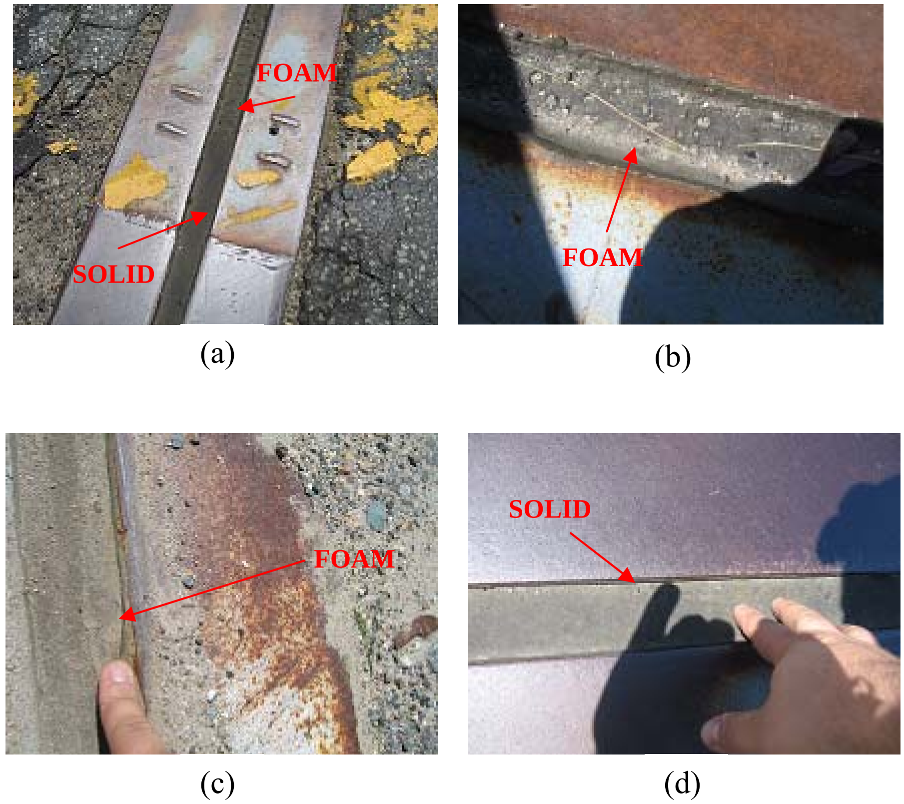

(a) (b) (c) (d)

Figure 55. Monitoring: Rhode Island Bridge Sealant, May 7, 2010 with (a) Foam and Solid Sealant, (b) Solid Sealant, (c) Foam Sealant, and (d) Solid Sealant

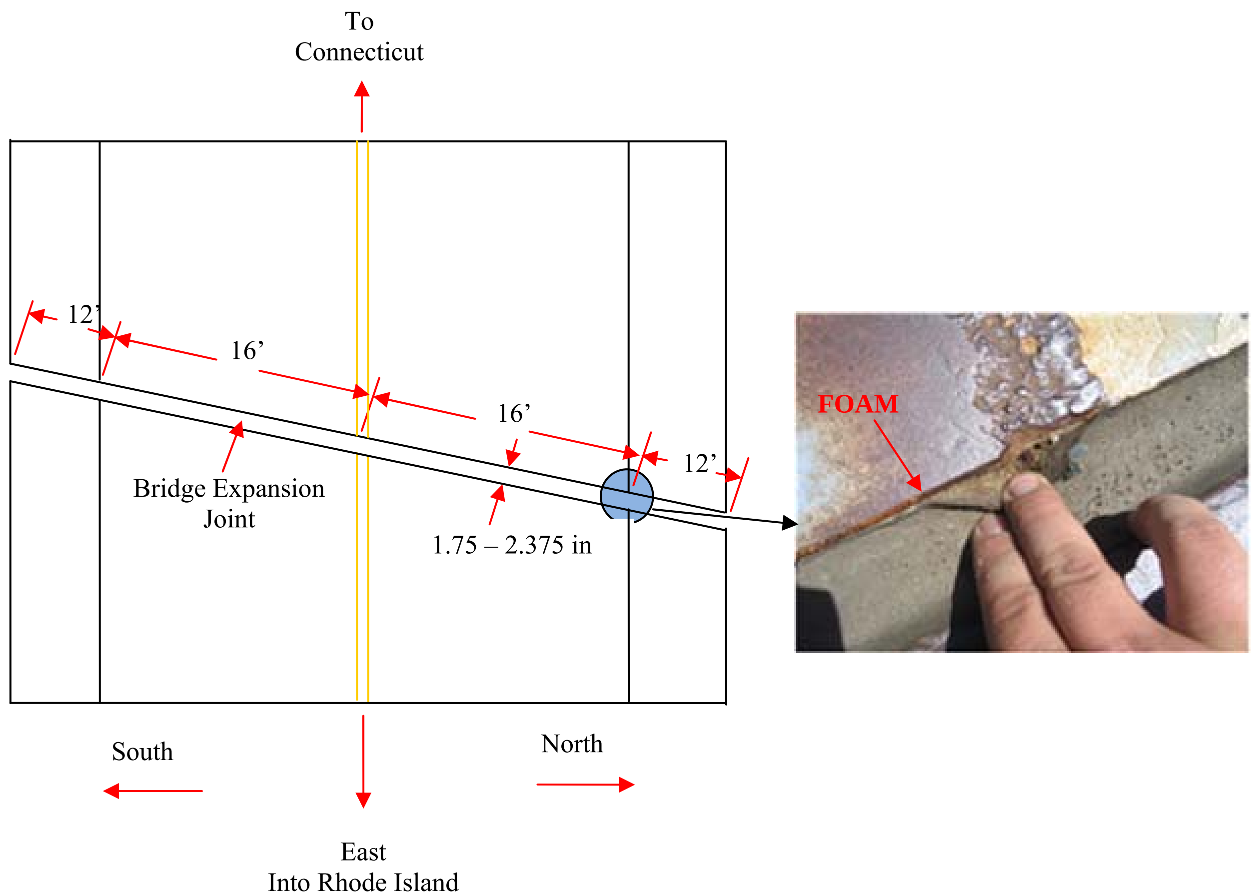

Figure 56. Monitoring: Damage to the Foam Sealant, May 7, 2010

During the second trip to the bridge site, damage was seen in the solid sealant. At about 6 inches north of the center line of the road, a 2 inch section of the solid has detached from the steel header. Also, a section of solid 10 feet from the curb on the north side of the bridge has detached from the substrate, causing slight damage to the adjacent foam sealant. The section of foam that was peeling due to, perhaps, a damaged section of the steel has worsened as the hole that was created has seemed to deepen. Pictures of the damage are shown in Figure 57.

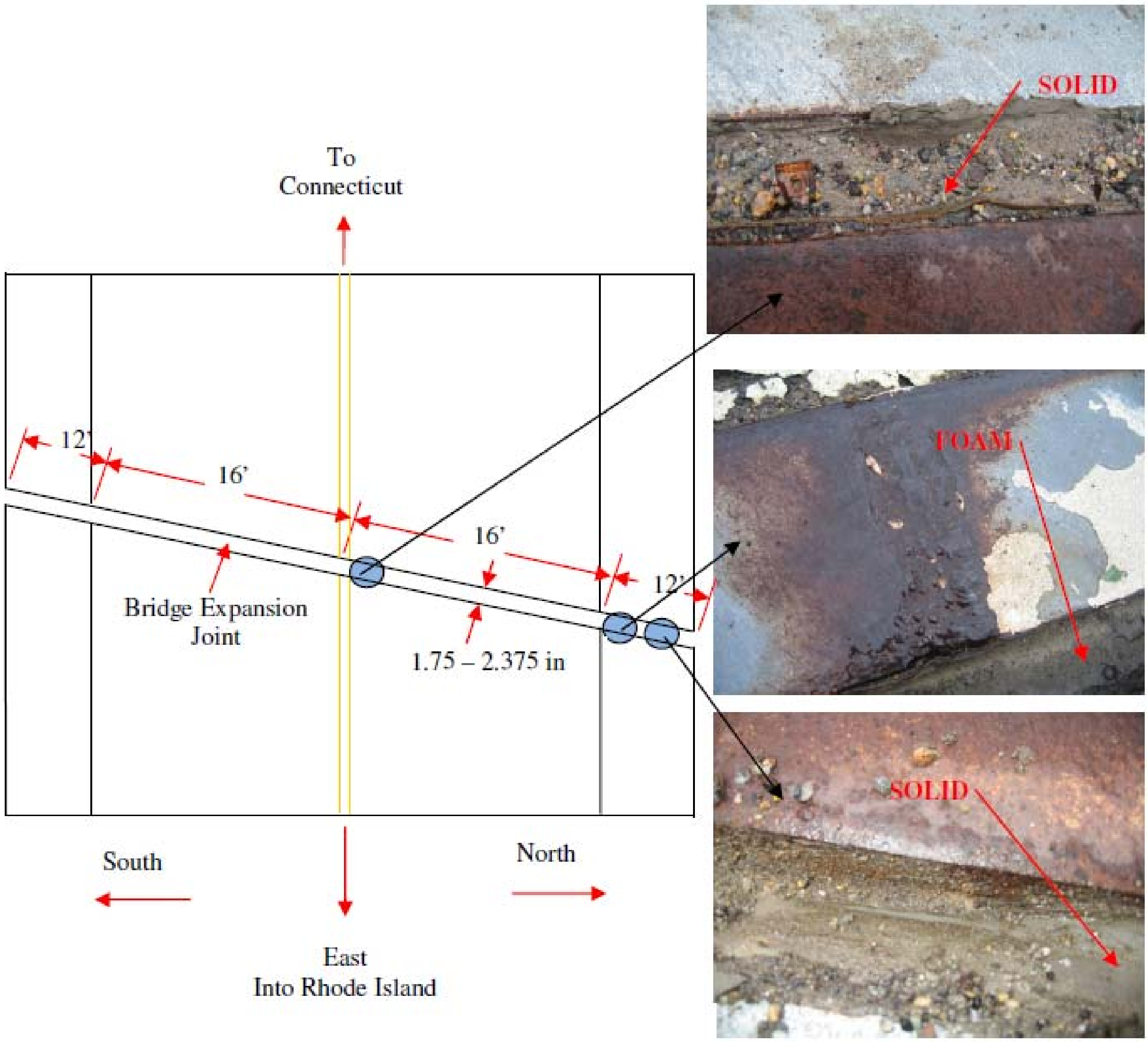

Figure 57. Monitoring: Damage to the Rhode Island Bridge, October 1, 2010

On May 24, 2011, the damage to both sealants had become more severe. Pictures of the damage and the location of the damage are shown in Figures 58 and 59. Damage to the solid sealant was extensive. On the north-side shoulder, the solid sealant had completely peeling off the steel header down the backer rod. The length of this debonding was about 8 inches. In the 8-ft long section of the solid sealant on the north-side of the roadway, the solid was seen to be damaged. In this section, the sealant was ripping at two places. The first rip was less than 1-in in length and did not go down the backer rod. The other rip was about 2.5-in and did go down the backer rod. The solid was also debonding from the steel header down to the backer rod in this section of the bridge. In the final solid sealed section of the bridge (10-ft long south-side), the solid was seen to have some slight debonding. The foam sealant was seen to be slightly peeling off the header at five locations at the bridge, but none of these damages went down to the backer rod. The locations of foam peeling were two in the south-side shoulder, two in the 8-ft long section on the south-side of the bridge, and one in the north-side shoulder. There was damage to the steel header at the north-side shoulder, where the foam peeling. Also, the foam had a small tear in the 10-ft long section on the north-side of the bridge. This tear may have been a defect caused by a large bubble, while installing the foam sealant.

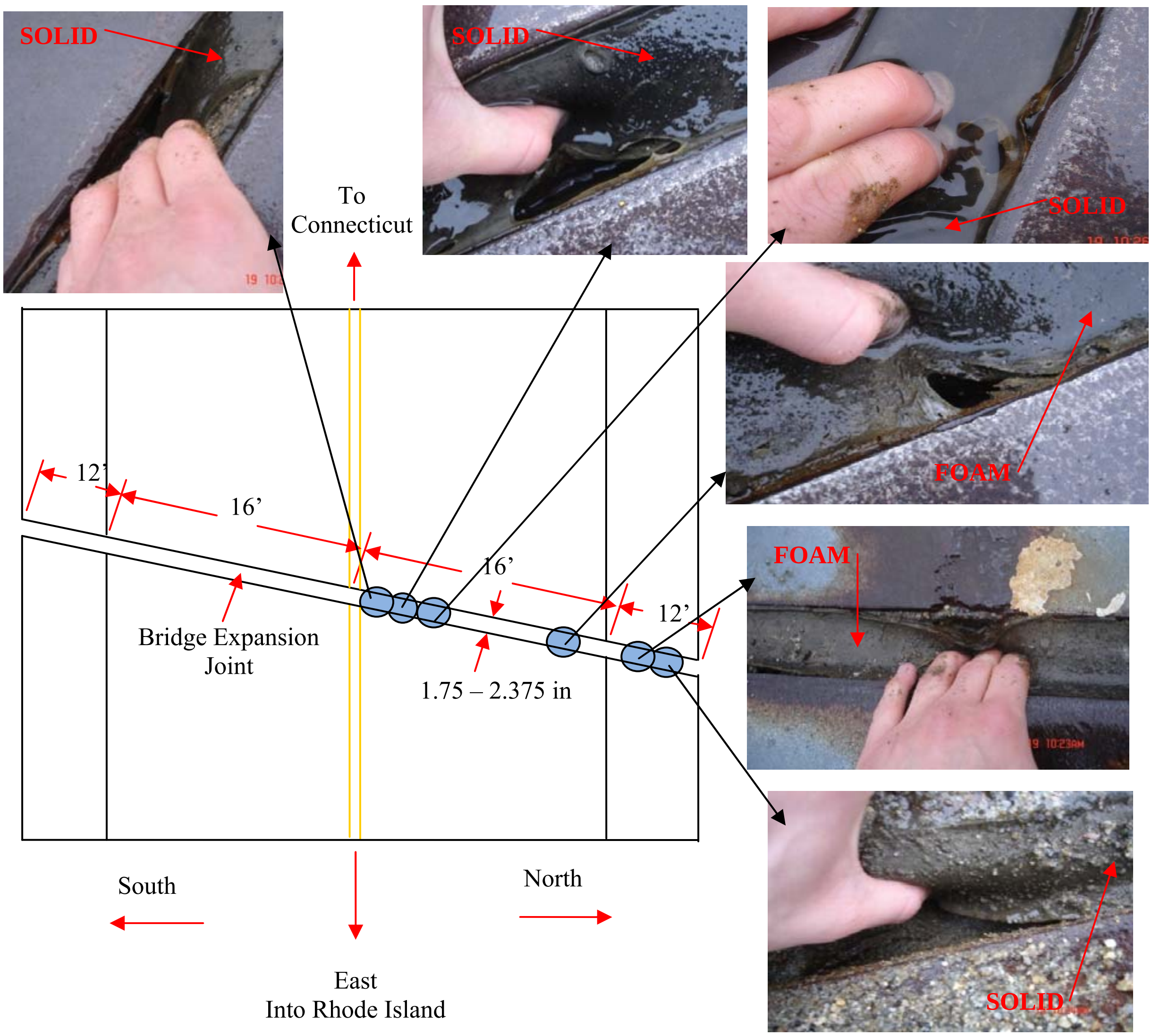

Figure 58. Monitoring: Damage to the Rhode Island Bridge, May 19, 2011

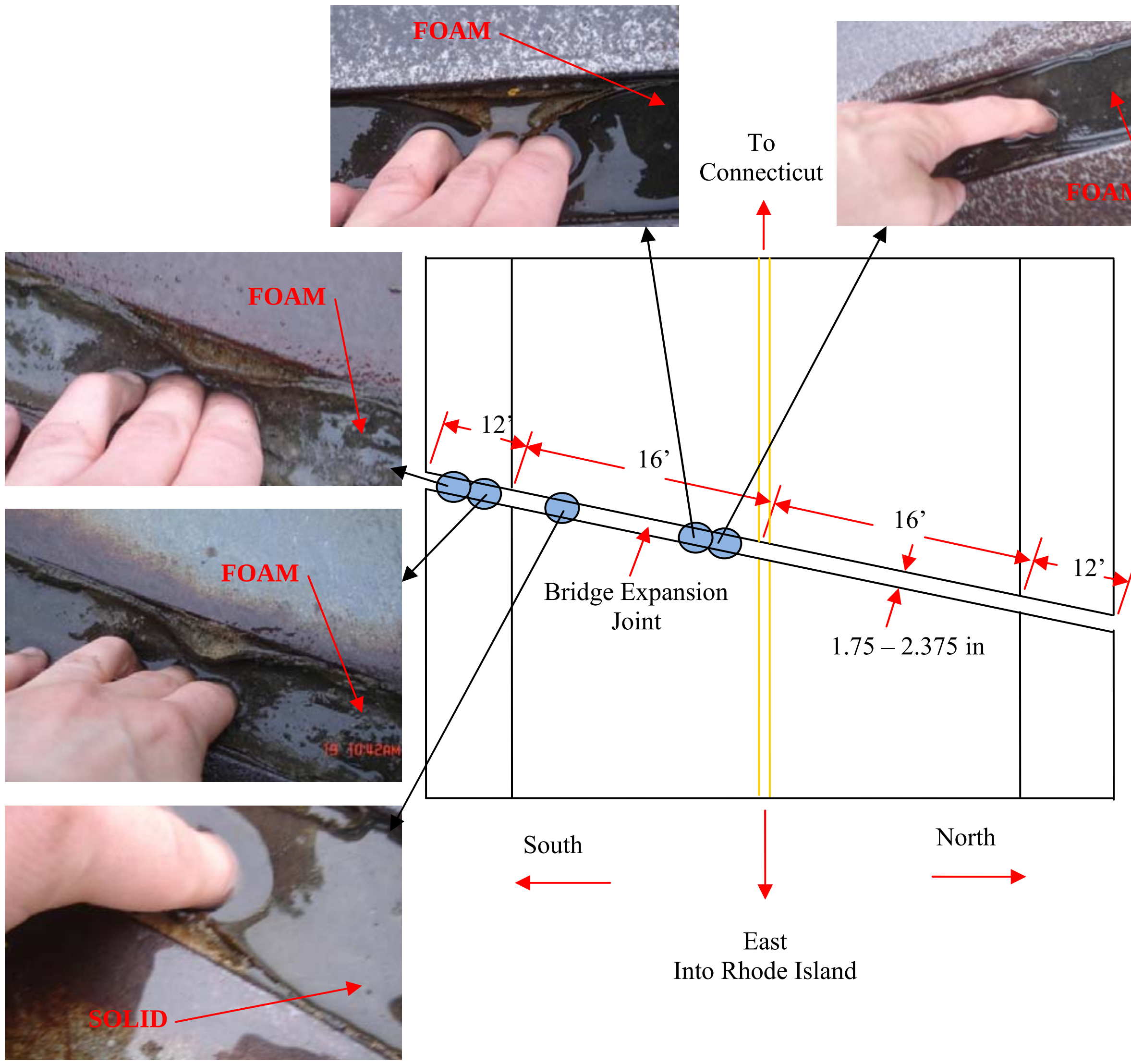

Figure 59. Monitoring: Damage to the Rhode Island Bridge, May 19, 2011

6.4 New York Bridge

The data collected for temperature, humidity, and precipitation are displayed, below, in Figure 60 and Table 25. Table 25 displays, for each month, the average of daily average temperatures, the average of daily maximum temperatures, the average of daily minimum temperatures, the average of daily humidities, the average of daily maximum humidities, the average of daily minimum humidities, and the total precipitation for a month.

Since the sealing application, the bridge has been visited on May 11, 2010 (8 months after joint sealing), October 6, 2010 (13 months after joint sealing), and May 18, 2011 (20 months after joint sealing). During the first visit to the bridge no visible damage seen in either sealant. Pictures form this visit are seen in Figure 61.

During the second visit to the bridge on October 6, 2010, the foam section still seemed to remain intact, but damage was seen to the solid sealant. Slight peeling of the solid sealant away from the substrate was noticed towards the road surface, however the sealant underneath maintained its adhesion to the joint header. On the solid side a 2 inch section of the header, 8 feet from the curb, began to break off, causing the solid sealant to tear slightly, as shown in Figure 62. The rest of the solid sealant seems to be intact, however the solid sealant, around the area where a piece of the header broke off, when pressed upon, did not exhibit much resistance, and it felt as though that the backer rod had detached from the sealant and had fallen deeper into the expansion joint.

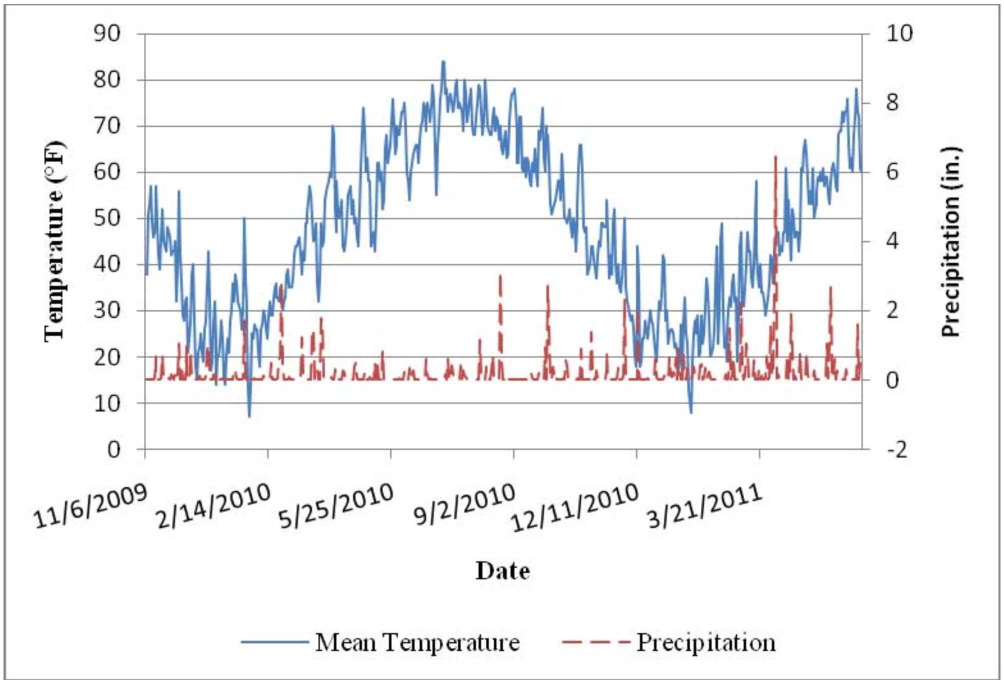

Figure 60. Average Daily Temperature and Total Daily Precipitation Data Collected in Dover Plains, NY for the Period Starting November 6, 2009 and Ending October 4, 2010

Table 25. Post – Installation Monitoring: Temperature, Humidity and Precipitation Data

Collected in Dover Plains, NY for the Period Starting November 6, 2009 and June 12, 2011

Month	Monthly Average of Daily Temperatures (˚F)	Monthly Average of Daily Maximum Temperatures (˚F)	Monthly Average of Daily Minimum Temperatures (˚F)	Monthly Average of Daily Humidities (%)	Monthly Average of Daily Maximum Humidities (%)	Monthly Average of Daily Minimum Humidities (%)	Total Monthly Precipitation (in.)
November, 2009	45.2	55.2	34.7	76.0	93.4	53.4	1.45
December, 2009	29.5	37.2	21.4	72.3	90.0	51.3	3.75
January, 2010	26.3	35.3	16.8	73.4	91.3	52.3	2.04
February, 2010	28.7	36.1	21.0	73.3	89.9	57.4	4.08
March, 2010	43.3	53.5	32.7	66.6	88.9	43.1	4.56
April, 2010	53.3	66.9	39.03	62.3	92.5	32.6	1.74
May, 2010	61.9	74.9	48.4	71.2	95.7	41.6	1.77
June, 2010	70.0	81.8	57.8	73.1	97.6	45.3	1.88
July, 2010	76.2	89.4	62.7	68.8	96.3	39.2	1.4
August, 2010	71.9	83.4	59.8	75.7	96.7	46.3	6.97
September, 2010	65.0	76.4	53.2	75.4	95.4	46.7	3.61
October, 2010	53.5	62.2	45.6	76.3	93.5	46.0	4.22
November, 2010	42.6	50.3	35.0	69.2	88.4	47.5	3.49
December, 2010	28.1	34.5	22.1	71.9	84.6	56.6	5.59
January, 2011	24.4	30.7	17.4	74.0	87.0	53.8	4.98
February, 2011	29.8	38.1	20.1	62.9	80.8	41.4	4.38
March, 2011	37.5	45.4	29.4	61.9	81.8	40.8	8.00
April, 2011	50.1	60.1	41.8	69.5	91.2	40.8	15.94
May, 2011	60.8	70.4	52.5	74.4	91.8	51.8	6.80
June, 2011	67.5	77.9	57.5	68.3	90.1	43.5	2.77

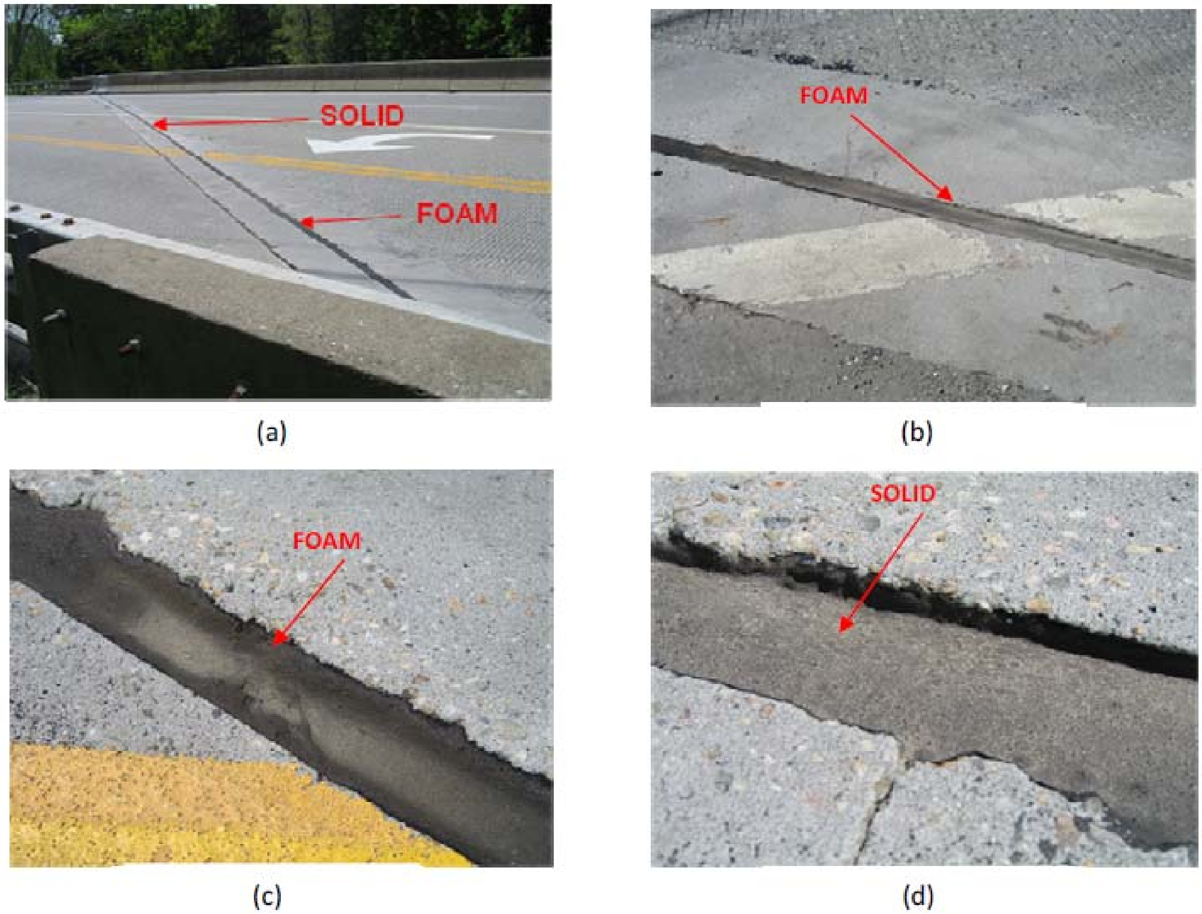

Figure 61. Monitoring: Foam and Solid Sealants on New York Bridge, May 11, 2010

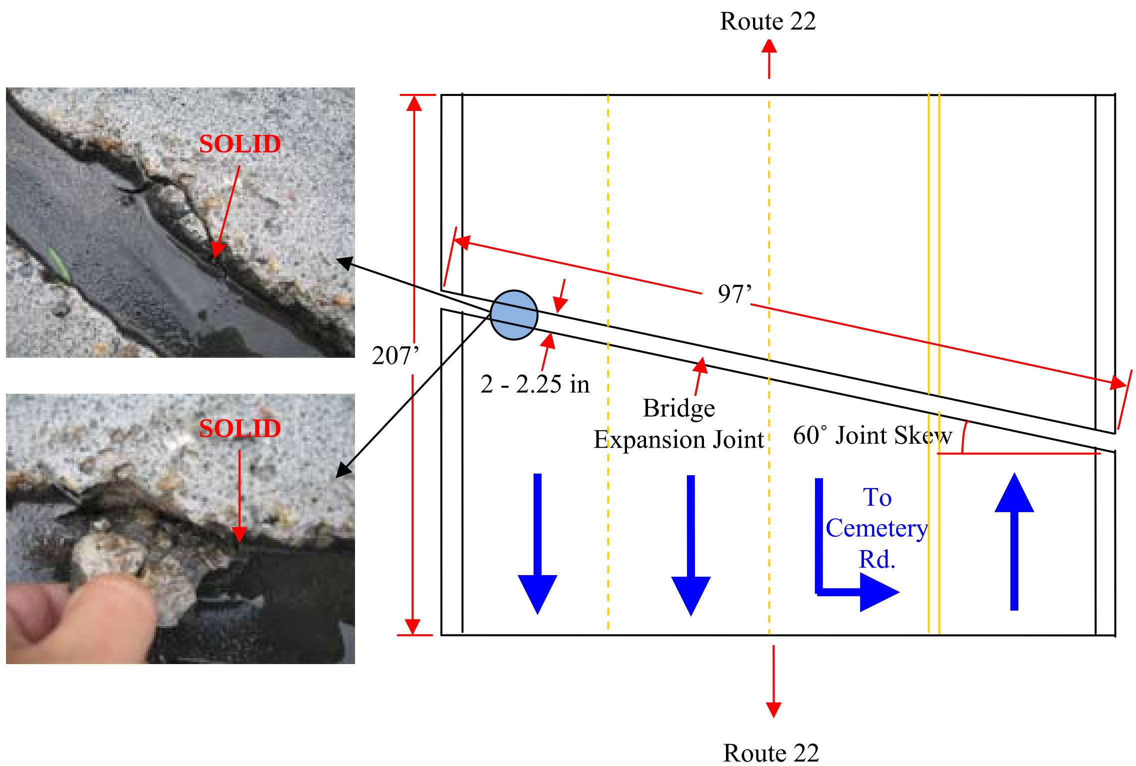

Figure 62. Monitoring: Damage to the Solid Sealant, October 6, 2010

On May 18, 2011, both sealants were seen to be damaged as shown in Figures 63 and 64. The solid sealant was damaged in four places. In three places, the solid sealant had detached from the header, because the header was breaking apart. At the shoulder of the first south-bound lane and at the center of the second south-bound lane, the debonding was only present at the roadway surface, but the sealant remained underneath remained adhered. However, at the center of the first south-bound lane, the solid sealant had completely detached from the header down to the backer rod. Additionally, at this debonding point, the solid sealant was also starting to rip and fail in cohesion. This was likely caused by vehicles driving over and pulling the unbounded sealant, while the adjacent sealant was still attached to the substrate. The last damage to the solid sealant was a rip in the sealant about 2-in in length. The rip did not go down to the backer rod. The foam sealant exhibited peeling from the header in many places. The peeling was minor, except at locations where header damage was also present, and at no place was the foam sealant seen to completely debond from the header.

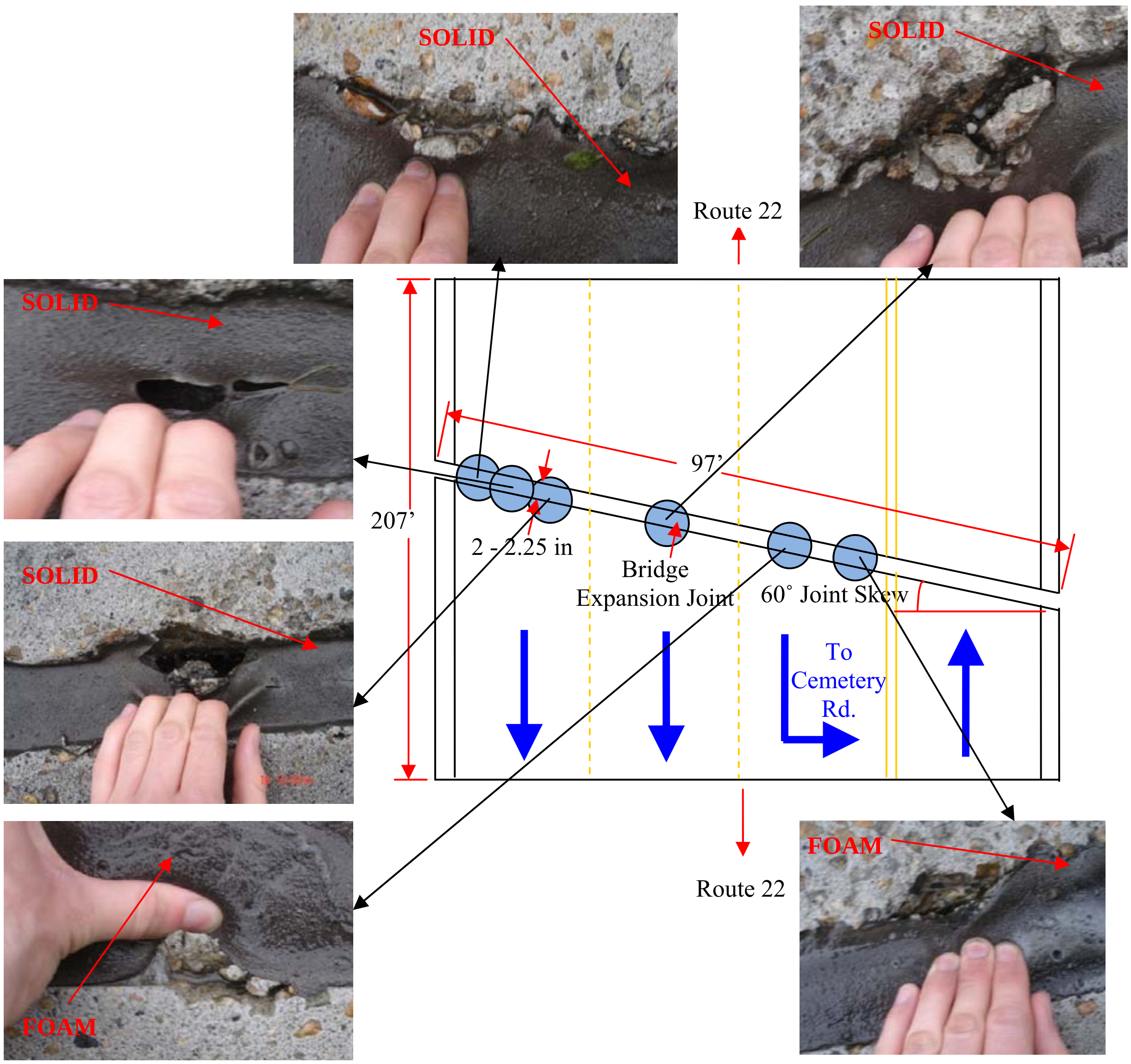

Figure 63. Monitoring: Damage to the New York Bridge, May 18, 2011

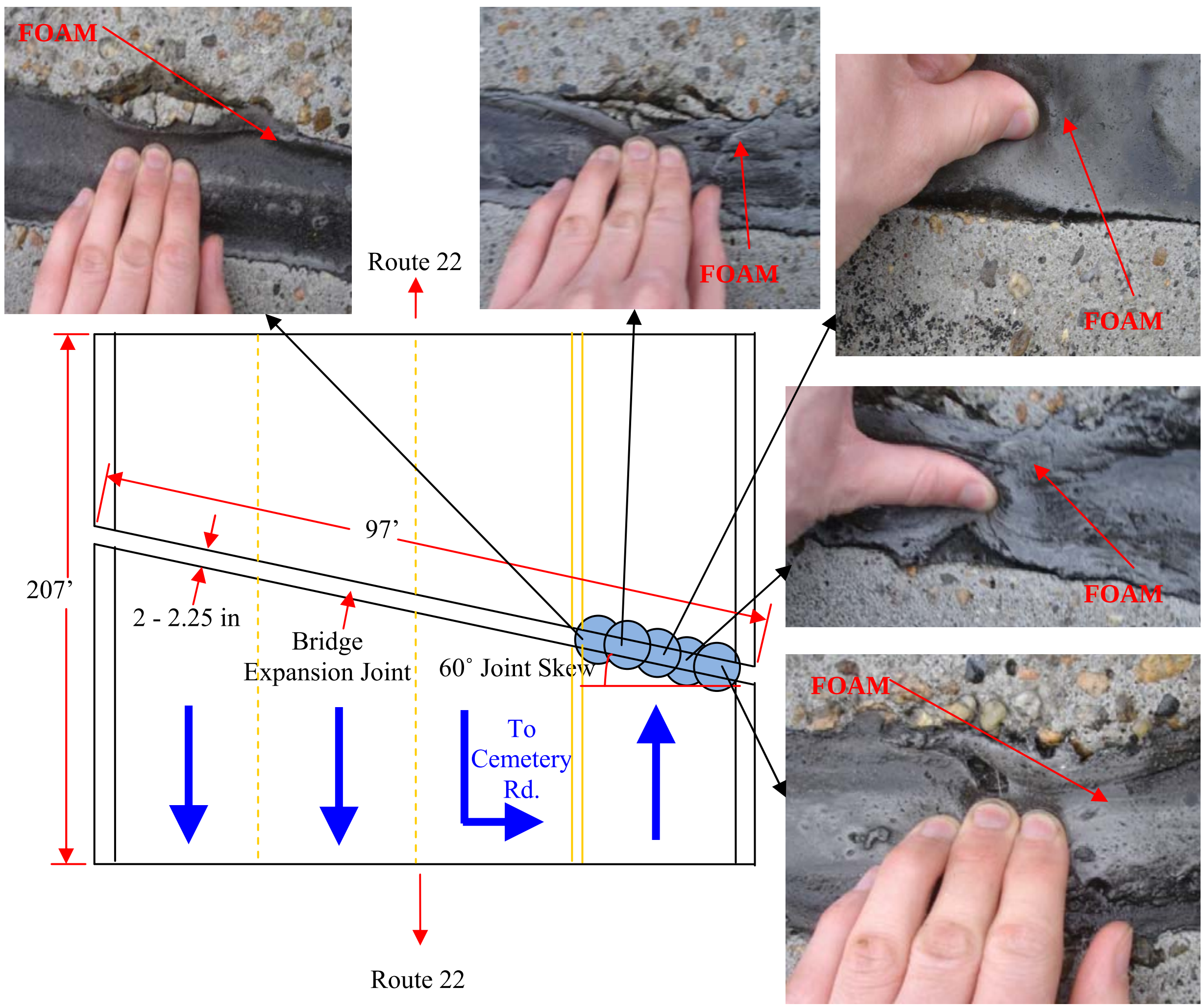

Figure 64. Monitoring: Damage to the New York Bridge, May 18, 2011

7.0 SUMMARY, CONCLUSIONS, AND RECOMMENDATION FOR THE FUTURE WORK

This research study discusses the various laboratory testing, field installation, and monitoring of a newly developed silicone foam sealant. The laboratory tests were conducted to understand the material and engineering characteristics of the foam sealant in comparison to those of a commercially available solid sealant (herein, termed the solid sealant). The laboratory tests conducted were two types of tension tests (pull-to-fail and loading/unloading), repair/retrofit test, oven-aged bond test, salt water immersion test, modulus over time test, freeze-thaw test, cure rate test, and a water ponding test. The field installation and monitoring were conducted after the development and thorough evaluation of a sealant application procedure. Based on the results from the laboratory tests, field installation, and monitoring specific conclusions can be drawn as well as recommendations for future work.

7.1 Conclusions

The following covers the conclusions drawn from the laboratory experiments, field installation, and monitoring of the silicone foam sealant.

- The silicone foam has the capability of bonding to commonly used joint header materials (such as concrete, steel, and polymeric concrete) in bridge expansion joints. The sealant also exhibits an ability to accommodate movement of small-movement expansion joints as these types of joints are designed to expand as much as 100 to 200% of its original strain. The foam sealant was observed to elongate more prior to failure than the solid sealant when bonded to all of these substrates. The majority of the test specimens showed the foam failing cohesively (internal material failure) rather than at the sealant-substrate bond interface. On the other hand, the solid sealant was observed to fail at the sealant-substrate interface at a much lesser strain (elongation) value. The reason is quite evident; the lower modulus of the foam applies a much lower stress to the interface at a given deformation. This result is seen despite the likely similar structures of the two sealants in the interfacial region.

- After oven aging, the foam and solid sealants were observed to exhibit a loss in stress after each cycle of freezing and elongation to 100% strain. The trends exhibited by both the foam and solid sealants the suggest that had there been more than 5 cycles of freezing and elongation, both the sealants would achieve a minimum 100% modulus (i.e. modulus E_∞ when cure time is infinite) and not continue to lose strength. .
- Immersion test units in salt water had no discernable negative effect on the bonding of the foam and solid sealants to asphalt. For the steel substrate, the salt-water immersion was observed to cause the foam and solid sealants to have a lower ultimate strain than that of the dry test specimens.
- Both the newly prepared foam and solid sealants, when bonded to old (aged) foam, have higher average ultimate strains compared to when they were bonded to old solid sealant. The average ultimate strain of new foam/aged foam test samples is not statistically different from new solid/old foam or new foam/old solid. There is a statistical difference in the average ultimate strain between new foam added to old foam and new solid added to old solid. Based on the test results, if the foam sealant is damaged, either by tearing or separating from the substrate, it can be repaired with better results than can the solid.

- As both the foam and solid sealants approach the ultimate modulus (modulus at infinite time E_∞), the rate of increase of the modulus (stress at 100% strain) will slow and plateau. The cure rate is consistent with the second-order kinetics of the cross linking reaction. While it appears that the foam sealant has a slower rate of increase of the modulus, it is not significantly different from that of the solid sealant.
- The results from the freeze-thaw test had shown that the ultimate strength of the foam sealant after submersion and freezing in fresh water was not different from the ultimate strength from a control, dry set of foam sealant specimens. On the other hand, the ultimate strength of the solid sealant appeared to be weakened by its initial submersion in fresh water in comparison to a control, dry set of specimens.
- The foam sealant, having been submersed in water after 1 and 2 hours of curing, was observed to have prevented leakage of water over the course of 7 days of ponding.
- Instructions for producing the foam sealant in large quantities and a procedure for installing the foam sealant in bridge expansion joints were developed. The best applicator tools and a step-by-step application process were determined. Then, the sealing process was practiced on a 7-ft long x 2-in wide joint prototype in the laboratory.
- The application procedure developed in the lab was used successfully in the installation of the silicone foam sealant in expansion joints on bridges in four New England states, namely, Connecticut, Rhode Island, New Hampshire, and New York. The same method was used for the installation of the solid sealant as well for comparison purposes. Overall, the application procedure proved to be effective in the field.
- Over the course of the 20 month monitoring period, the foam sealant in bridge expansion joints has displayed resiliency and was in much better condition than the solid sealant. At

the Connecticut, Rhode Island, and New Hampshire bridges, the foam sealant sealants had experienced only minor peeling from the header. At the New York bridge, more significant peeling of the foam from the substrate was present, but that was due to header damage. The foam did not detach from the header down to the backer rod at any of the bridges. Conversely, the solid sealant had significant damage. While only minor peeling of the solid was present at the Connecticut bridge, at the other three bridges, the solid was failing both cohesively (internal ripping) and adhesively (detaching from the header). More importantly, much of the damage to the solid was severe going from the roadway surface down to the backer rod allowing water to get into the joints. It is apparent from the field monitoring of the sealants that the foam sealant was much more durable and therefore provided longer lasting protection to the expansion joints than did the solid sealant

7.2 Recommendations for Future Research

This section discusses the recommendations for future research on the silicone foam sealant.

- A recommendation for future laboratory testing involves the repair/retrofit test. In the original test conducted, the new batch of sealant was bonded to an old batch of sealant that was attached to concrete. Unfortunately after the sealants were pulled to fail it took a lot of time to determine if the new sealant separated from the old sealant. It is recommended that for future repair/retrofit tests the old sealant needs to be marked in such a way so that it can easily be picked out in the presence of the new sealant.
- For the oven-aged bond test it would be worthwhile to conduct further investigations on the effects of oils that may seep from the asphalt onto the foam and solid sealants when

they are placed in an oven. Currently, there is no direct evidence for this possible reaction of the sealants when placed in an oven while bonded to asphalt.

- Changes in the specimen preparation for the cure rate test need to be made if the test is to be repeated for future research. As stated in Chapter 3, the specimens were not made on the same day due to limited resources. For example, the specimens allowed to cure for 3 days were not made on the same day as specimens allowed to cure for 10 days. If all the specimens were not made on the same day then many variables are introduced; the mixing of the sealant could have been slightly different on each day and the room temperature may have been different on each day. These varying factors could have been the reason why the testing did not produce data that could be effectively analyzed. For future cure rate tests, all test specimens need to me made on the same day.
- New laboratory tests not conducted in this study may be beneficial. One test, in particular, could analyze dynamic loading and unloading. A loading and unloading test was conducted in this research, however, it only involved 5 cycles. This dynamic testing would require many, continuous cycles of loading and unloading at fast crosshead velocities.
- While the application procedure proved to be effective, there is room for refinement. One major upgrade to the procedure would be establishing a way to prepackage the materials together so that, instead of 5 separate containers for 5 materials, everything is in 2 containers. In this situation, the applicator gun used by Watson Bowman for its two-part, silicone sealant can be used.

- The vertical joints were a problem with all four bridges. Because the foam and solid sealants easily flow before they begin to cure it is very difficult to seal vertical joints. A procedure to accomplish this needs to be developed and taken to the field.
- It is recommended that, for future monitoring of the bridge sites, new procedures for evaluating the sealant, while remaining installed in the expansion joint, be used. These procedures focus on non destructive analysis of the sealant. ASTM has a standard for evaluating the adhesion of weatherproofing joint sealants, and the procedure used can be very applicable to this study. This test places strain on the sealant, while also applying a stress to the sealant/bonding substrate interface, closely simulating the tests conducted in the laboratory (ASTM 1997). Along with the ASTM standard for non destructive testing, there are devices that can be used to monitor the sealant. Ultrasonic (UT) NDT material testers can be used to measure changes in the material's elastic modulus, while density variations can be measured by radiation adsorption or sound wave attenuation. These types of devices can help in evaluating the potential characteristic changes of the silicone foam sealant as it remains installed in the bridge expansion joint.

8.0 REFERENCES

1. AASHTO (2007). *AASHTO LRFD Bridge Design Specifications 2007.* American Association of State Highway and Transportation Officials, Washington D.C.
2. ASTM (1997). “Standard Specification for Cold Applied, Single Component, Chemically Curing Silicone Joint Sealant for Portland Cement Concrete Pavements. *ASTM D 5893”, Annual Book of ASTM Standards*, Vol.04.03, Am. Society for Testing and Materials, West Conshohocken, PA.
3. Cantournet, S., Desmorat, R., and J. Besson (2008). “Mullins Effect and Cyclic Stress Softening of Filled Elastomers by Internal Sliding and Friction Thermodynamics Model,” *International Journal of Solids and Structures*, 46(11-12), 2255-2264.
4. Chang, L.M., and Lee, Y.J. (2002). “Evaluation of Performance of Bridge Deck Expansion Joints,” *Performance of Constructed Facilities*, 16(1), 3-9, 2002.
5. Chen, W. and Duan, L. (2000). *Bridge Engineering Handbook*. CRC Press, NY.
6. Dornsife, Ralph J., “Expansion Joints,” *Bridge Engineering Handbook,* CRC Press, NY., 1999, 25-1 to 25-14.
7. Dow Corning Silicones (2008). “Dow Corning 902 RCS Joint Sealant.” Form No. 62-181F-01, Dow Corning Corporation, Midland, MI.
8. Drozdov, A.D., (2008). “Mullins Effect in Thermoplastic Elastomers: Experiments and Modeling.” *Mechanics and Research Communications*, 36(4), 437-443.
9. Federal Highway Administration (2010). “FHWA Vehicle Classification.” <http://www.fhwa.dot.gov>, Federal Highway Administration, Washington, DC.

10. French, J.W. and McKeel, W.T. (2003). "An evaluation of Bridge Deck Joint Sealing Systems in Virginia." *Technical Assistance Report VTRC 03-TAR,* Charlottesville, VA.

11. Fogler, H. S. (1992). *Elements of Chemical Reaction Engineering*, Prentice-Hall, Inc., Englewood Cliffs, NJ, 2nd Edition.

12. GE Bayer Silicones (2003). <http://www.gesilicones.com/gesilicones/eu1/en/home.jsp>., Wilton, CT.

13. Gelest, Inc. (2008). <http://www.gelest.com> (Oct. 2008), Morrisville, PA

14. Guzaltan, F. (1993). *Bridge Inspection and Rehabilitation: A Practical Guide*, Silano, L.G., ed., Wiley, NY.

15. Malla, R., Shaw, M., Shrestha, M., and Boob, S. (2006). "Sealing Small Movement Bridge Expansion Joints," *NETCR-58, Final NETC 02-6 Project Report*, New England Transportation Consortium, Fall River, MA; June 29, 2006, 112 pages.

16. Malla, R., Shaw, M., Shrestha, M., and Brijmohan, S.B. (2007). "Development and Laboratory Analysis of Silicone Foam Sealant for Bridge Expansion Joints," ASCE *J. of Bridge Engineering*, 12 (4), 438-448.

17. Malla, R.B., Shrestha, M.R., Shaw, M.T., and Brijmohan, S. (2010). "Temperature Aging, Compression Recovery, Creep, and Weathering of a Foam Silicone Sealant for Bridge Expansion Joints." *J. of Materials in Civil Engineering*, Vol 23, No. 3, March 2011, pp 287-298. (Published online, http://dx.doi.org/10.1061/(ASCE)MT.1943-5533.0000166; Sept. 16, 2010).

18. Malla, R.B., Swanson, B. and Shaw M.T. (2010a). "Laboratory Evaluation of a Silicone Foam Sealant for Field Application of Bridge Expansion Joints," *Proceedings* of the 2010 SEM Annual Conference & Exposition, SEM, Bethel, CT, 12 pages, June 2010.

19. Malla, R.B., Swanson, B. and Shaw M.T. (2010b), "Development and Installation of Foam Sealant for Small Movement Bridge Expansion Joints," *Proceedings,* 27th Annual International Bridge Conference , Pittsburgh, PA, June 6-9, 2010. (Poster Presentation).

20. Malla, R.B., Swanson, B. and Shaw M.T. (2011), "Laboratory Evaluation of a Silicone Foam Sealant Bonded to Various Header Materials used in Bridge Expansion Joints," *Construction and Building Materials-An International Journal ((*http://dx.doi.org/10.1016/j.conbuildmat.2011.04.050; *in Press, May* 2011).

21. Momentive Performance Materials (2008). "Silicones." <http://www.momentive.com/Internet/Silicones/Brand/Silopren*/U_Crosslinker430?productid=16b927d09d67d110VgnVCM1000002a25340a____>, Momentive Performance Materials, Albany, New York.

22. National Weather Service (2009). <http://www.erh.noaa.gov>, Taunton, MA.

23. New Hampshire Department of Transportation (2010). "Lyme Traffic Detail Sheets – Traffic Volume Report." <http://www.nh.gov/dot/org/operations/traffic/tvr/detailsheets/lyme> , New Hampshire Department of Transportation, Concord, NH.

24. Omega Engineering, Inc. (2008). "Temperature Products." < http://www.omega.com/temperature/tsc.html> , Omega Engineering, Inc., Stamford, CT.

25. Polymath Software (2010). <http://www.polymath-software.com> , Willimantic, CT.

26. Price, A.R. (1984). "The Performance in Service of Bridge Deck Expansion Joints."*TRRL Report LR 1104*, Transportation and Road Research Laboratory, Crowthorne, U.K., 4-10.

27. Purvis, R. (2003). "Bridge Deck Joint Performance." *NCHRP Synthesis 319*, Transportation Research Board, Washington D.C.

28. Shaw, M. T. and W. J. MacKnight, (2005). *Introduction to Polymer Viscoelasticity*, Wiley, New York, Chapter 6.

29. Shrestha, M.R., Malla R.B., Boob, S., and Shaw M.T. (2006). “Laboratory Evaluation of Weathering and Freeze-Thaw Effects on Silicone.” *Proceedings of the 2006 SEM Annual Conference & Exposition*, St. Louis, Missouri, June, 8 pages.

30. Stevens, M. P. (1999). *Polymer Chemistry, an Introduction*, 3rd edition Oxford, New York, pp. 427-430.

31. Vipulanandan, C., and Paul, E. (1993). “Characterization of Polyester Polymer and Polymer Concrete,” *J. of Materials in Civil Engineering,* 5(1), 62-82.

32. Volk, W. (1956). “Industrial Statistics.” *Chemical Engineering*, 165-190.

33. Watson Bowman Acme Corp. (2008). **“**Wabo®SiliconeSeal,” Watson Bowman Acme, Corp., Amherst, NY. <http://www.watsonbowman.com/Products/ViewProductLine.aspx?ProductLine D=48> (September 2008).

34. Washington State DOT (2005). *Bridge Design Manual*, Washington State Department of Transportation, Olympia, WA.

35. Weather Underground (2008). Ann Arbor, MI <http://www.wunderground.com> (August 2009).